



THE UNIVERSITY OF  
**WAIKATO**  
*Te Whare Wānanga o Waikato*

Research Commons

<http://waikato.researchgateway.ac.nz/>

## Research Commons at the University of Waikato

### Copyright Statement:

The digital copy of this thesis is protected by the Copyright Act 1994 (New Zealand).

The thesis may be consulted by you, provided you comply with the provisions of the Act and the following conditions of use:

- Any use you make of these documents or images must be for research or private study purposes only, and you may not make them available to any other person.
- Authors control the copyright of their thesis. You will recognise the author's right to be identified as the author of the thesis, and due acknowledgement will be made to the author where appropriate.
- You will obtain the author's permission before publishing any material from the thesis.

**CHARACTERISATION OF WATER-  
SOLUBLE POLYSACCHARIDES  
PRODUCED DURING PREHYDROLYSIS  
OF *PINUS RADIATA***



THE UNIVERSITY OF  
**WAIKATO**  
*Te Whare Wānanga o Waikato*

A thesis  
submitted in partial fulfillment  
of the requirements for the degree  
of  
**Master of Science in Chemistry**  
at  
**The University of Waikato**  
by  
**John McDonald-Wharry**

---

The University of Waikato  
2010

## Abstract

An aqueous prehydrolysate (or prehydrolysis liquor) was produced during a mild hot-water prehydrolysis (90 minute ramp to 175°C) of commercial radiata pine wood chips. Oligosaccharide and polysaccharide material was separated from the concentrated prehydrolysate using solvent precipitation after most of the non-carbohydrate material was removed.

These polymeric carbohydrates were fractionated based on charge and molecular weight by size-exclusion chromatography (SEC). The fractions were each analysed by a number of methods including MALDI-ToF mass spectrometry, and NMR. A number of different types of carbohydrate polymer structures were found that were produced due to the partial de-polymerisation of the wood hemicelluloses during the prehydrolysis process.

The *O*-acetylated (galacto)glucomannans were the most extensively characterised. These partially-acetylated hexose-based polymers were the main type found and accounted for approximately 54% by mass of the polymeric carbohydrates. Most appeared to contained between 5 and 79 hexose units with differing degrees of acetylation. The average mol ratio of components in these polymers was calculated to be approximately 3.7 : 1.3 : 1 : 0.2 (D-mannosyl : acetyl : D-glucosyl : D-galactosyl). They had a structure consistent with a linear backbone of  $\beta$ -1,4-linked D-mannopyranosyl and  $\beta$ -1,4-linked D-glucopyranosyl units with acetyl groups attached at C-2 and C-3 positions of some D-mannopyranosyl units. The terminal D-galactopyranosyl units were likely to be attached at 1,4,6-linked D-mannopyranosyl branch points. Of the neutral (non-anionic) polysaccharides, this type was most prevalent in the higher molecular weight fractions.

Anionic pentose-based polymers with a backbone of  $\beta$ -1,4-linked D-xylopyranosyl units were also characterised. Identified as (arabino)glucuronoxylans, they featured uronic acid groups consistent with 4-*O*-methyl- $\alpha$ -D-glucopyranosyluronic acids attached to the C-2 position of some D-xylopyranosyl units. Smaller amounts of terminal  $\alpha$ -L-arabinofuranosyl units likely to be attached at  $\beta$ -1,3,4-linked D-xylopyranosyl branch points were also detected. These polymers appeared to mostly contain between 5 and 40 pentose units with between 1 and 4 uronic acid groups attached.

The anionic fractions (approximately 30% by mass) also contained large amounts of D-galactopyranosyl and L-arabinosyl units along with some D-glucuronic and D-galacturonic acid residues. This suggested the presence of carbohydrates produced from the partial hydrolysis of arabinogalactans and pectins.

The smaller molecular weight fractions of non-anionic polysaccharides were enriched in both 1,4-linked D-galactopyranosyl units and non-acetylated hexose-based polymers that contained between 5 and 30 hexose units; this suggested that significant amounts 1,4-galactan derived carbohydrates were present. Small amounts of oligomers containing only pentose units were detected in these smaller molecular weight fractions along with what appeared to be other uncharged fragments of the polysaccharide-types that were present in the anionic fractions.

## Acknowledgements

I would like to thank Dr Marilyn Manley-Harris and John Lloyd for their crucial advice and support throughout this work.

Thanks also to those in the Chemistry Department at the University of Waikato for their assistance, especially the following people.

Katie de Lange for help in developing the ion chromatography method.

Martyn Faville, Jonathan Puddick and Wendy Jackson for their advice on MALDI-ToF-MS. Ben Deadman and Chris Adams for advice on the HPLC systems. Jolene Brown and Professor Alistair Wilkins for NMR training and advice on the GC-MS setup.

I would also like to acknowledge the advice, assistance, and training from those in the Papro team at Scion, especially Sylke Champion.

The financial assistance of the Dumont d'Urville NZ/France S&T Support Programme is acknowledged for providing the opportunity for collaboration with EFPG in Grenoble. Thanks must go to Dr Ian Suckling and many others for the considerable work that went into organising this collaboration.

# Table of Contents

<b>Abstract</b> .....	i
<b>Acknowledgements</b> .....	iii
<b>Table of Contents</b> .....	iv
<b>List of Figures</b> .....	vii
<b>List of Tables</b> .....	ix
<b>List of Abbreviations</b> .....	x
<b>Chapter 1 Introduction &amp; Background</b> .....	1
1.1 Introduction .....	1
1.2 Literature Review .....	3
1.2.1 General Wood Composition and Structure .....	3
1.2.2 The Structural Diversity of Softwood Hemicelluloses .....	7
1.2.3 Hemicelluloses from Other Plant Sources .....	10
1.2.4 The Biology of Hemicelluloses.....	11
1.2.5 Current and Potential Industrial Utilisation of Hemicelluloses .....	12
1.2.6 Extraction of Hemicelluloses from Wood.....	16
1.2.7 Recovery and Purification of Hemicelluloses.....	19
1.2.8 Methods for Fractionating and Characterising Polysaccharides.....	21
<b>Chapter 2 Experimental</b> .....	27
2.1 Prehydrolysis and Isolation of Polymeric Carbohydrates .....	27
2.1.1 Aims .....	27
2.1.2 Methodology .....	27
2.2 Fractionation by Size Exclusion Chromatography.....	29
2.2.1 Aims .....	29
2.2.2 Methodology .....	29
2.3 Matrix Assisted Laser Desorption Ionisation – Time of Flight-Mass Spectrometry (MALDI-ToF-MS) Analysis.....	32
2.3.1 Aims .....	32
2.3.2 Methodology .....	32
2.4 Nuclear Magnetic Resonance Spectrometry (NMR) Analysis.....	36

2.4.1	Aims .....	36
2.4.2	Methodology .....	36
2.5	Acid Hydrolysis and Monomer Composition Analysis .....	37
2.5.1	Aims .....	37
2.5.2	Methodology .....	37
2.6	Linkage Analysis .....	43
2.6.1	Aims .....	43
2.6.2	Methodology .....	43
	<b>Chapter 3 Results and Discussion</b> .....	48
3.1	Fractionation by Size Exclusion Chromatography.....	48
3.2	Matrix Assisted Laser Desorption Ionisation – Time of Flight-Mass Spectrometry (MALDI-ToF-MS) Analysis.....	51
3.2.1	Anionic (Acidic) Polysaccharides.....	51
3.2.2	Neutral Polysaccharides .....	57
3.2.3	Alkaline De-acetylation of Neutral Polysaccharides .....	60
3.3	Nuclear Magnetic Resonance Spectroscopy (NMR) Analysis.....	67
3.3.1	Anionic (Acidic) Fractions.....	67
3.3.2	Neutral Fractions.....	70
3.4	Acid Hydrolysis and Monomer Composition Analysis .....	77
3.4.1	Analysis of Neutral Components by Conversion to Alditol Acetates.....	77
3.4.2	Analysis of Acidic Components by Ion Chromatography and NMR .....	79
3.4.3	Interpretation of Monomer Composition Information .....	83
3.5	Linkage Analysis .....	88
	<b>Chapter 4 Summary and Conclusions</b> .....	95
4.1	Types of Polysaccharides in the Prehydrolysate .....	95
4.1.1	<i>O</i> -acetylated (galacto)glucomannans (AcGGMs).....	96
4.1.2	(Arabino)4- <i>O</i> -methylglucuronoxylans.....	99
4.1.3	(Arabino)xylans.....	101
4.1.4	Galactans .....	101

4.1.5	Arabinogalactans.....	101
4.1.6	Glucans.....	102
4.1.7	Arabinans .....	103
4.1.8	Other Polysaccharides .....	103
4.2	Causes of the Diversity and Complexity of Polysaccharides in this Prehydrolysate.....	104
4.3	Future Research Suggestions.....	106
4.3.1	NMR.....	106
4.3.2	Enzyme Hydrolysis .....	108
4.3.3	Ion Chromatography .....	108
4.3.4	MALDI-ToF-MS .....	109
4.3.5	Linkage Analysis.....	109
4.3.6	Larger Scale Processing of Prehydrolysates .....	110
	<b>Appendix 1</b> .....	111
	<b>Appendix 2</b> .....	113
	<b>References</b> .....	115

## List of Figures

Figure 1: Polymer structure of cellulose .....	4
Figure 2: Example of structural features of softwood <i>O</i> -acetylated galactoglucomannan.....	7
Figure 3: Example of structural features of softwood arabino-4- <i>O</i> - methylglucuronoxylans.....	8
Figure 4: M/K 6 L digesters (left) and <i>P. radiata</i> woodchips (right). .....	28
Figure 5: Size-exclusion chromatography calibration curve. ....	31
Figure 6: Chromatogram of SEC fractionation of hemicelluloses polymers.....	31
Figure 7: Calibration plot for the quantification of uronic acid concentration using ion chromatography (using logarithmic scales). ....	42
Figure 8: Retention time correlation to literature SP-2330 column for known standards.....	46
Figure 9: Retention time correlation to literature OV-275 column for known standards.....	46
Figure 10: Chromatogram of SEC fractionation of hemicelluloses polymers.....	48
Figure 11: Apparent molecular weights of neutral fractions by SEC. Blue divisions indicate where each fraction was collected. These nine smaller fractions were each re-injected and retention times of peak tops measured. ....	49
Figure 12: MALDI-ToF mass spectrum of Fraction A1 (S-DHB matrix, negative ion mode). ....	53
Figure 13: MALDI-ToF mass spectrum of Fraction A2. (S-DHB matrix, negative ion mode). ....	53
Figure 14: MALDI-ToF mass spectrum of Fraction A3. (S-DHB matrix, negative ion mode). ....	54
Figure 15: MALDI-ToF mass spectrum of Fraction N1. (S-DHB matrix, negative ion mode). ....	54
Figure 16: MALDI-ToF mass spectrum of Fraction N3. (THAP matrix, positive ion mode). ....	57

Figure 17: MALDI-ToF mass spectrum of Fraction of N2. (THAP matrix, positive ion mode). .....	57
Figure 18: MALDI-ToF mass spectrum of Fraction N3 control before de-acetylation (THAP matrix, positive ion mode). .....	61
Figure 19: MALDI-ToF-MS Fraction N3 after de-acetylation with NH <sub>4</sub> OH (THAP matrix, positive ion mode). .....	61
Figure 20: MALDI-ToF-MS of Fraction N2 after de-acetylation with NH <sub>4</sub> OH (THAP matrix, positive ion mode). .....	62
Figure 21: Ion gating changes on N1 after de-acetylation with NH <sub>4</sub> OH (THAP matrix, positive ion mode). .....	62
Figure 22: <sup>1</sup> H NMR of Fraction A2 in D <sub>2</sub> O (70°C probe temperature). .....	67
Figure 23: Anomeric region of <sup>1</sup> H NMR of Fraction A2 in D <sub>2</sub> O (70°C probe temperature) .....	68
Figure 24: <sup>1</sup> H NMR of Fraction N1 in D <sub>2</sub> O. (27°C probe temperature) .....	70
Figure 25: <sup>1</sup> H NMR of Fraction N2 in D <sub>2</sub> O. (70°C probe temperature) .....	70
Figure 26: <sup>1</sup> H NMR of Fraction N2 in D <sub>2</sub> O acquired two weeks after Figure 25. .....	71
Figure 27: <sup>13</sup> C DEPT135 of Fraction N2 in D <sub>2</sub> O. (37°C probe temperature).....	76
Figure 28: Estimated uronic acid content of the fractions as a proportion of fraction dryweight. ....	79
Figure 29: Plot of correlations between estimated content of D-galactosyl and L-arabinosyl.....	84
Figure 30: Relative enrichment and depletion of detected linkages .....	93
Figure 31: Estimated distribution of different types of polymer across the major fractions.....	96
Figure 32: Postulated structure of a typical <i>O</i> -acetylated (galacto)glucomannan molecule ≈ 2780 Da that could be found in the prehydrolysate. ....	98
Figure 33: Postulated structure of a typical (arabino)4- <i>O</i> -methylglucuronoxylan molecule ≈ 2511 Da that could be found in the prehydrolysate. ....	100
Figure 34: Ways that the native softwood xylan could fragment during prehydrolysis. ....	105

## List of Tables

Table 1: Average MW values for major acidic pentose polymers (calculated using Polytools). .....	55
Table 2: Simplified hypothetical hexose polymer sample <sup>a</sup> .....	64
Table 3: Average MW values for de-acetylated neutral hexose polymers (calculated using Polytools). .....	65
Table 4: Estimated degrees of acetylation for neutral fractions and comparison to literature values. ....	74
Table 5: Monosaccharide components by mol ratio relative to D-mannose .....	77
Table 6: Monosaccharide composition of samples in mol% .....	77
Table 7: Estimated mol% of monomer components .....	83
Table 8: Useful linear correlations between mol % estimates of different components .....	85
Table 9: Linkages deduced from detected partially methylated alditol acetates, approximate proportions represented as percentage of total indentified PMAA peak area within each sample. ....	91
Table 10: Partial methylated alditol acetates detected and identified. ....	92
Table 11: Estimated yields of different polymer types identified. ....	95
Table 12: Extended table of linear correlations between mol % estimates of different components of correlation graphs between monomer components .....	111
Table 13: Summary Table. ....	113
Table 14: Summary Table (continued). ....	114

## List of Abbreviations

DP	Degree of polymerisation
AcGGM(s)	<i>O</i> -acetylated (galacto)glucomannan(s)
SEC	Size exclusion chromatography
DS <sub>Ac</sub>	Degree of substitution with acetyl groups
GPC	Gel permeation chromatography
DHB	2-5-dihydroxybenzoic acid
TFA	Trifluoroacetic acid
RI	Refractive index
THAP	2,4,6-trihydroxyacetophenone
MeGlcA	4- <i>O</i> -methyl-D-glucuronic acid
MW	Molecular weight
MALDI	Matrix assisted laser desorption ionisation
ToF	Time of flight
MS	Mass spectrometry
S-DHB	Super-DHB (DHB with added 2-hydroxy-5-methoxybenzoic acid)
RT	Retention time
HPLC	High performance liquid chromatography
NMR	Nuclear magnetic resonance spectroscopy
DMSO	Dimethylsulfoxide
HOD	Deuterium hydrogen monoxide

COSY	Correlation spectroscopy
NOESY	Nuclear overhauser effect spectroscopy
DEPT	Distortion enhancement by polarisation transfer
HSQC	Heteronuclear single quantum coherence
HMBC	Heteronuclear multiple bond coherence
TOCSY	Totally correlated spectroscopy
AA(s)	Alditol acetate(s)
PMAA(s)	Partially methylated alditol acetates(s)

# Chapter 1 Introduction & Background

## 1.1 Introduction

Radiata pine (Monterey pine, *Pinus radiata*) is New Zealand's principal plantation forests species covering approximately 1,500,000 ha in 2006 [1]. Radiata pine wood is processed into a number of different products, including those manufactured by the pulp and paper industry. The industrial-scale facilities and processes used in pulp and paper mills have the potential to act as biorefineries in the future, producing renewable wood-derived chemicals and reducing the reliance on petrochemical-based products [2].

Hemicelluloses are a diverse group of polysaccharides that are found in structural plant materials such as wood. Lignocellulosic biomass such as wood is primarily composed of three general types of organic polymers, cellulose, lignins, and hemicelluloses. As they account for approximately 30% of the dry weight of radiata pine wood, hemicelluloses are a large sustainable resource [3, 4].

In the normal kraft pulping process the alkaline pulping liquor is added directly to the wood chips and the mixture heated to 160-170°C, and held at that temperature until the target amount of lignin has been extracted out of the chips. During this stage more than half of the hemicelluloses and a small amount of the cellulose are also extracted and pass to the pulping liquor along with the lignin. The spent liquor at the end of pulping is sent to the recovery boiler where the extracted organic material is burnt to provide energy for the process [3].

A variation of the kraft process is the prehydrolysis-kraft process where a steam or hot-water hydrolysis stage is inserted prior to the main kraft pulping stage. The reason for including the prehydrolysis stage is to increase the extraction of hemicelluloses in order to produce a cellulose-rich final pulp with a low hemicellulose content. These pulps are called dissolving pulps and are often not used for paper manufacture, but for manufacturing textiles along with cellulose derivatives such as cellulose esters and cellulose ethers. The water heated to over 100°C under pressure, will cause hydrolysis of some glycosidic linkages within the hemicelluloses. This causes the extracted hemicellulose-derived material in the resulting prehydrolysis liquor to be mainly a mix of polysaccharides, oligosaccharides, and monosaccharides. The prehydrolysis liquor (or prehydrolysate) is traditionally combined with the main kraft pulping liquor and sent to the recovery boiler [2, 3].

The prehydrolysis stage may offer an opportunity to extract and recover potentially valuable hemicelluloses from wood provided the conditions during the prehydrolysis stage are sufficiently mild to minimise degradation of the hemicelluloses.

This study aimed to characterise the water-soluble polymeric carbohydrates present in such a prehydrolysis liquor (or prehydrolysate). The prehydrolysate used for the study described in this thesis was produced by heating water up to 175°C over 90 minutes while circulating it through *P. radiata* woodchips in a sealed digester. Once the water reached 175°C, the prehydrolysis process was completed by passing the hot process water through a condenser to yield the prehydrolysate solution. The elucidation of polysaccharide structures contained within this solution are the subject of this thesis.

## **1.2 Literature Review**

This section gives a brief overview of previous research and established knowledge on hemicelluloses. The composition, distribution, biosynthesis, function, and structures of hemicelluloses will be covered with a focus on those found in softwoods, especially radiata pine. Literature methods for the extraction, purification, fractionation, analysis, and structural characterisation of plant derived polysaccharides will also be covered in some detail.

### **1.2.1 General Wood Composition and Structure**

#### **1.2.1.1 Composite and Cellular Structure**

Wood is a composite material that has evolved over millions of years to provide trees with a number of important functions needed for their survival. These functions include transporting water from roots to the leaves, structural support of plant, and the long-term storage of chemicals required for the plants metabolism [5, 6].

Through the cross-section of a tree's trunk an outer layer of bark is followed by a sapwood zone, and finally a heartwood zone around the tree's core. Sapwood contains metabolically active parenchyma cells that allow the conduction of sap, shorter-term storage, and synthesis of biochemicals. The heartwood is generally comprised of cell walls which do not contain a protoplast or metabolically active cell. These empty or dead cells provide the functions of structural support, transport of water and the long-term storage of some biochemicals [5].

In softwoods such as *P. radiata*, long tracheid cell structures make up a large proportion of the wood's volume. They provide support and a pathway for water flow. The walls of wood cells are comprised of a number of microscopic layers. These include the middle lamella, primary wall, and three layers of secondary wall. Each layer of the wall is a composite material consisting of the polymers: cellulose, lignin, hemicelluloses, and pectic polysaccharides [5, 6].

### 1.2.1.2 Cellulose

Cellulose typically makes up 40-50% of wood's dry weight. Cellulose is a very long homopolymer containing only repeating monomer units of anhydro D-glucose (or more specifically,  $\beta$ -(1 $\rightarrow$ 4)-D-glucopyranosyl units). Due to the regular linear structure of cellulose, polymers tend to aggregate and form strong inter-molecular hydrogen-bonds. Multiple cellulose polymers will form crystalline and fibre structures that are very difficult to dissolve. The degree of polymerisation (or DP) of cellulose molecules is estimated to be  $\approx$  10,000 on average and represents a chain length of approximately 5  $\mu$ m [6].

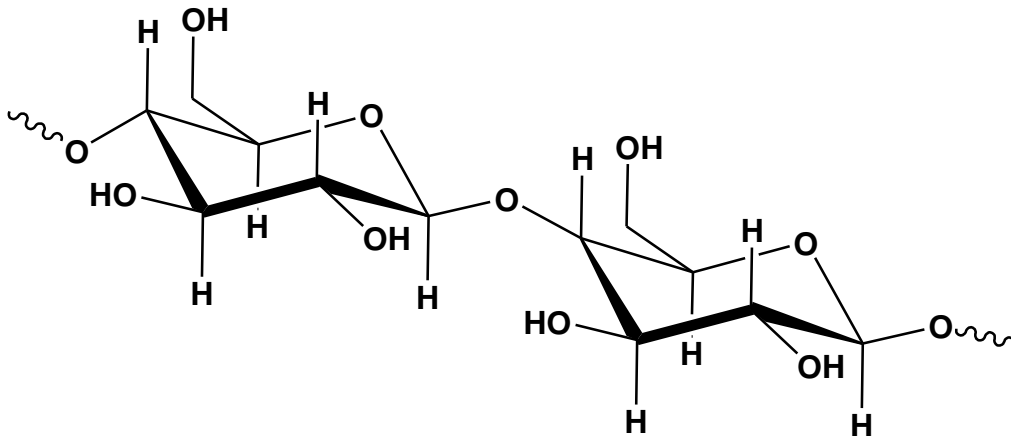


Figure 1: Polymer structure of cellulose

### 1.2.1.3 Lignin

Lignin is a complex three-dimensional polymer composed of many different linkages between a diverse range of substituted phenolic units [6]. Lignin acts as a matrix in cell walls to hold fibre components such as cellulose in a rigid structure. The aim of most pulp & paper processing is to remove lignin from wood in order to obtain cellulose-rich fibres. Lignin is known to be covalently linked to some hemicelluloses [6-10]. The existence and/or extent of covalent linkages between lignin and cellulose in native wood is currently in dispute [6, 11].

#### **1.2.1.4 Hemicelluloses**

In contrast to the homogeneous cellulose polymer chain, hemicelluloses are a diverse group of different polymer types, most of which are heterogeneous in composition. They are polymers of the monosaccharide sugars D-glucose, D-galactose, D-mannose, D-xylose, and L-arabinose. Other common components of hemicelluloses include: acetyl groups, D-glucuronic acid, D-galacturonic acid, and 4-*O*-methyl-D-glucuronic acid [3, 6]. The structural diversity of hemicelluloses is discussed later in this chapter. Hemicelluloses generally function in cell walls by assisting with binding cellulose fibres and other components such as lignin together at a molecular level [12].

#### **1.2.1.5 Pectic Polysaccharides**

Pectic polysaccharides are another class of carbohydrate polymers that occur in plants. A higher content of uronic acids (usually galacturonic and glucuronic acid) tends to distinguish pectic polysaccharides from hemicelluloses [3, 6]. However most non-cellulose wood polysaccharides exist somewhere on a continuum between what are considered pectins and what are considered hemicelluloses. On one extreme is homogalacturonan [13], a polymer that is entirely composed of galacturonic acid and esterified galacturonic acid [14] which is definitely considered a pectin. On the other extreme, galactoglucomannans are a major type of softwood polymer that usually contain no attached uronic acids and are definitely considered hemicelluloses. A grey area can exist near the middle of this continuum where polymers such as some arabinogalactans [13] are considered to be both pectins due to their high uronic acid content and hemicelluloses due to the rest of their structure and properties. Pectins and other carbohydrates with high uronic acid content are what is sometimes referred to in the pulp and paper industry as “anionic trash” [15].

### **1.2.1.6 Extractives**

Extractives are usually the more non-polar substances in wood that may be extracted from the wood using organic solvents. They can include resin acids, fats, terpenes, waxes, oleoresin, tannins, flavonoids, and pitches. There is a great deal of diversity in the compounds generally considered as extractives [3, 6]. For the scope of this thesis, extractives are only relevant as softwoods contain significant levels and some polysaccharides can help solubilise these extractives in aqueous solutions [15-17].

### **1.2.1.7 Inorganics (Ash)**

As most of wood is comprised of compounds that contain only carbon, oxygen, and hydrogen, other elements usually make up a very small percentage of wood weight. Ash contains the inorganic elements that remain after the combustion of wood. Calcium, magnesium, potassium, silicon, sodium, and boron are elements which are often abundant in wood ash [6].

### **1.2.1.8 Variations in Wood Composition**

The chemical composition of wood is likely to be influenced by a number of factors including the genetics of the tree, the environment in which it has grown, which part of the tree the wood comes from, the age of the tree and its life history [4].

Softwoods contain much higher levels of glucomannan hemicelluloses when compared to hardwoods, and *P. radiata* tends to contain higher glucomannan levels compared to many of the other softwoods, including Norway spruce (*Picea abies*) [3, 6]. At a microscopic level the distribution of lignin, cellulose, pectin and hemicellulose components changes across the different layers in the cell wall [6].

The influence of genetics, environment, and life history, on chemical composition is demonstrated in compression wood. Compression wood often forms as a localised response to structural stresses and involves an increase in  $\beta$ -(1 $\rightarrow$ 4)-D-galactosyl-based hemicelluloses and changes in lignin composition [18-20]. Compression wood content tends to be higher in early stages of a tree's life [6].

## 1.2.2 The Structural Diversity of Softwood Hemicelluloses

### 1.2.2.1 *O*-Acetylated galactoglucomannans (AcGGMs)

This type of mannan or glucomannan, is the main type of hemicellulose present in most softwoods, including *P. radiata*. It is a hexose-based polymer with a linear backbone of (1 $\rightarrow$ 4)-linked  $\beta$ -D-mannopyranosyl and  $\beta$ -D-glucopyranosyl units [3]. Attached almost exclusively to some D-mannosyl units on the backbone are acetyl groups at positions C-2 & C-3, and terminal  $\alpha$ -D-galactopyranosyl units at position C-6 (Figure 2) [17, 21].

The degree of acetylation (or  $DS_{Ac}$ ) for these polymers is  $\approx 0.3$  which means there is on average one acetyl group attached per 3 or 4 hexoses in the backbone. Attached D-galactosyl units are rare compared to acetyl groups, meaning that most mannosyl units in the backbone bear no attached groups [17, 22, 23].

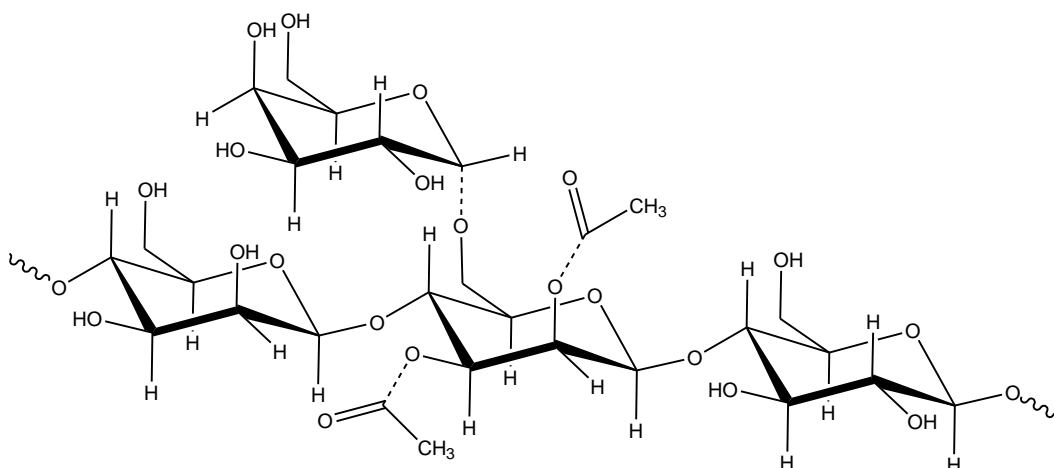


**Figure 2: Example of structural features of softwood *O*-acetylated galactoglucomannan. Dashed lines represent the bonds that can attach side groups to some backbone D-mannosyl units.**

The (1→6)-linkage between  $\alpha$ -D-galactopyranosyl branches and the D-mannopyranosyl backbone is especially vulnerable to acid hydrolysis [3]. In softwoods, ‘native’ galactoglucomannans were thought have a DP of approximately 100 [3, 6]. However, recent evidence has suggested molecular weights as high as 60,000 Da may well be present and this corresponds to a DP well over 300 [17, 21].

### 1.2.2.2 Arabino-4-*O*-methylglucuronoxylans

This type of xylan is the second most abundant type of hemicellulose found in softwoods. It is predominantly pentose-based with a linear backbone of (1→4)-linked  $\beta$ -D-xylopyranosyl units [3]. It is known to contain some 4-*O*-methyl- $\alpha$ -D-glucopyranosyluronic acid groups attached to the C-2 position [4, 24-30] and fewer  $\alpha$ -L-arabinofuranosyl units at C-3 positions along the D-xylopyranosyl backbone (Figure 3) [21].

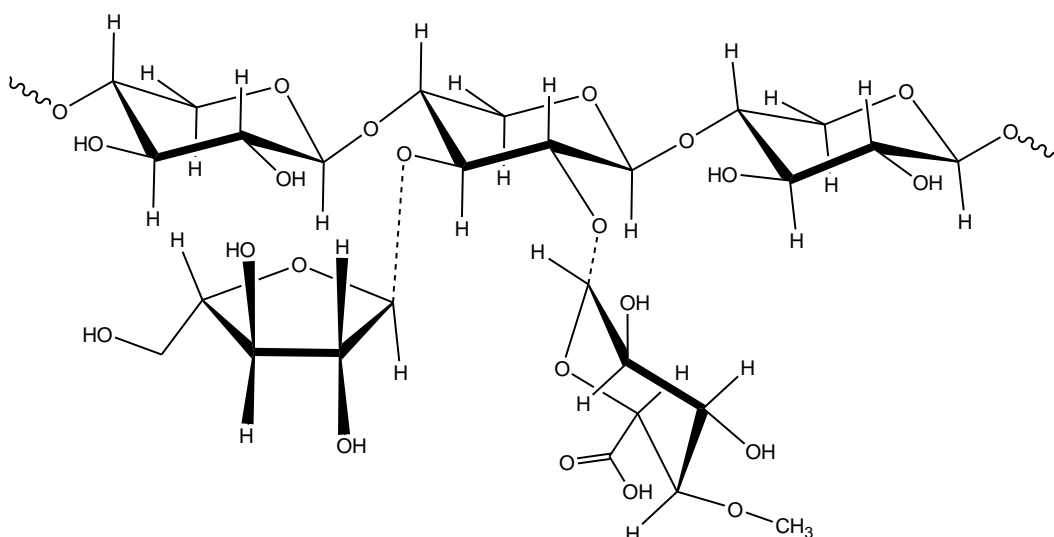


**Figure 3:** Example of structural features of softwood arabino-4-*O*-methylglucuronoxylans. Dashed lines represent the bonds that can attach side groups to some backbone D-xylosyl units.

The (1→3)-linkage between  $\alpha$ -L-arabinofuranosyl branches and the D-xylopyranosyl backbone is especially vulnerable to acid hydrolysis [3]. In softwoods, ‘native’ arabino-4-*O*-methylglucuronoxylans are thought have a DP of approximately 100 [3, 6].

### 1.2.2.3 Arabinogalactans

With the exception of larch species, most softwoods contain only minor amounts of arabinogalactans. Considered to be a highly branched polymer with a backbone of (1→3)-linked β-D-galactopyranosyl units and with many branches at the C-6 position [3]. Branches of (1→6)-linked β-D-galactopyranosyl units along with both terminal and (1→5)-linked L-arabinofuranosyl units have been reported [31]. Arabinogalactans in softwood have been reported to contain 3-8 times more D-galactosyl residues than L-arabinosyl residues and some attached D-glucuronic acid [4, 29].

### 1.2.2.4 Galactans

Compression wood contains high levels of a galactan polysaccharide found to have a linear backbone of (1→4)-linked β-D-galactopyranosyl units and in some cases attached D-glucuronic acid and D-galacturonic acid [6, 19].

### 1.2.2.5 Arabinans

There is uncertainty about the structures of L-arabinosyl-rich hemicelluloses. Some research on softwoods has attributed L-arabinose residues and evidence of (1→5)-linked L-arabinofuranosyl units as belonging to arabinans [32, 33]. The name “arabinans” suggests that these polysaccharides are mostly comprised of L-arabinosyl units. Questions remain as to the existence and extent of any polysaccharides in softwoods that are primarily L-arabinose-based. Arabinans might not exist as a type of ‘native’ softwood hemicellulose. However other ‘native’ hemicelluloses such as arabinogalactans [29] could undergo partial hydrolysis during their extraction and create “arabinans” as the small proportion of fragments that happen to be L-arabinose-rich and D-galactose-poor.

### 1.2.2.6 Other Xylans

Oligomers containing only pentose units have been identified as originating from softwoods such as *P. radiata* and could be composed of D-xylosyl and/or L-arabinosyl units [32]. As with arabinans there is uncertainty as to the existence of any pure xylan polymers in the original wood. Oligomers containing only D-xylosyl units might only form due to partial hydrolysis of arabino-4-*O*-methylglucuronoxylans during the extraction process.

### **1.2.2.7 Pectic Polysaccharides**

Galacturonan, a polymer of D-galacturonic acid units have been found in both softwoods and hardwoods [14]. (1→4)-linked β-D-galactopyranosyluronic acid backbones with some attached methyl esters are the general structural features of these pectins [6]. Other polysaccharides with high uronic acid content including arabinogalactans are sometimes considered pectins [13].

## **1.2.3 Hemicelluloses from Other Plant Sources**

### **1.2.3.1 Hardwoods**

Hardwoods are known to contain large amounts of an acetylated type of 4-*O*-methylglucuronoxylan [3]. These have been extensively characterized and found to have similar structures to the softwood xylans (page 8), with the main differences being that they have far fewer uronic acid groups and some of the D-xylopyranosyl units are acetylated at positions C-2 and C-3 [25, 34, 35].

Small amounts of glucomannans (2-5% by mass) are present in hardwoods, they differ from those in softwoods as they usually contain increased D-glucosyl levels and no D-galactopyranosyl branches [3, 6, 36].

### **1.2.3.2 Agricultural Residues & Herbaceous Vegetation**

A variety of different hemicelluloses have been characterised in non-tree plants [37, 38]. Agricultural residues have attracted attention due to their abundance, accessibility, and because their utilisation can solve waste disposal issues [39].

4-*O*-methylglucuronoxylans have been identified in sugar beet pulp [40] along with other hemicelluloses classed as xyloglucans and glucomannans [41, 42]. Xylans have been extracted from parts of flax and kenaf plants, some of these xylans have 4-*O*-methyl-α-D-glucopyranosyluronic acid groups attached to the C-2 position of the backbone [37, 43-45].

### **1.2.3.3 Seeds and Fruits**

A galactoglucomannan has been extracted from *Acrocomia aculeate* and differs from softwood galactoglucomannans because the D-galactopyranosyl branches are attached at the C-3 position on the D-glucosyl units of the backbone [46].

A galactoglucomannan has been extracted from kiwifruit (*Actinidia deliciosa*) that has more branching and higher D-glucosyl levels when compared to those found in softwoods. A large proportion of its backbone was found to be alternating D-glucosyl and D-mannosyl units [47].

## **1.2.4 The Biology of Hemicelluloses**

### **1.2.4.1 Biosynthesis of Hemicelluloses**

A number of enzymes have been discovered that are involved in the biosynthesis of hemicelluloses in biosynthetic pathways that involve different sugar-nucleotides and the Golgi apparatus [13].  $\beta$ -(1,4)-Galactosyltransferase has been discovered as being involved in the formation of compression wood in pines [18].

### **1.2.4.2 Biological Functions of Hemicelluloses**

The primary biological function of hemicelluloses is as a structural component of the cell wall where they help hold cellulose fibrils together using hydrogen bonding. Other functions include acting as long-term carbohydrate storage [13, 48]. Hemicelluloses and pectins also function along with celluloses and lignin to create physical barrier structures that protect parts of the plant from the wider environment and attack from other organisms [49].

### **1.2.4.3 The Attachment of Hemicelluloses to Lignin, Cellulose and Proteins**

Hemicelluloses are attached to cellulose mainly through extensive hydrogen bonding [13, 50]. Attachment to lignin is known to occur through ester and ether covalent linkages [7]. Uronic acids form esters with the hydroxyl groups on some lignin structures [51]. Arabinogalactan-protein complexes are also present in *P. radiata* and other softwoods [31, 52].

## **1.2.5 Current and Potential Industrial Utilisation of Hemicelluloses**

### **1.2.5.1 The Integrated Forest Biorefinery Concept**

A forest biorefinery would be industrial facility that converts biomass, such as wood chips, into a range of material, chemical and energy products, analogous to a petroleum refinery [53, 54]. A number of pulp and paper industry processes that have been operating for over 150 years would be called a biorefinery by the current definition [2, 55]. Recent interest around forest biorefineries has been driven by the realisation that petroleum is a finite resource and that we will increasingly have to use renewable resources to create products to replace those currently produced from petrochemicals [2]. Hemicelluloses make up a large proportion of forest biomass, so alongside cellulose and lignin they are a key target for research and development towards industrial conversion into value-added products [55].

### **1.2.5.2 Kraft Pulp and Paper Mills**

Alkaline degradation during the kraft pulping process causes a peeling reaction that converts much of the hemicelluloses and some of the celluloses into monomers then acidic degradation products. Composed largely of glucoisosaccharinic acids these sugar degradation products, along with the bulk of the lignin, are sent as black liquor to the recovery furnace for combustion [3].

Some hemicelluloses survive the kraft process in polymeric form. Xylans have been found to dissolve in the kraft pulping liquor during the early stages of the kraft cook then re-bind to the cellulose pulp fibres towards the end of the cook [3]. The hemicelluloses left in pulp contribute to the pulp yield (mass) and properties of final products [55-59].

### **1.2.5.3 Emulsifying Agent in Thermo-mechanical Pulping (TMP)**

*O*-Acetylated (galacto)glucomannans (or AcGGMs) extracted from spruce have been studied with regard to their ability to help keep hydrophobic extractives soluble in thermo-mechanical process water. This utilisation appears to be serendipitous as the AcGGMs released from the wood during the pulping process act as an emulsifier for the wood resins reducing pitch deposition problems that are costly in paper making [17, 50].

#### 1.2.5.4 Monomers as Feedstocks

Hemicelluloses can be converted into their sugar monomers by hydrolysis treatments catalysed by acids, bases, or enzymes. The monomers may then be processed further, usually fermented by fungi and bacteria in order to produce a range of products. Xylose, usually hydrolysed from hardwood xylans can be used as a feedstock to produce xylitol by chemical reduction [3]. Xylitol can also be produced by the fermentation of D-xylose and has applications as a sweetener suitable for diabetics [60].

Hexose sugars, such as D-glucose, D-mannose and D-galactose produced from the total hydrolysis of hemicelluloses and cellulose have been used to produce ethanol by fermentation [3]. A large amount of research between 1995 and 2010 has focused on improving the conversion of lignocellulosic materials into monosaccharides for the production of fuel ethanol by fermentation [57, 61-67]. The conversion of the pentose monomers (D-xylose and L-arabinose) into ethanol has proven to be more challenging [55, 68].

A promising use for monosaccharides produced from hemicelluloses, is in the production of lactic acid by fermentation. Fermentation organisms exist that can convert both the pentoses and hexoses found in hemicellulose hydrolysates into lactic acid with reasonably high yields. Examples of suitable fermentation organisms might include *Rhizopus oryzae* [69, 70] and *Lactobacillus pentosus* [71]. Lactic acid is the monomer building block for producing polylactide (PLA) plastics that have experienced strong market demand which is expected to grow in the foreseeable future [69, 72].

### **1.2.5.5 Additives for Pulp, Paper or Textile Products and Processes**

Mannans of various types have been utilised for many centuries as additives in the paper and textile industries. Non-wood mannans such as guar gum and locust bean gum have been used as beater and wet-end additives in the pulp and paper industry, often to lower operating costs and improve product strength [50]. Wood-derived galactoglucomannans and the galactomannans from guar gum have been compared for their sorption to pulp and paper products and the improvement in tensile strength that they can provide [58, 73].

Polymers containing backbones of 1-4 linked  $\beta$ -D-mannopyranosyl units (mannans) have a tendency to line up parallel to 1-4 linked  $\beta$ -D-glucopyranosyl chains in cellulose polymers and form a great number of hydrogen bonds. This sorption is very strong, and if the mannan is free of branches, that is no acetyl groups or galactose side chains, it can result in complete crystallisation [50]. Using this sorption tendency, applications for *O*-acetylated (galacto)glucomannans have been suggested involving their modification and sorption to cellulose fibres for abrasion-resistant clothing and functionalised medical bandages [17].

### **1.2.5.6 Emulsifiers, Thickeners, and Stabilizers**

Polysaccharides such as guar gum and gum arabic are already used as thickeners, emulsifiers, and stabilisers in the food and beverage industry and softwood hemicelluloses have been investigated for these applications [17, 74, 75]. Although softwood hemicelluloses have shown some potential in this area [74], they would have to compete commercially with well-established products that likely have the advantage of more economical production.

### **1.2.5.7 Hydrogels and Thin Films.**

Softwood hemicelluloses like many polysaccharides can be used to create thin films and hydrogels [17, 76, 77]. Thin films have applications such as edible oxygen barriers on foods and pharmaceuticals [78]. Hydrogels are basically polymer materials that can absorb large amounts of water and form gels. These gels also have applications in slow release drug delivery, and tissue engineering [79, 80]. Hemicelluloses in any of these potential applications are likely to be used as a blend along with other polymers (natural or synthetic) to adjust the properties of the final products [81, 82].

### **1.2.5.8 Bioactivity**

Hemicellulose-derived polymers and oligomers can induce changes in living cells exposed to them. 4-*O*-Methylglucuronoxylans with an estimated DP of 200 extracted from Spanish chestnut (*Castanea sativa*) have been shown to inhibit the proliferation, migration and invasion of certain aggressive cancerous tumors in human cell cultures [83]. Influencing plant growth regulation have also been suggested as possible applications for some hemicellulose-derived products such as de-acetylated galactoglucomannan oligosaccharides [17].

### **1.2.5.9 Flocculating Agents**

Hemicelluloses such as mannans can have the ability to bind onto many different types of particle and act as flocculating agents. This property leads to potential applications in water cleaning and mineral extraction processes [50].

### **1.2.5.10 Niche Biotechnology and Nanotechnology Applications**

Arabinogalactan hemicelluloses have been used to aid the formation of metal nanoparticles [84]. Micelles can be assembled using derivatised xylans [85].

## **1.2.6 Extraction of Hemicelluloses from Wood**

Hemicelluloses occurring within wood are entangled with, hydrogen bonded and covalently linked to the other components of the wood, thus in order to extract large amounts of hemicelluloses from wood, breaking some of these bonds is required. The intermolecular hydrogen bonding between hemicelluloses and other carbohydrates such as cellulose may need to be broken and the covalent bonds (often ester or ether) between hemicelluloses and lignin or those between lignin units may also need to be broken allowing release of hemicelluloses. The covalent linkages within the hemicellulose polymer itself can be broken by hydrolysis, which releases the hemicelluloses as shorter partially de-polymerised carbohydrates. In most extraction methods heat and/or catalysts are required to facilitate the breaking of these bonds. In some situations, advantage may be taken of differences in solubility between hemicelluloses, lignins and cellulose components in order to extract one type of component from the others [3, 6, 86].

### **1.2.6.1 Hot Water Hydrolysis**

Treatment with hot water is a convenient process for extracting hemicelluloses. A wide range of processing conditions have been used and this has resulted in many different terms being used to describe this process. However, the principal reaction taking place in all the variations of the process is the partial hydrolysis of the hemicelluloses allowing the degraded fragments to be dissolved, or colloiddally suspended, in the hot water. The hydrolysis reaction is an acid catalysed reaction, but in many instances no additional catalyst needs to be added to the process water because the acidity is sufficient to initiate the hydrolysis. In such cases the process is often called autohydrolysis. The source of the catalytic acid is probably a combination of the increased dissociation (ionic product) of water at higher temperatures [68] along with the acidic groups found on the pectins, hemicelluloses and sometimes the extractives [3].

Thermo-mechanical pulping (TMP) represents one of the more mild hot water hydrolysis processing conditions. The mildly acidic conditions present during processing solubilises and hydrolyses the hemicelluloses to some extent, although the extracted polymers are relatively large (20-60kDa for spruce AcGGM) [15] due to limited hydrolysis under mild conditions.

The hot water prehydrolysis used to extract polysaccharides for this thesis was carried out under moderate conditions. The chips and water were heated from ambient to 175°C over 90 minutes, reaching a maximum pressure of  $\approx 7 \times 10^2$  kPa. Similar prehydrolysis/autohydrolysis conditions have been used to extract hemicelluloses from southern pine [87] and spruce [88].

Steam explosion [28, 62] and microwave initiated hydrolysis [34, 89, 90] are other procedures that have been used to extract hemicelluloses from wood using hot water. Generally steam explosion tends to be a more severe hydrolysis, thus resulting in the extraction of smaller polymeric carbohydrates, more sugar monomers, but also an increase in losses due to sugar degradation [87].

Supercritical water represents an extreme form of hot water hydrolysis at temperatures above 374°C and pressures above  $22.1 \times 10^3$  kPa. Under these conditions even cellulose is quickly hydrolysed into oligomers, monomers and large quantities of sugar degradation products [68].

#### **1.2.6.2 Catalysed Hydrolysis**

Higher amounts of hemicelluloses may be removed from the wood if the hydrolysis reaction is catalysed by the addition of acids, bases, or enzymes. The type of catalyst used influences the size and composition of the carbohydrates extracted. The applications of catalyzed hydrolysis are best suited to situations where the primary aim of the treatment is to obtain large amounts of monosaccharides for fermentation into products such as ethanol [59, 65-67, 86, 91]. Sulfuric acid and sulfur dioxide gas are acidic catalysts commonly used for this purpose. For example, treatment of *P. radiata* wood chips with sulfur dioxide followed by steam explosion converts most of the hemicelluloses and some of the cellulose into monosaccharides or disaccharides that are easily separated from remaining insoluble wood components [28].

Addition of acid catalysts aids hydrolysis of most glycosidic linkages but at different rates [92], whereas basic catalysts tend to catalyse the removal of acetyl groups from hemicelluloses [26]. Generally, basic conditions produce a higher proportion of polymeric material in the hydrolysate in comparison with acidic conditions [59]. Enzymes hydrolyse only the linkages between specific monomers depending on the type of enzyme used [91, 93, 94]. The specific action of enzymes offers scope to control the amount, type, structure and molecular size of hemicelluloses extracted from wood.

### **1.2.6.3 Other Extraction Methods**

Traditionally, hemicelluloses used for research purposes were often extracted after conversion of the wood to holocellulose which is a term used to describe wood after the removal of the extractives and lignin components. Holocellulose is prepared by using delignification reagents such as sodium chlorite to degrade the lignin allowing it to be washed easily out of the wood matrix [35, 83, 95].

On an industrial scale the pulp and paper industry uses many different processes to remove considerable amounts of lignin and hemicelluloses from wood with the aim of producing cellulose-rich fibres. Kraft processes use strong alkali that causes peeling reactions that degrade many types of polysaccharide. However, some xylans are solubilised in a polymeric form in the kraft processes [3]. Organosol processes, *i.e.* treatment of the wood with organic solvents such as organic acids or alcohols, can also be used to remove hemicelluloses and lignin from lignocellulosic biomass [96, 97].

## **1.2.7 Recovery and Purification of Hemicelluloses**

In most cases, aqueous extraction of wood produces an extraction liquor, often called a hydrolysate, or a prehydrolysate if the treatment is followed by a pulping operation. This hydrolysate is a complex mixture comprising water and hemicelluloses together with a range of contaminants that could include lignin, extractives, sugar degradation products, proteins, salts, monosaccharides, organic acids, alcohols and degraded cellulose polymers as contaminants. Thus recovering the hemicelluloses in a pure form from such a complex mixture may be a difficult assignment. At both analytical and industrial scale, various techniques for separating either the contaminants, or the polysaccharides, from the complex mixture are required.

### **1.2.7.1 Precipitation**

Precipitation techniques are useful for separating carbohydrates into different fractions based on molecular weight and structural features. The technique takes advantage of the differences in solubility of carbohydrates based on their size and structure in order to isolate and concentrate target carbohydrates from a solution. For example, a series of precipitations from solutions comprising combinations of acetone, methanol, acetic acid, water, and barium hydroxide was used to fractionate the carbohydrates from a prehydrolysate of southern pine chips [87]. Ethanol can also be used to precipitate and purify polymeric hemicelluloses [17].

### **1.2.7.2 Microfiltration, Ultrafiltration and Dialysis**

Microfiltration, ultrafiltration and dialysis are ideal techniques for separating and concentrating the polysaccharides based on their molecular size and would probably be the preferred methods on a commercial scale. A combination of techniques, including filtration and ultrafiltration allowed *O*-acetylated galactoglucomannans to be isolated from thermo-mechanical process waters at the kilogram scale [17].

### **1.2.7.3 Ion Exchange**

As most prehydrolysates contain both charged and neutral components, ion exchange resins may be used for separating the components on a charge basis. For example, ion exchange resins were used to deionise a prehydrolysate prior to characterisation of the polysaccharides [87] and acidic polysaccharides can be also be removed by anion exchange chromatography [17]. Treatment with different types of ion exchange resins can also be effective at removing many of the contaminants in a prehydrolysate, including phenolics, furfural, and organic acids [66].

### **1.2.7.4 Adsorption Treatments**

Activated carbons, charcoal, and other solid phase extraction techniques can be used to remove some non-carbohydrate contaminants such as furfural and lignin fragments from wood hydrolysates [87, 98, 99].

### **1.2.7.5 Chemical Cleaning**

Isolated hemicellulose fractions may still require further purification before they can be a useful product. Bleaching with peroxide is one way of accomplishing this as the peroxide reacts with lignin-derived contaminants and changes the chemical structures responsible for colour resulting in a hemicellulose preparation with higher brightness. [100]. The lignin-derived contaminants are likely to still be physically present in the hemicelluloses but their colour contribution is removed.

Solvents such as methyl ethyl ketone, chloroform, supercritical CO<sub>2</sub> and ethyl acetate have all been used to remove contaminants such as lignin fragments and furfural from lignocellulosic hydrolysates [66, 87, 101, 102].

### **1.2.7.6 Concentration techniques**

Large quantities of water are often required to extract hemicelluloses efficiently from wood chips during a wood hydrolysis operation and this results in the hemicelluloses being at low concentration in the wood hydrolysate. Spray drying, lyophilisation, and evaporation can all be used to reduce the amount of water in the hydrolysate and concentrate the polysaccharides [17, 87].

## **1.2.8 Methods for Fractionating and Characterising Polysaccharides**

### **1.2.8.1 Size Exclusion Chromatography (SEC)**

Size exclusion chromatography (SEC) or gel permeation chromatography (GPC) can be used to fractionate carbohydrates based mainly on their hydrodynamic volume. Hydrodynamic volume is usually based on the size and molecular weight of the carbohydrate molecules. The term “apparent molar mass” has been used to describe estimates of polysaccharide molecular weight using calibration with standards of similar polymers [17]. SEC columns operated using eluents with very low ionic strength (usually de-ionised water), often results in anionic polysaccharides being excluded from the column and therefore separated from the neutral polysaccharides due to an “ion exclusion effect” [34, 103]. Fractionating polysaccharides using SEC is often carried out prior to characterisation of the fractions by other techniques such as mass-spectrometry, linkage analysis, sugar compositional analysis and NMR [25, 32, 34-36, 43].

### **1.2.8.2 Ion Chromatography**

Ion chromatography using pulsed amperometric detection has been used to quantify both the neutral sugar monomers and uronic acids from hydrolysed hemicelluloses [27, 89]. Ion exchange chromatography has also been employed to separate acidic (anionic) polysaccharides and neutral polysaccharides [43, 104].

### **1.2.8.3 Matrix Assisted Laser Desorption Ionisation – Time of Flight-Mass Spectrometry (MALDI-ToF-MS)**

MALDI-ToF-MS has been used extensively in determining the size and structure of many oligosaccharides and polysaccharides extracted from plants [25, 34-36, 43, 105-107]. For example, this technique has been used to determine the distribution of uronic acid groups and pentose units in arabino-4-*O*-methylglucuronoxylans extracted from spruce wood [25, 26], to study the degree of acetylation on spruce-derived AcGGM, and to characterise the acetylated hemicelluloses in hardwoods [26, 35, 36, 106]. 2,5-Dihydroxybenzoic acid (DHB) and 2,4,6-trihydroxyacetophenone (THAP) have been established as being suitable matrix compounds to aid the ionisation of neutral polysaccharides from a variety of plant sources as Na<sup>+</sup> and K<sup>+</sup> adducts [108, 109].

When attempting to analyse the average molecular weight of neutral polymers, MALDI-ToF-MS will often have a bias toward lower molecular weight polymers [110]. The other main limitation is that the mass spectrum does not allow different structural components with the same molecular weight to be distinguished. Therefore MALDI-ToF-MS will provide evidence of hexose-based polymers or pentose-based polymers, but will not indicate if the pentoses are D-xylosyl units or L-arabinosyl units or a mix of both [26].

#### **1.2.8.4 Electrospray Ionisation Mass spectrometry**

Electrospray Ionisation Mass Spectrometry has been applied to polysaccharides to determine molecular masses, degree of acetylation and to distinguish hexose-based polymers from the pentose-based polymers [32]. Generally, the techniques will provide similar kinds of information to MALDI-ToF-MS methods.

Tandem mass spectrometry and electrospray ionisation after derivatisation with ferrocene boronic acid can allow detailed structural characterisation of low molecular weight carbohydrates such as monosaccharides and disaccharides through analysing their fragmentation patterns under collisionally induced dissociation [111].

#### **1.2.8.5 Nuclear Magnetic Resonance (NMR) Spectroscopy**

One-dimensional proton and  $^{13}\text{C}$  NMR analysis along with two-dimensional techniques such as NOESY, COSY, DEPT, HSQC, HMBC, and TOCSY have been used to provide detailed information about the structural features of hemicelluloses [21-23, 89].

Proton NMR is very effective at detecting  $\text{CH}_3$  groups attached to polysaccharides such as the methyl groups on 4-*O*-methylglucuronoxylans [35, 90], and the acetyl groups on AcGGM [21, 22, 89]. NMR is an important tool for determination of  $\alpha$  or  $\beta$  anomeric linkages between hexose and pentose units [21, 22].

Signals tend to broaden and lose intensity when larger polysaccharides are analysed using NMR. To minimise this problem polysaccharides can be reduced in size using partial hydrolysis and/or the spectra can be acquired at an elevated temperature [21].

#### **1.2.8.6 Degradation and Hydrolysis Techniques.**

Acid catalysts are used to hydrolyse polysaccharides into oligosaccharides and monosaccharides. Often the goal is to carry out a complete hydrolysis of the polymer, releasing all its components as monomer units so these can be analysed by other techniques. A number of different acids may be used including sulfuric, hydrochloric, acetic, and trifluoroacetic acid (TFA). The choice of acid catalyst and the concentration used is influenced by how resistant the target polysaccharide is to hydrolysis and the steps required to remove the acid after the hydrolysis process. Volatile organic acids such as trifluoroacetic acid are often preferred over mineral acids because they may be easily removed by evaporation whereas mineral acids require neutralisation and/or extensive washing steps. In acid catalysed hydrolysis targeting complete hydrolysis of the polymer there is a need to find a balance in reaction conditions in order to minimise the formation of undesirable products. This balance is to be found between a too severe hydrolysis that will degrade the released monosaccharides (especially uronic and aldonic acids which may de-carboxylate in severe conditions), and a too mild hydrolysis that will leave a high proportion of resistant linkages unhydrolysed. Generally, increasing the acid concentration, reaction temperature, and/or reaction time will lead to a more severe hydrolysis [92]. A partial hydrolysis can be applied in order to generate smaller oligomers for a further analysis and gain detailed information on the structure of the original polysaccharide [23].

Alkaline degradation may also be used for structural elucidation of polysaccharides. The degradation products are often oligomers and metasaccharinic acid residues and can be analysed with techniques such as NMR [112].

Enzyme catalysis can be used to selectively hydrolyse certain linkages in the hemicelluloses. The released oligomers may be purified and analysed allowing the original structure to be deduced in greater detail [45, 113, 114].

#### **1.2.8.7 Alditol Acetates and Gas Chromatography**

Reduction and acetylation of monosaccharides to form alditol acetates allows for their qualitative and quantitative analysis using gas chromatography with flame ionisation or mass spectrometry detection [39, 97, 115].

#### **1.2.8.8 Partially Methylated Alditol Acetates (PMAAs)**

Linkage analysis can allow the points of attachment and ring form of each sugar monomer present in a sample of oligomers or polymers to be deduced. The formation of partially methylated alditol acetates (PMAAs) from a polysaccharide usually involves the following steps; (i) reduction of the reducing end of the polysaccharide to an alditol, (ii) methylation of the hydroxyl groups, (iii) complete hydrolysis of the partially methylated polymer, (iv) reduction (deuterium labelling) of the partially methylated monosaccharides to alditols, and finally (v) acetylation of the new hydroxyl groups (*i.e.* those that were involved in linkages between monosaccharide units, or within the monosaccharide unit such as part of pyranose and furanose ring structures). The resulting PMAAs may then be separated by gas chromatography and identified using mass spectrometry[115].

Linkage analysis using PMAAs has been carried out on a number of softwood derived hemicelluloses [19, 22, 23, 30-32] to establish many of the linkages described earlier (pages 7, 8, 9, 10).

#### **1.2.8.9 Other Derivatisation Techniques and Applications**

Methanolysis involves the reaction of the polysaccharide with methanol and hydrogen chloride under anhydrous conditions. Methanolysis is a particularly useful technique for structural elucidation of polysaccharides such as hemicelluloses and pectins because the analysis of neutral and acidic fragments can be performed in a single step. The acid hydrolysis releases both neutral and acidic monosaccharide fragments from the polymer and the neutral monosaccharides and uronic acids are then converted into their corresponding methyl glycosides and methyl esters, respectively, which may be analysed by gas chromatography [27, 88] or HPLC [92].

Silylation is often required to make monosaccharides and oligosaccharides sufficiently volatile to allow analysis by gas chromatography. Methyl glycosides produced by methanolysis often require silylation prior to gas chromatography [27].

#### **1.2.8.10 Solvent/Reagent Precipitation Techniques**

Fractional precipitation using combinations of solvents such as ethanol, methanol and acetone, sometimes together with reagents such as barium hydroxide, enables polysaccharides to be fractionated based on differences in solubility [87]. These precipitation techniques have been used to separate galactans from galactoglucomannans in extracts of *P. radiata* compression wood [19].

#### **1.2.8.11 Light Scattering**

Light scattering detection has been used for determining the molecular weight of polysaccharides, often used coupled to an SEC chromatography system. For example, the average molar mass of Norway spruce AcGGMs isolated from thermomechanical pulping water was estimated to be 21.5 kDa using multiangle laser light scattering [116].

#### **1.2.8.12 Measuring Uronic Acid Content**

Uronic acid content of lignocellulosic materials may be determined by several different techniques, including combinations of methods such as acid methanolysis, anion exchange chromatography, gas chromatography, capillary electrophoresis and ion chromatography using pulsed amperometric detection [27]. It may also be determined with methods that use various reagents such as 3-phenylphenol [117] and *m*-hydroxydiphenyl with detection involving colorimetric assays [118]. The uronic acid content can also be estimated using NMR [101].

## Chapter 2 Experimental

### 2.1 Prehydrolysis and Isolation of Polymeric Carbohydrates

#### 2.1.1 Aims

This mild prehydrolysis method was chosen because the low severity of the conditions would maximise polymeric carbohydrates at the expense of monosaccharides sugars. Lower severity conditions were also chosen with the aim of minimising any negative impacts on the kraft pulp [55, 59].

The isolation and clean-up method was aimed at efficiently separating and concentrating gram-scale amounts of the polymeric carbohydrates present in this prehydrolysate. Ideally the isolation method should remove the non-carbohydrate contaminants and monosaccharides and produce a high-yield representative sample of the polymeric carbohydrates in the prehydrolysate.

#### 2.1.2 Methodology

Commercial *Pinus radiata* wood chips were treated with water using a 90 minute ramp to 175°C in the prehydrolysis stage of a prehydrolysis-kraft cook as detailed in Lloyd *et. al.*[59]. Woodchips (1168 g, from top logs and thinning of younger radiata pine, 42.8% dry matter content) were placed in a stainless steel digester with liquor recirculation capability (M/K, 6 L) and tap water added (1830 mL) giving a ratio of 5 : 1 (liquor : wood). When the temperature in the digester reached 175°C, the free prehydrolysis liquor (approximately 1600 mL) was collected by draining through a condenser.

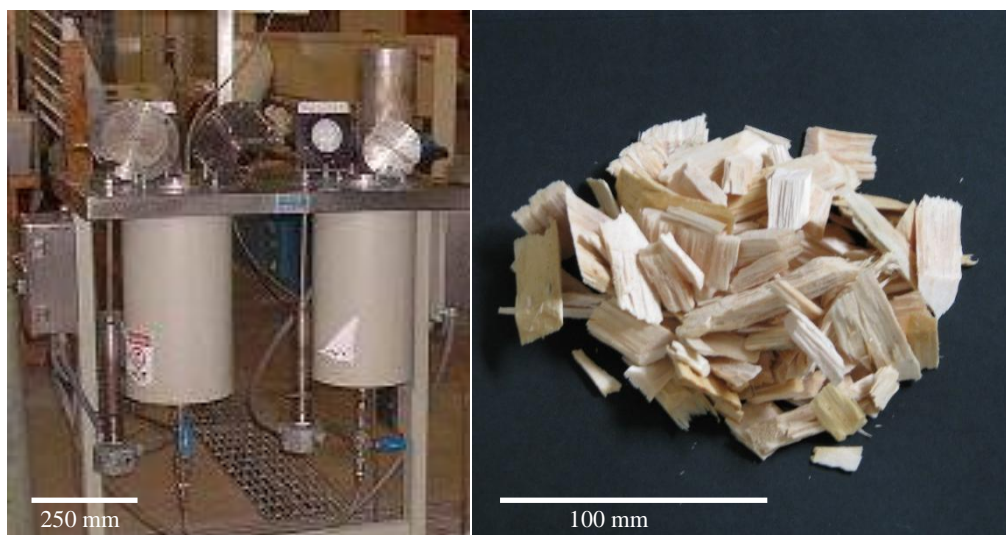


**Figure 4: M/K 6 L digesters (left) and *P. radiata* woodchips (right).**

The hemicelluloses in this prehydrolysate were isolated using an extensively modified version of the method used by Sears *et. al.* to fractionate prehydrolysates from Southern pine [87]. Free prehydrolysis liquor (860 mL) was mixed with activated charcoal powder (7.4 g BDH Chemicals, UK) and concentrated to 200 mL by rotary evaporation at 60°C. The concentrate was centrifuged at 2000 rpm for 20 minutes and the supernatant filtered through a 0.45 µm Nylon membrane (Millipore, USA). The filtrate was further concentrated to 50 mL and then added dropwise with stirring into acetone/methanol (9:1, 650 mL).

The precipitate containing oligosaccharides and polysaccharides was separated by centrifugation (2000 rpm for 20 min) and the supernatant containing monosaccharides and other contaminants was discarded. The precipitate was re-suspended and washed in acetone/methanol (9:1, 450 mL) before a final separation by centrifugation and discarding of the supernatant. This precipitate of crude polymeric carbohydrates was re-dissolved in distilled water, lyophilised and weighed (yield of 2% based on the oven dry weight of original woodchips).

## **2.2 Fractionation by Size Exclusion Chromatography**

### **2.2.1 Aims**

The use of high pressure size-exclusion chromatography (SEC) was aimed at fractionating the polymeric carbohydrates based on their charge and molecular weight [26, 103]. Fractions were collected for the purpose of further analysis by a wide range of different methods. The SEC method was calibrated using standards with the aim of estimating the apparent molecular weights [17] of the uncharged polymeric carbohydrates isolated from the prehydrolysate.

### **2.2.2 Methodology**

Size-exclusion chromatography was carried out with three Shodex columns (KS-805, KS-804 and KS-803) linked in series at 50°C and preceded by a KS-G guard column (Showa Denko, Japan). This combination of three columns was suited to the size range of the neutral components in the crude sample and gave sufficient separation of acidic and neutral components at the large loading volume. Injection was made with a 50 µL loop (Rheodyne, USA) and detection was by refractive index (Waters Assoc., USA). The eluent was de-ionised distilled water at a flow rate of 1.0 mL/min. The signal from the RI detector was recorded and processed by Empower Pro software (Waters Assoc., USA).

Molecular weight calibration of this system was achieved using, sucrose (BDH Chemicals Ltd., UK), glucose (Aldrich, USA), and a set of fractionated dextran standards (1200 Da, 4,440 Da, 9,890 Da, 43,500 Da, and 70,000 Da, Pharmacia Biotech, Sweden). Each molecular weight standard was mixed with a small amount of 2,000,000 Da dextran, dissolved in de-ionised water, and injected into the SEC system. The 2,000,000 Da dextran was used to check consistence of the retention time ( $18.53 \pm 0.06$  min) from a complete excluded polysaccharide. Refractive index (RI) chromatograms were recorded and the retention times of these standards were used to construct an apparent molecular weight calibration plot. The term ‘apparent molecular weight’ is used with reference to standards like dextrans, because in reality the hydrodynamic behaviour of hemicelluloses during SEC could be different thus adding additional uncertainty [29].

Approximately 1.2 mg of the crude polymeric hemicelluloses was dissolved in de-ionised water and injected into the SEC system on each run. Seven 3.0 mL fractions (A1, A2, A3, N1, N2, N3, and W1) were collected at three minute intervals from the outlet of the RI detector, covering the entire chromatogram as shown in Figure 6. The equivalent fractions from fourteen independent runs were pooled, lyophilised, and weighed. A small sub-sample of each fraction was separated and used for MALDI-ToF analysis, the remainder was used for NMR analysis. A second set of equivalent fractions from another 24 independent runs were later collected under the same conditions, pooled as two batches and lyophilised. One batch of this second set was used for determination of monomer composition and the other batch was used for further MALDI-ToF analysis with most of the N1 fraction used for methylation linkage analysis.

Another fourteen independent runs were used to collect two composite fractions, an acidic fraction (A1, A2, and A3 combined) and a neutral fraction (N1, N2, and N3 combined). These were used in methylation linkage analysis.

Nine smaller fractions of the neutral polysaccharides (three for each of N1, N2, and N3) were collected in one minute intervals from the SEC system on a single run. Each fraction was re-injected independently and RI chromatograms were recorded. Retention times from the peaks for each of the nine fractions were measured. The SEC calibration formula (Figure 5) was used to estimate apparent molecular weights from the nine fraction's retention times. These MW estimates were graphed against the retention time of peak tops for each fraction (Figure 11, page 49).

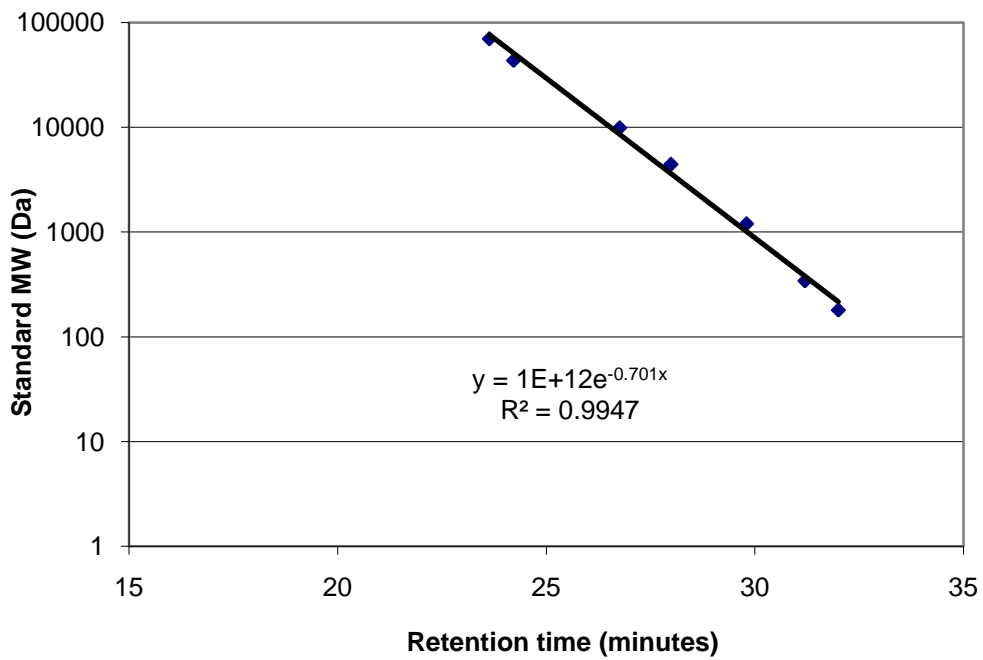


**Figure 5: Size-exclusion chromatography calibration curve.**  
 Constructed using standards of various sized dextrans, sucrose, and glucose.

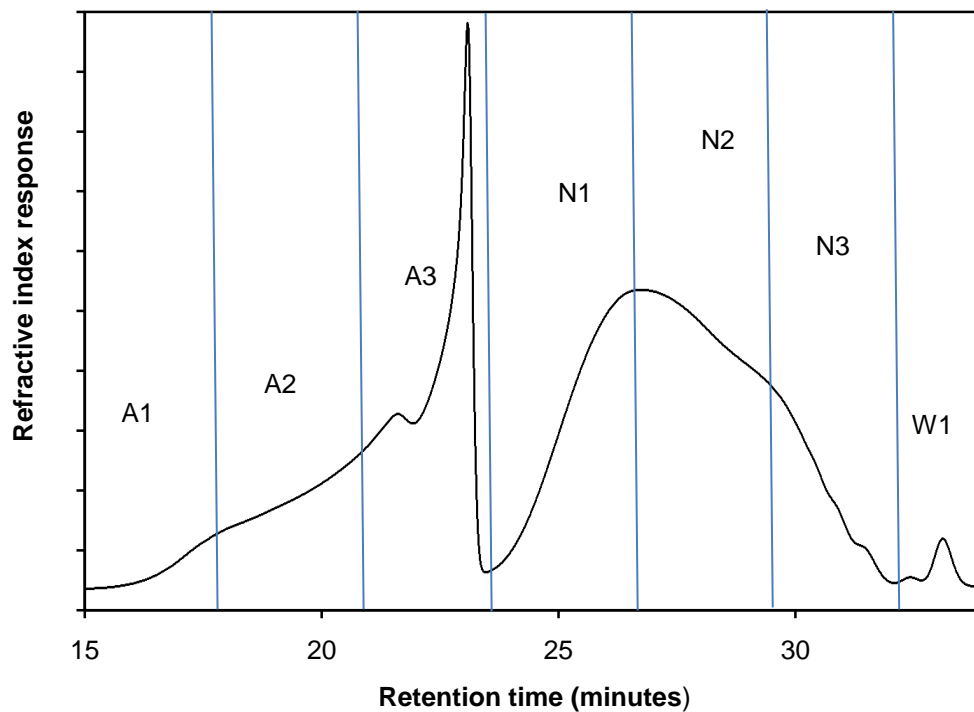


**Figure 6: Chromatogram of SEC fractionation of hemicelluloses polymers.**

## **2.3 Matrix Assisted Laser Desorption Ionisation – Time of Flight-Mass Spectrometry (MALDI-ToF-MS) Analysis**

### **2.3.1 Aims**

These methods were aimed at analysing the molecular weights of the polymeric carbohydrates in each fraction. MALDI-ToF mass spectrometry was also utilised to provide information about which monomer units are present in the isolated polymers. Pentose or hexose based polymers can be distinguished along with the distribution and types of other groups attached to the backbone. This is revealed by patterns in the various masses detected [25, 26, 35, 36].

### **2.3.2 Methodology**

#### **2.3.2.1 Equipment and Calibration**

Matrix-assisted laser desorption ionisation-time of flight (MALDI-ToF) mass spectra were acquired with an Autoflex II LIFT-ToF/ToF mass spectrometer using FlexControl and FlexAnalysis software. (Bruker Daltonics, Germany).

Calibration was carried out using peptide and protein calibration standards (Bruker Daltonics, Germany) co-crystallised with S-DHB (2,5-dihydroxybenzoic acid/ 2-hydroxy-5-methoxybenzoic acid) and spotted adjacent to each sample on the MALDI plate.

### **2.3.2.2 Trials for Choice of Matrix and Conditions**

4-HCCA ( $\alpha$ -cyano-4-hydroxycinnamic acid), S-DHB, 4-aminophenol, and THAP were trialled as matrix compounds in both positive and negative ion modes. Trials were also made by varying polysaccharide dilution, plate type, matrix solvents, ion suppression/gating conditions, laser power and pulse rate, and addition of NaCl. These variations were trialled using mainly S-DHB as a matrix due to it being well established in the literature for use on polysaccharides [25, 26, 35, 110]. Both linear and reflectron modes on the time of flight detector were trialled on each sample that was analysed. These trials were guided and adapted from methods in the literature [25, 26, 35, 109, 119] and were used in the development of the following methods used to analyse the polymeric carbohydrates isolated from this prehydrolysate. This was not intended to be a complete and thorough systematic study of polysaccharide ionisation and MALDI-ToF-MS response designed to find the optimum conditions, but rather a series of checks of which available combination of conditions and matrix appeared to provide adequate mass spectra, and which did not.

### **2.3.2.3 General Conditions and Sample Preparation**

Small sub-samples from each of the seven SEC fractions were dissolved in de-ionised water to give solutions of concentrations less than 0.5 mg/mL. Equal volumes (1.00  $\mu$ L) of the sample and saturated matrix solution (S-DHB or THAP) were then mixed together and spotted onto the surface of a MALDI-ToF plate and allowed to co-crystallise with evaporation of the solvent. Mass spectra were obtained using pulsed ion extraction at 130 ns unless stated otherwise. Each mass spectrum represents the sum of 300 laser shots obtained from 10 different crystalline locations on the sample spot.

#### **2.3.2.4 Analysis of Anionic (Acidic) Polysaccharides**

Saturated Super-DHB (2,5-dihydroxybenzoic acid / 2-hydroxy-5-methoxybenzoic acid) dissolved in de-ionised water was found to be effective as a matrix for detecting acidic polysaccharides in negative ion mode. Negative ions were likely to be de-protonated uronic acid groups attached to the polysaccharides [25]. Laser power at 45% of maximum was usually used because ionisation often became inadequate when laser power was drastically increased or decreased. In cases in which linear mode did not detect many ions with  $m/z$  values larger than 5000, reflectron mode was used to increase resolution.

#### **2.3.2.5 Analysis of Neutral Polysaccharides**

Saturated THAP (2,4,6-trihydroxyacetophenone) dissolved in acetonitrile: de-ionised water (3: 1) was used as a matrix to ionise neutral polysaccharides. Laser power at 95% of maximum was usually used, although adequate spectra could be obtained at most laser powers above 50%. Neutral hemicelluloses were detected in positive ion mode and had  $m/z$  values consistent with mainly  $\text{Na}^+$  adducts. Another series of ions was often observed that had  $m/z$  values consistent with  $\text{K}^+$  adducts.

#### **2.3.2.6 Alkaline De-acetylation of Neutral Polysaccharides**

Alkaline de-acetylation, similar to that described by Jacobs *et. al.* [34], was carried out on sub-samples of fractions N1, N2, and N3. A small amount of each lyophilised fraction was dissolved in de-ionised water (200  $\mu\text{L}$ ) and an aliquot (50  $\mu\text{L}$ ) from each solution transferred to a separate vial.  $\text{NH}_4\text{OH}$  solution (10  $\mu\text{L}$ ,  $\approx 2 \text{ mol L}^{-1}$ ) was added to each vial before they were covered and heated in an oven (90°C, 16 min). Vials were cooled in ice before small aliquots (0.5  $\mu\text{L}$ ) were removed, mixed with saturated THAP solution (0.5  $\mu\text{L}$ ) and spotted onto a MALDI-ToF plate and allowed to co-crystallise.

Small aliquots (0.5  $\mu\text{L}$ ) from the original 200  $\mu\text{L}$  solutions of each fraction were also mixed with saturated THAP solution (0.5  $\mu\text{L}$ ) and spotted onto a MALDI-ToF plate and allowed to co-crystallise as pre-de-acetylation controls. Mass spectra were obtained from the control and de-acetylated samples for each fraction using pulsed ion extraction at 400 ns. Each mass spectrum represents the sum of 300 laser shots obtained from 10 different locations on the sample spot and was obtained in linear mode.

### **2.3.2.7 Polytool Calculations**

Peaks were picked manually for the distinct higher abundance ions in the mass spectra of anionic polysaccharides and de-acetylated neutral polysaccharides. These mass list and peak area data were further analysed using Bruker Polytools 1.08g software.

## 2.4 Nuclear Magnetic Resonance Spectrometry (NMR) Analysis

### 2.4.1 Aims

NMR was used with the aim of identifying and quantifying the *O*-acetyl groups. It also provided evidence for the presence of *O*-methyl groups in some fractions. Another aim of NMR was to provide supporting evidence for the presence of various structural features and linkages through comparison with hemicelluloses analysed in the literature [21, 35, 36] and results obtained from other methods used in this study.

### 2.4.2 Methodology

Samples of the seven SEC fractions (0.2 mg - 5.0 mg) were dissolved in 1.0 mL of D<sub>2</sub>O (99.9 atom %D, Aldrich, USA), lyophilised, and re-dissolved in approximately 0.5 mL of D<sub>2</sub>O. Spectra were obtained using either a Bruker 300MHz or 400MHz spectrometer and processed using Bruker Topspin software. Early spectra were acquired with a probe temperature of 27°C. However, a probe temperature of 70°C gave sharper signals and was used for subsequent NMR acquisition.

Standards of acetic acid, *t*-butanol, and acetone were run in D<sub>2</sub>O at 27°C and 70°C and their chemical shifts were used for initial referencing. However, the sharp ≈1.9 ppm peak present to some extent in all fractions was often used as a reference point for calibrating the proton spectra for comparison. This 1.9 ppm peak is assigned as acetate in a number of literature <sup>1</sup>H NMR spectra of wood hemicelluloses [35, 36, 90], and using it as a reference point assisted with assigning and comparing various peaks with those in the literature.

Basic one-dimensional <sup>1</sup>H spectra were acquired on all seven fractions.

Basic one-dimensional <sup>13</sup>C experiments such as DEPT135 were attempted on some fractions. However these spectra often took over 12 hours to collect and tended to provide adequate results only in a few high-yield fractions such as N1.

## **2.5 Acid Hydrolysis and Monomer Composition Analysis**

### **2.5.1 Aims**

With the aim of finding out the proportions of different monomer components that constitute the crude polysaccharides and each SEC fraction, samples were subjected to severe acid hydrolysis before the acidic and neutral components were separated for quantification by different methods.

### **2.5.2 Methodology**

#### **2.5.2.1 Severe Acid Hydrolysis**

Three samples of the crude polysaccharides and samples of the six fractions from SEC (A1, A2, A3, N1, N2 and N3) were each dissolved in de-ionised water (400  $\mu$ L) and TFA (400  $\mu$ L, 99%, Acros) was added. The solution was recapped under N<sub>2</sub> in a vial and placed in a heating block (120°C, 120 min). The hydrolysed samples were evaporated to dryness under a stream of N<sub>2</sub> at 40°C, re-dissolved in de-ionised water (2.00 mL), evaporated to dryness under a stream of N<sub>2</sub> at 40°C for a second time, and re-dissolved in de-ionised water (2.00 mL).

#### **2.5.2.2 Separation of Acidic and Neutral Components**

Liquid chromatography was carried out with a packed column ( $\approx 25 \times 1000$  mm) of Bio-Gel<sup>®</sup> (P-2 Gel, Bio-Rad Laboratories, USA) kept at approximately 20°C. The eluent was de-ionized distilled water at a flow rate of 0.5 mL/min. Injection was made with a 2.000 mL loop (Rheodyne, USA) and detection was by refractive index (Shodex, Japan). The signal from the RI detector was recorded and processed by Empower Pro software (Waters Assoc., USA). Fractions were collected using an automated fraction collector (Waters Assoc., USA).

Each of the TFA hydrolysis solutions (2.00 mL) of the samples were injected into the above chromatography setup. A clear separation was obtained between the acidic components (likely to be uronic acids, aldobiouronic acids [24], acetic acid, and residual TFA) and the neutral components (mainly monosaccharides). This separation was likely to be due to an ion exclusion effect [103], and was confirmed by the injection of standards (glucuronic acid, lactose, and glucose).

Two fractions (acidic components and neutral components) were collected from each hydrolysed sample injected onto the Bio-Gel column. The acidic component fractions were lyophilised, re-dissolved in de-ionised water (3.000 mL) and analysed using ion chromatography (Page 40). The neutral component fractions were lyophilised, converted to alditol acetates, and analysed by GC-MS.

In addition, four narrower acidic fractions were collected from the Bio-Gel system from a single injection of hydrolysed crude sample. Although there was little apparent separation of different acidic components in the chromatogram, when samples of these four narrower fractions were analysed by ion chromatography and NMR they showed differing relative enrichment and depletion of various components.

### **2.5.2.3 Analysis of Neutral Components by Conversion to Alditol Acetates and Gas Chromatography**

The lyophilised samples (neutral components) of each of the six SEC fractions (0.2 mg - 5.0 mg) were dissolved in de-ionised water (250  $\mu$ L). Aqueous NaBH<sub>4</sub> solution (6 mg in 250  $\mu$ L) was stirred into to each sample and they were left to stand (room temperature, 120 minutes). Washed IRC-50 resin (Amberlite) was added until the sample stopped effervescing. The resin was then removed by filtration (glass filter paper GC-50, Advantec<sup>®</sup>) under vacuum.

The reduced samples were evaporated to dryness under a stream of N<sub>2</sub> at 40°C. Methanol (1.0 mL) was added to each sample and then evaporated to dryness under a stream of N<sub>2</sub> at 40°C; this was repeated an additional 5 times. The dry samples were each re-dissolved in pyridine (2.00 mL). Acetic anhydride (2.00 mL) was added and the samples capped, stirred, and left to stand at room temperature. After approximately 15 hours standing, de-ionised water (5.00 mL) was mixed into each sample.

The aqueous phase was extracted with chloroform ( $3 \times 1.00$  mL). The combined chloroform extracts for each sample were placed in freezer ( $-20^{\circ}\text{C}$ ) until any aqueous residue had frozen. Part of the chloroform phase ( $\approx 1.5$  mL) was then transferred to a GC vial for analysis. In the case of some too concentrated samples, the chloroform phase was later diluted 1/100 with chloroform and the GC-MS analysis repeated.

The above derivatisation method was also applied to standards of D-galactose, D-glucose, D-xylose, D-mannose, and L-arabinose, and some known mixes of these standards. These known mixes of sugar standards were used to estimate relative response factors (Equation 1). These response factors were used to calculate mol% and mole ratios of different monosaccharides from relative peak areas

**Equation 1: Molar and mass response factors between different monosaccharide alditol acetates.**

$$\frac{(\text{Peak area of mannose AA}) \div (\text{Peak area of glucose AA})}{(\text{Mass of mannose}) \div (\text{Mass of glucose})} = 1.0$$

$$\frac{(\text{Peak area of xylose AA}) \div (\text{Peak area of glucose AA})}{(\text{Mass of xylose}) \div (\text{Mass of glucose})} = 1.4$$

$$\frac{(\text{Peak area of mannose AA}) \div (\text{Peak area of glucose AA})}{(\text{Mol amount of mannose}) \div (\text{Mol amount of glucose})} = 1.0$$

$$\frac{(\text{Peak area of xylose AA}) \div (\text{Peak area of glucose AA})}{(\text{Mol amount of xylose}) \div (\text{Mol amount of glucose})} = 1.3$$

Gas chromatography and mass spectrometry was carried out on 7890A GC System with a 7683B Series Injector and a 5975c inert MSD with Triple-Axis Detector (Agilent Technologies).

A 15 m SP-2330 column (Supelco, USA) was operated under the following oven program: hold at  $60^{\circ}\text{C}$  for 0.3 min,  $20^{\circ}\text{C}/\text{min}$  ramp to  $100^{\circ}\text{C}$ ,  $6^{\circ}\text{C}/\text{min}$  ramp to  $230^{\circ}\text{C}$  and then held at  $230^{\circ}\text{C}$  for 20 min.

Injection was carried out in splitless mode at 220°C, helium was used as the carrier gas at 9.4973 psi, and 2.00 µL of sample was injected. The mass spectrometer source temperature was 220°C and the MS Quad temperature was 150°C. MS monitoring was carried out in total ion mode with a solvent delay of 4.50 min.

#### **2.5.2.4 Analysis of Acidic Components by Ion Chromatography and NMR**

Ion Chromatography was carried out on a DIONEX ICS2000 system using a hydroxide cartridge (EGC II KOH). Chromeleon Software (Version 6.80 SP4) was used to operate the system and record chromatograms.

IonPac<sup>®</sup> AS11-HC columns (one Analytical 4×250 mm column, preceded by a Guard 4×50 mm column) were operated at 30.0°C. The detector (DS6 Heated conductivity Cell) was maintained at 35.0°C and the suppressor (Type 6.0) current set to 23 mA. An injection loop (25 µL) was used to deliver samples and standards.

At a constant flow rate (1.5 mL/min) and an isocratic eluent concentration (6mM NaOH in de-ionised water) the ICS2000 system was found to separate standards of acetic acid, TFA, D-galacturonic acid, D-glucuronic acid and some minor peaks associated with neutral sugar standards.

Each of the four narrower Bio-Gel fractions of acidic components (Page 37) was dissolved in D<sub>2</sub>O (1.0 mL, 99.9 atom %D, Aldrich, USA), lyophilised, and re-dissolved in approximately 0.5 mL of D<sub>2</sub>O. One-dimensional proton NMR spectra were acquired with a probe temperature of 27°C using a Bruker 300 MHz spectrometer and processed using Bruker Topspin software. The integrals of the *O*-methyl signal (3.48ppm) were compared to integrals of carbohydrate signals to determine which of the four narrower fractions had the highest relative enrichment in *O*-methyl groups. This relative enrichment information from NMR was compared to relative enrichment information from the different ion chromatograms of the four narrower fractions to determine which ion chromatograph peaks could contain the *O*-methyl groups. A proton NMR spectrum was acquired of the acidic components isolated from the Fraction N2.

A series of D-glucuronic acid standards of different concentration were run on the ICS2000 system and the peak areas recorded. D-Glucuronic acid had a retention time of approximately 4.7 min. Peak area was plotted against D-glucuronic acid concentration (Figure 7) to produce a linear calibration line ( $R^2 = 0.9989$ ). Two standards of D-galacturonic acid were run in order to confirm that their molar response was similar to D-glucuronic acid. D-Galacturonic acid had a retention time of approximately 3.9 min and had baseline resolution from D-glucuronic acid at the concentrations injected.

A series of spiked samples were also injected onto the ICS2000 system including hydrolysed (4M TFA) crude polysaccharides successively spiked with D-galacturonic acid, D-glucuronic acid, and finally the unhydrolysed crude polysaccharides.

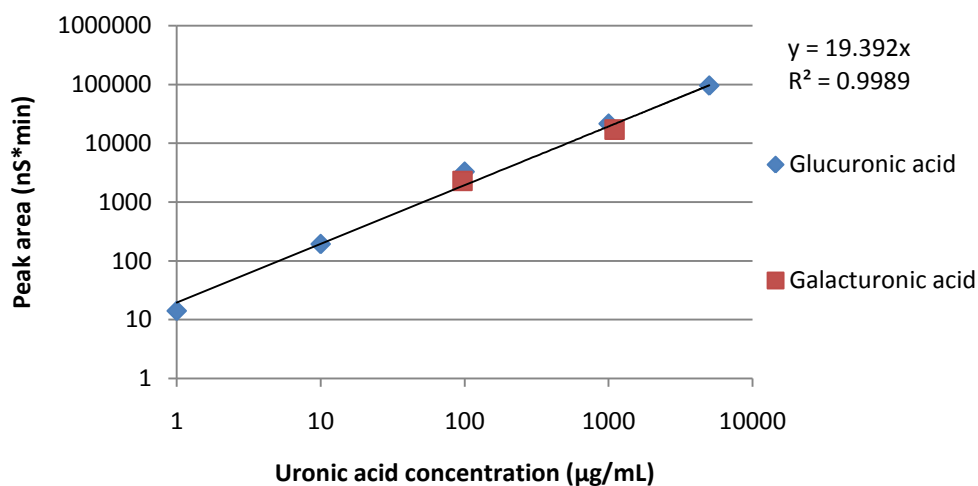


**Figure 7: Calibration plot for the quantification of uronic acid concentration using ion chromatography (using logarithmic scales).**

Samples (25 µL) of each of the acidic component solutions (3.000 mL) from each of the six fractions were injected onto the ICS2000 system and the concentration of uronic acid components were estimated using integrated peak areas and the uronic acid response calibration curve plot (Figure 7).

## 2.6 Linkage Analysis

### 2.6.1 Aims

Linkage analysis through the conversion of polymeric sugar residues into partially methylated alditol acetates, aims to allow the main linkage points of each carbohydrate unit to be deduced. Separate samples of acidic and neutral fractions were analysed to determine if any linkages are more prevalent in the acidic or neutral fractions. A sample of Fraction N1 was also analysed due to it being a high-yield fraction and evidence (Table 6, page 77) suggesting it was mostly a single type of polymer.

### 2.6.2 Methodology

Two samples of the crude polysaccharides, one standard of lactose, one composite sample of acidic polysaccharides (fractions A1, A2, and A3 combined), one composite sample of neutral polysaccharides (fractions N1, N2, and N3 combined), and one sample of Fraction N1 were each converted to partially methylated alditol acetates (PMAAs) and analysed by GC-MS using repeats of the following method (adapted from a number of published methods [115]).

The lyophilised sample was dissolved in de-ionised water (250  $\mu$ L) before NaBH<sub>4</sub> (Aldrich, 99%) solution (6.0 mg in 250  $\mu$ L de-ionised water) was stirred into to each sample. After 120 minutes washed IRC-50 resin (Amberlite) was added until the sample stopped effervescing. The resin was removed by filtration (glass filter paper, GC-50, Advantec<sup>®</sup>) and washing ( $\approx$  5 mL, de-ionised water) under vacuum. The reduced sample was concentrated then evaporated to dryness under a stream of N<sub>2</sub> at 40°C.

Methanol (1 mL) was added to the sample and then it was evaporated to dryness under a stream of N<sub>2</sub> at 40°C. This was repeated an additional 5 times before the sample was dried under vacuum for  $\approx$  15 hours.

The sample was re-dissolved in dry DMSO (1.00 mL), powdered NaOH ( $\approx 100$  mg, Baker Chemical Co.) was added and this mixture vigorously stirred (40 min) in a capped vial while being cooled in a beaker of ice and water.  $\text{CH}_3\text{I}$  (250  $\mu\text{L}$ , 99%, Aldrich) was added, the vial recapped and the sample stirred (40 min) while being cooled in a beaker of ice and water. The vial was opened and a stream of  $\text{N}_2$  was bubbled through the sample at  $40^\circ\text{C}$  for approximately 2 hours to remove excess  $\text{CH}_3\text{I}$ . The vial was returned to cool in a beaker of ice and water, before de-ionised water (2.00 mL) was added. Chloroform (2.00 mL) was added and the sample vigorously stirred and shaken before being left to stand. Once the aqueous and chloroform layers had separated, the chloroform phase was transferred to a clean vial and the aqueous phase discarded.

De-ionised water (1.0 mL) was added to the chloroform phase, followed by vigorous stirring, centrifuging ( $\approx 1500$  g, 10 min), and removal/discarding of the aqueous phase. This wash step was repeated two additional times before the sample was placed in the freezer ( $-20^\circ\text{C}$ ). Once the aqueous residue had frozen, the chloroform phase was transferred to a clean vial and blown dry under a stream of  $\text{N}_2$  at  $40^\circ\text{C}$ .

The dry methylated sample was dissolved in TFA (200  $\mu\text{L}$ , 99%, Acros). The vial was recapped under  $\text{N}_2$  and placed in a heating block ( $120^\circ\text{C}$ ). After heating for 10 minutes the vial was removed and cooled under running water. Once cool, the vial was uncapped, de-ionised water (1.000 mL) added, and the vial recapped under  $\text{N}_2$ . The vial was returned to the heating block ( $120^\circ\text{C}$ ) for a further 60 minutes. The vial was cooled to room temperature under running water before it was uncapped and the sample blown dry under a stream of  $\text{N}_2$  at  $40^\circ\text{C}$ . The dry sample was re-dissolved in aqueous  $\text{NH}_4\text{OH}$  solution (100  $\mu\text{L}$ , 1 M),  $\text{NaBD}_4$  (99%, Aldrich) solution (0.02 mg/mL in dry DMSO) was added and the mixture stirred before being capped and placed in heating block ( $40^\circ\text{C}$ ) for approximately 3 hours.

Glacial acetic acid (100  $\mu\text{L}$ ) was added to the sample with stirring followed by the sequential addition of 1-methylimidazole (100  $\mu\text{L}$ ) and acetic anhydride (2.000 mL). The vial was capped, mixed and left to stand at room temperature. After 10 minutes, de-ionised water (5.00 mL) was added to the vial and it was recapped and stirred. Once the sample had cooled, the aqueous solution was extracted with chloroform (3 x 1.00 mL). The combined chloroform extract was placed in a freezer ( $-20^{\circ}\text{C}$ ) until any aqueous residue had frozen and then a portion of the chloroform phase containing PMAAs ( $\approx 1.5$  mL) was transferred to a GC vial for analysis.

Each of the PMAA samples was injected and analysed using the same GC-MS system and methodology (including oven temperature program) detailed in section 2.5.2.3.

The retention times of the alditol acetates of standards (D-xylose, L-arabinose, D-glucose, D-galactose and D-mannose) along with that of the terminal-D-galactopyranosyl PMAA from the lactose standard were plotted against literature relative retention times [115] to produce calibration plots and correction factors (Figure 8 and Figure 9). These calibration and correction factors were used to predict at what times PMAAs from the literature tables would elute on the Waikato University SP-2330 column and GC method.

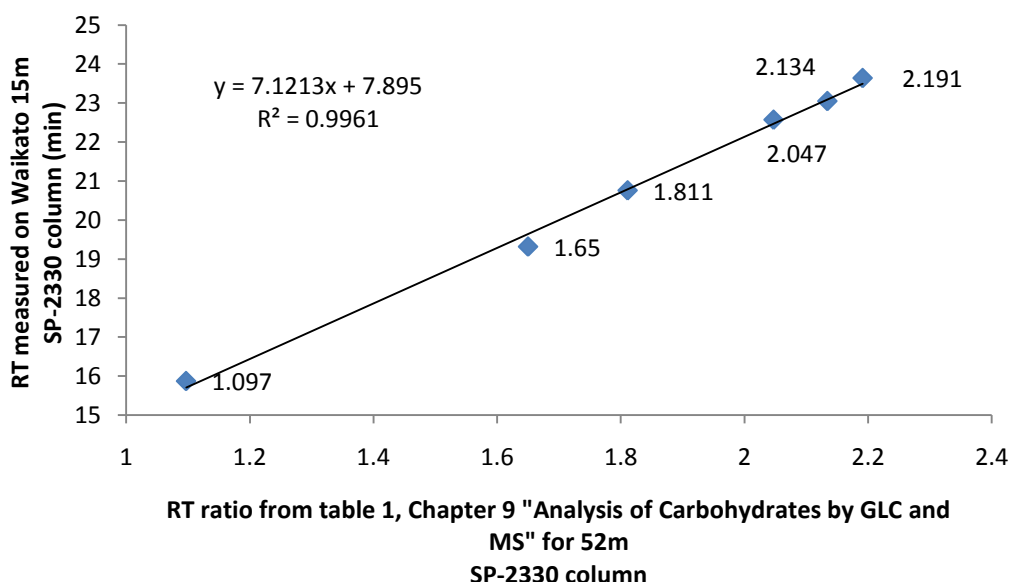


**Figure 8: Retention time correlation to literature SP-2330 column for known standards.** Standards used were the alditol acetates prepared from D-xylose (1.811) , L-arabinose (1.65), D-glucose (2.191), D-galactose (2.134) and D-mannose (2.047), along with 1,5-di-*O*-acetyl-1-deuterio-2,3,4,6-tetra-*O*-methyl-D-galactitol produced from a lactose standard (1.097). The retention time of each standard on the gas chromatography method used in this thesis, was plotted against the RT ratio in the literature for a 52m SP-2330 column [115].

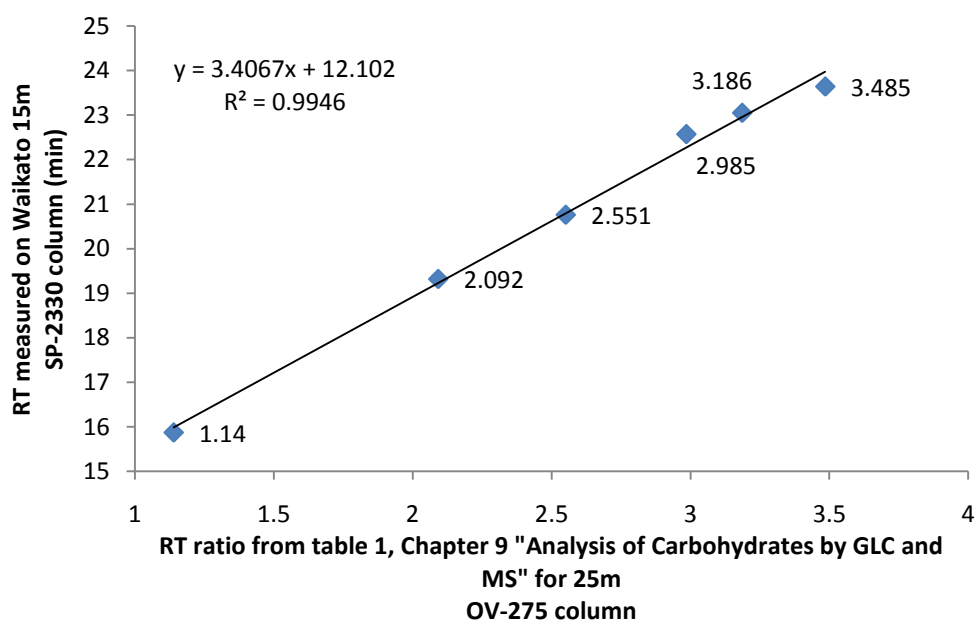


**Figure 9: Retention time correlation to literature OV-275 column for known standards.** Standards used were the alditol acetates prepared from D-xylose (2.551), L-arabinose (2.092), D-glucose (3.485), D-galactose (3.186) and D-mannose (2.985), along with 1,5-di-*O*-acetyl-1-deuterio-2,3,4,6-tetra-*O*-methyl-D-galactitol produced from a lactose standard (1.14). The retention time of each standard on the gas chromatography method used in this thesis, was plotted against the RT ratio in the literature for a 25m OV-275 column [115].

The mass spectrum of each peak was checked against the equivalent spectrum in the CCRC database [120] to provide evidence for the identity of the PMAA. Predicted fragmentation patterns were also deduced and used especially when the CCRC database lacked the mass spectrum (*e.g.* for the PMAA derived from 1,4-linked D-xylopyranosyl). Peaks present in the GC-MS chromatogram of the PMAA samples had their identity confirmed based on matching converted retention times to those in a literature table [115] using the correction formulas from the graphs (Figure 8 and Figure 9).

## Chapter 3 Results and Discussion

### 3.1 Fractionation by Size Exclusion Chromatography

The crude polysaccharide preparation that was isolated from the prehydrolysate separated into two broad groups when fractionated by SEC (Figure 10). A similar separation into acidic and neutral polysaccharides has been reported for spruce hemicelluloses [34].

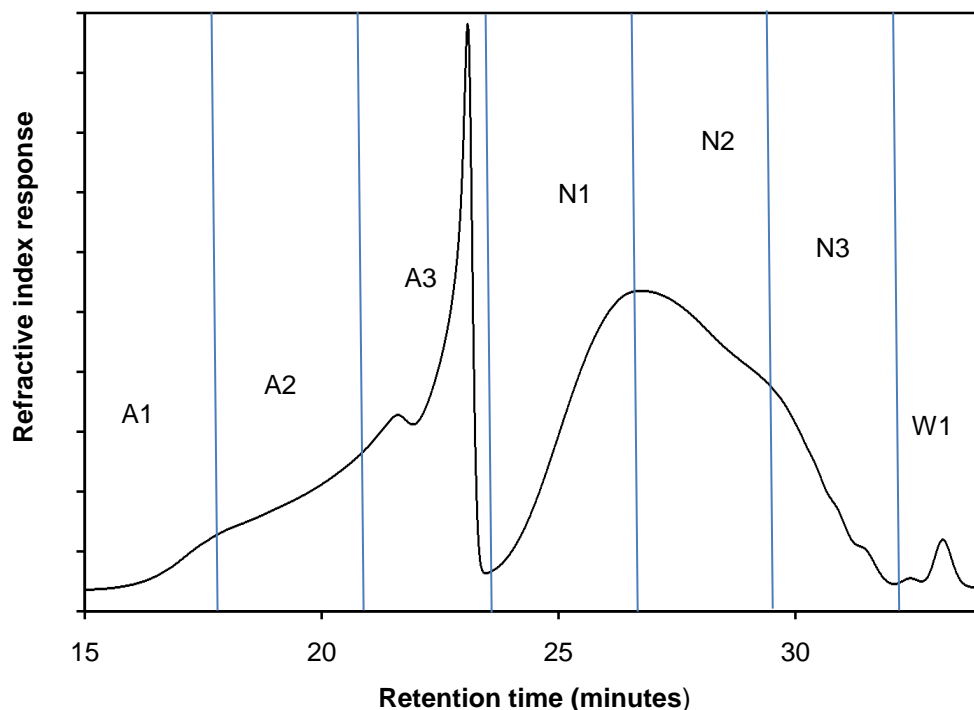


**Figure 10: Chromatogram of SEC fractionation of hemicelluloses polymers. Blue lines indicate where each fraction was collected.**

The first group, comprising fractions A1, A2, and A3 which eluted between 12 and 23.5 minutes (Figure 10), contained acid (anionic) functional groups and accounted for approximately 30% of the total dry mass injected (by weight). Acidic polysaccharides elute early and separate based on charge as well as size, due to an ion-exclusion effect when using low ionic strength eluents in SEC [103]

The second group, comprising fractions N1, N2, and N3 that eluted between 23.5 and 32.5 minutes (Figure 10), was considered to contain only neutral molecules with no charged groups. These neutral fractions accounted for approximately 70% of the dry weight injected.

The last fraction eluting from the columns, Fraction W1, accounted for less than 2% of the dry weight injected. This fraction may comprise non-carbohydrate contaminants, carbohydrate degradation products, or monosaccharides, but retention times for standards of D-xylose and hydroxymethylfurfural run on this SEC system did not match the major peak in Fraction W1, so their identity is still unknown.

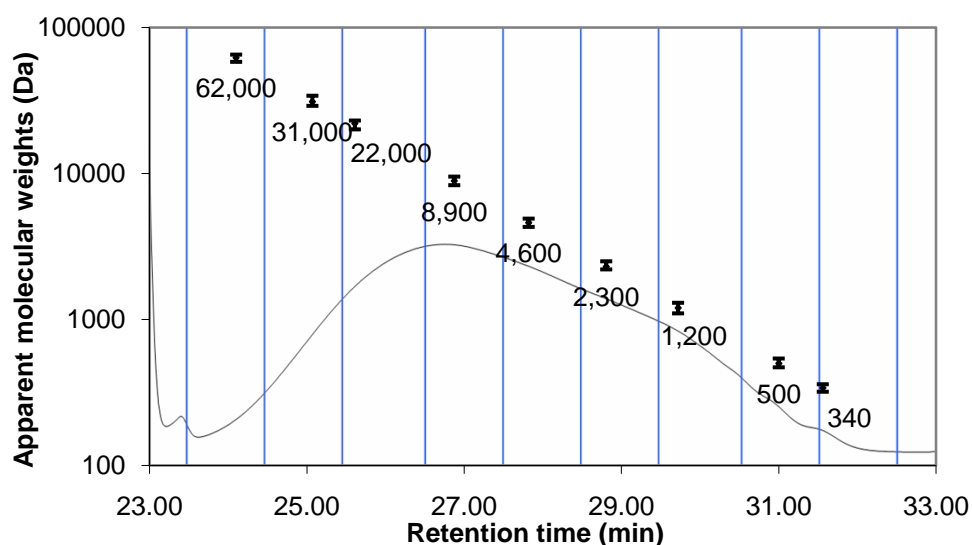


**Figure 11: Apparent molecular weights of neutral fractions by SEC. Blue divisions indicate where each fraction was collected. These nine smaller fractions were each re-injected and retention times of peak tops measured.**

As the acidic components are excluded from the SEC beads when using pure water as the eluent, their molecular weight cannot be calculated using the dextran calibration curve (Figure 5). Use of a higher ionic strength eluent might cause the acidic components to behave more like the neutral components [103]. However the calibration curve would need to be repeated due to change of operating conditions and the behaviour of eluent ions in SEC might cause additional problems.

The molecular weight estimates from re-injections of the nine smaller neutral fractions are graphed over the section of the chromatogram from which they were collected (Figure 11). If these polysaccharides produced from the partial depolymerisation of hemicelluloses have a similar hydrodynamic behavior to dextrans on the SEC columns, then most of the neutral polysaccharides in the crude sample have molecular weights between 30,000 Da and 1,000 Da.

## 3.2 Matrix Assisted Laser Desorption Ionisation – Time of Flight-Mass Spectrometry (MALDI-ToF-MS) Analysis

### 3.2.1 Anionic (Acidic) Polysaccharides

The mass spectra of acidic fractions (A1, A2, and A3) contained repeating patterns of 132 mass units with abundances in bell-curve shaped populations. This is consistent with polymer populations with a distribution of different numbers of pentose units. Different populations, each with the 132 mass unit repeats, overlap in the mass spectra of the acidic fractions (Figure 12-Figure 14). The difference between these populations is  $\approx 190$  mass units and produced a pattern consistent with different numbers of attached 4-*O*-methylglucuronic acid (MeGlcA) groups as found in other softwood hemicelluloses [19, 29]. Below  $m/z$  of 1200, matrix clusters caused interference. All major peaks above  $m/z$  of 1200 in these mass spectra may be attributed to  $[M-H]^-$  ions of pentose polymers of various DP values and different numbers of the  $\approx 190$  mass unit groups attached. Based on established softwood literature [24-30], these  $\approx 190$  mass unit groups were assumed to be 4-*O*-methylglucuronic acid (MeGlcA), however other *O*-methylated hexuronic acids such as 3-*O*-methylgalacturonic acid would be indistinguishable as they would also appear on the MALDI-ToF spectra as a 190 mass unit difference.

The mass spectrum of Fraction A2 contained four overlapping populations of pentose polymers (Figure 13). The population with the most abundant ions are attributed to pentose polymers (DP of approximately 6 to 28), with two 4-*O*-methylglucuronic acid groups attached to each polymer. The most intense ion at  $m/z$  2115 is consistent with a (4-*O*-methylglucuronic acid)<sub>2</sub>(pentose)<sub>13</sub> structure.

The next two most abundant populations observed in the spectrum of Fraction A2 have lower and higher DP ranges, respectively. The lower molecular weight population has pentose polymers (DP of approximately 5 to 19) with a single 4-*O*-methylglucuronic acid group attached, while the higher molecular weight population is distributed around the  $m/z$  3228 ion and is consistent with pentose polymers (DP of approximately 10 to 28) with three 4-*O*-methylglucuronic acid groups attached. The fourth population detected in Fraction A2 with very low abundance is consistent with pentose polymers of DP in the approximate range of 21-31 with four 4-*O*-methylglucuronic acid groups attached to each polymer.

No pentose-based polymers with attached 4-*O*-methylglucuronic acid groups were detected in fractions N2, N3 and W1 using this method, which is expected given the fractions are supposedly neutral. However, the mass spectrum of Fraction N1, a supposedly neutral fraction, contained a small amount of pentose polymer (DP of approximately 5 to 19) with one attached 4-*O*-methylglucuronic acid group (Figure 15). The presence of this acidic material is likely to be due some overlap of neutral and acidic polysaccharides as they elute near to the point where the collection of Fraction N1 commenced.

Polytools was used to analyse the major acidic pentose series that were detected in the MALDI-ToF spectra of Fractions A1, A2, A3, and N1 in negative ion mode. Polytools calculated a number of average values for the major pentose populations found in the four fractions (Table 1).

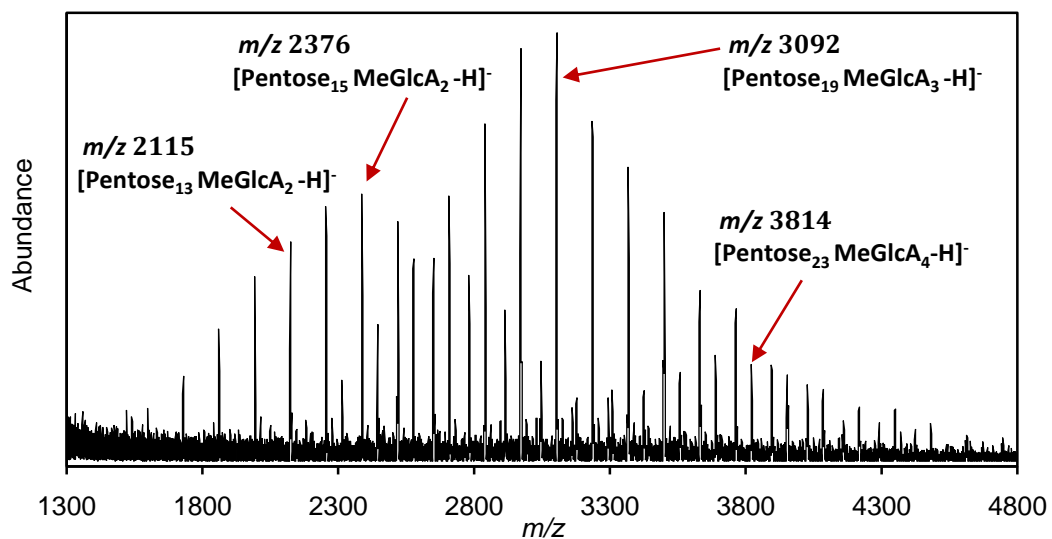


Figure 12: MALDI-ToF mass spectrum of Fraction A1 (S-DHB matrix, negative ion mode).

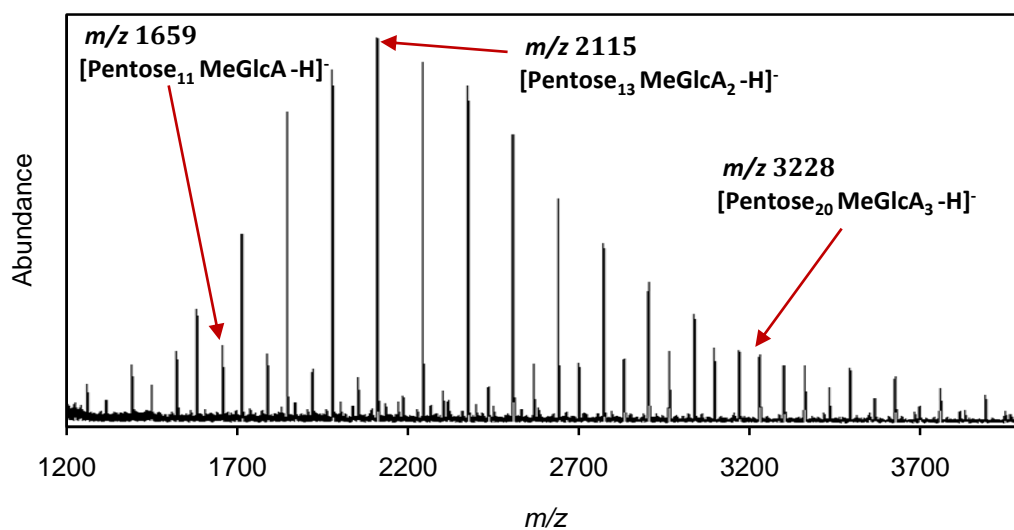


Figure 13: MALDI-ToF mass spectrum of Fraction A2. (S-DHB matrix, negative ion mode).

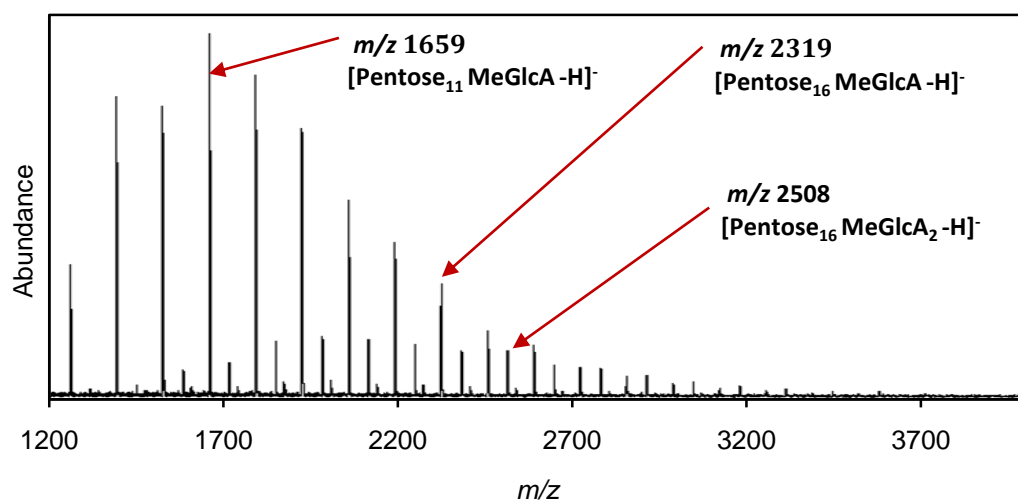


Figure 14: MALDI-ToF mass spectrum of Fraction A3. (S-DHB matrix, negative ion mode).

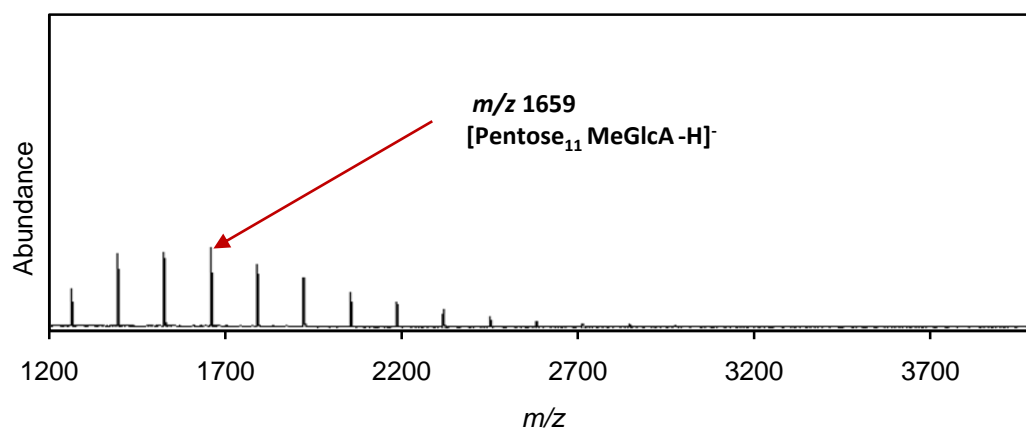


Figure 15: MALDI-ToF mass spectrum of Fraction N1. (S-DHB matrix, negative ion mode).

**Table 1: Average MW values for major acidic pentose polymers (calculated using Polytools).**

Fraction	Number of attached MeGlcA	$M_n$ (Da) <sup>a</sup>	$M_w$ (Da) <sup>b</sup>	pd <sup>c</sup>	DP <sup>d</sup>	Pentose : MeGlcA <sup>e</sup>
N1 <sup>f</sup>	1	1696.4	1775.2	1.04643	12.85	12.9:1
A3	1	1748.2	1831.8	1.04783	13.24	13.2:1
	2	2177.5	2270.9	1.04288	16.50	8.25:1
	3	2240.9	2365.2	1.05549	16.98	5.6 <sup>g</sup> :1
A2	1	1698.2	1753.4	1.03251	12.86	12.9:1
	2	2336.3	2440.4	1.04453	17.70	8.85:1
	3	3066.1	3121.8	1.01819	23.22	7.74:1
	4	3938.9	3999.6	1.01539	29.69	7.42:1
A1	2	2458.7	2523.1	1.02621	18.67	9.34:1
	3	3087.3	3144.2	1.01843	23.40	7.80:1
	4	3853.9	3897.9	1.01142	29.00	7.25:1
<p><sup>a.</sup> <math>M_n</math> = number-average molecular weight.</p> <p><sup>b.</sup> <math>M_w</math> = weight-average molecular weight.</p> <p><sup>c.</sup> pd = polydispersity.</p> <p><sup>d.</sup> DP = mean degree of polymerization.</p> <p><sup>e.</sup> Average pentose: MeGlcA ratio in the polymer population analysed.</p> <p><sup>f.</sup> The predominantly neutral Fraction N1 was contaminated with a small amount of acidic polysaccharides.</p> <p><sup>g.</sup> The population with 3 MeGlcA groups in Fraction A1 was of very low abundance ions and a number of ions could have been lost in the baseline noise.</p>						

These calculated values for average molecular weights ( $M_n$  and  $M_w$ ) were reasonably consistent when considering the population with one attached 4-*O*-methylglucuronic acid group across three different fractions (Table 1). This suggests that the SEC is separating the acidic hemicelluloses based on the number of acidic groups more than on the molecular weight of polymers. Populations with more attached 4-*O*-methylglucuronic acid groups would of course have higher average molecular weights.

### 3.2.2 Neutral Polysaccharides

In contrast to the mass spectra of acidic polysaccharides, the neutral polysaccharides gave spectra with low signal to noise ratios. This poor ionisation was likely due to the need for neutral polysaccharides to form  $\text{Na}^+$  or  $\text{K}^+$  adducts. In general the populations of these neutral polysaccharides appeared skewed towards the lower mass range.

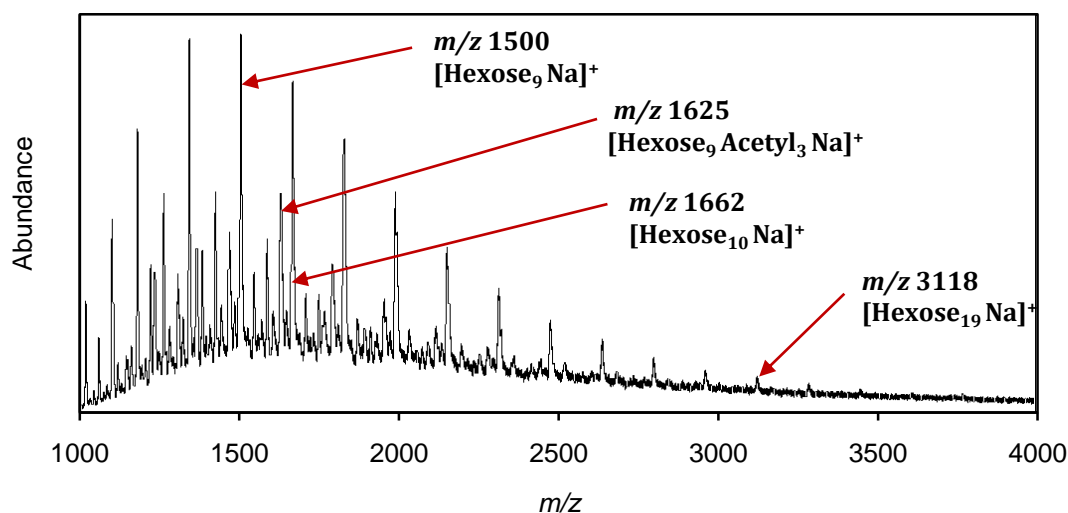


Figure 16: MALDI-ToF mass spectrum of Fraction N3. (THAP matrix, positive ion mode). Shows a dominant population of non-acetylated hexose polymers and smaller abundance populations of partially-acetylated hexose polymers around an  $m/z$  of 1600.

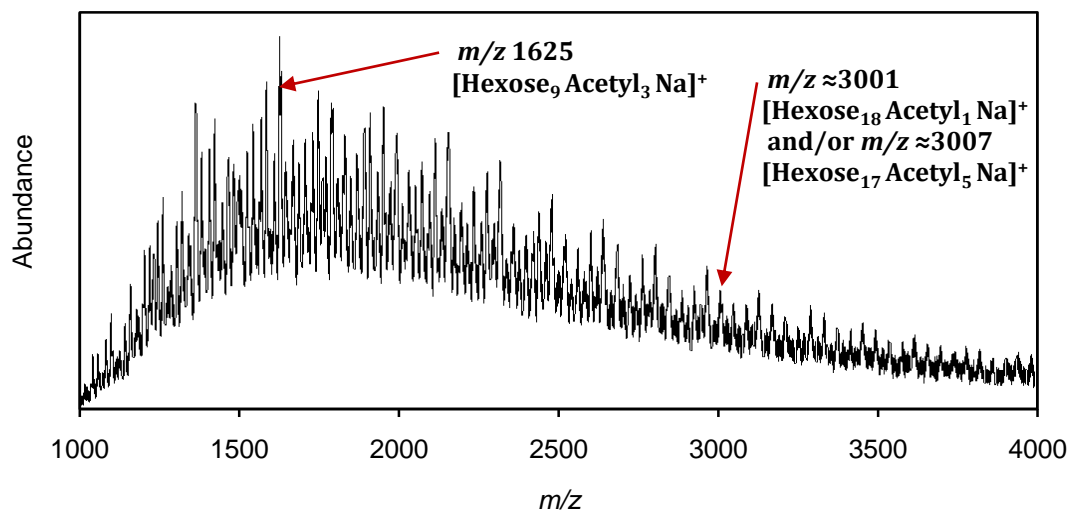


Figure 17: MALDI-ToF mass spectrum of Fraction of N2. (THAP matrix, positive ion mode).

The MALDI-ToF mass spectra of neutral fractions N2 and N3 were consistent with a mix of non-acetylated and partially-acetylated hexose polymers. Hexose polymers had repeating units of approximately 161 mass units, with each attached *O*-acetyl group adding approximately 42 mass units (Figure 16-Figure 17).

The most abundant series of ions in the spectrum of N3 (Figure 16) was Na<sup>+</sup> adducts of non-acetylated hexose polymers with DP range of approximately 4 to 22. Less abundant populations were present and were consistent with Na<sup>+</sup> adducts of hexose polymers with 1, 2, and 3 acetyl groups. A low abundance series of K<sup>+</sup> adducts of non-acetylated hexose polymers was also detected in fraction N3.

The mass spectra of N2 (Figure 17) showed more acetylated hexose polymers than non-acetylated hexose polymers. Series with 0, 1, 2, 3, and 4 acetyl groups were detected with DP range of approximately 4 to 36 hexose units. The *m/z* 1625 value of the most abundant ion in the mass spectrum was consistent with Na<sup>+</sup> adducts of (hexose)<sub>9</sub>(acetyl)<sub>3</sub> molecules with a DS<sub>Ac</sub> value of 0.33. DS<sub>Ac</sub> or degree of acetylation = (Number of acetyl groups)/ (Number of sugar units).

Higher DP polymers were more abundant in the spectra of N2 compared to N3. However, the difference between the spectra of Fractions N2 and N3 in terms of molecular weights was not as large as expected from the SEC estimates (Figure 11, Page 49). Possible reasons for this smaller than expected difference are that MALDI preferentially ionises smaller polymer molecules, fragmentation at the higher laser power setting, or that some overlap has occurred in SEC fraction collection. All three factors could be contributing to the small difference that is observed.

The large increase in the amount of completely de-acetylated hexose polymers in spectra of N3 compared to that of N2 appears to be more than can be explained by the concept that larger polymers are more likely to contain more acetyl groups (Figure 16 and Figure 17). Potential causes of this difference might include:

1. That N3 has undergone more de-acetylation than N2 after collection from the SEC system. Lower DP hexose polymers may perhaps be more vulnerable to de-acetylation than higher DP hexose polymers.
2. That non-acetylated hexose polymers have different hydrodynamic behaviour on the SEC and tend to elute later than the partially acetylated polymers of similar DP. Thus fraction N3 is enriched in non-acetylated hexose polymers of higher DP. Acetyl groups are known to disrupt hydrogen bonding [50] and could change the shape of a polysaccharide molecule in solution. This hypothesis might also help explain the appearance of two 'humps' in the neutral section of the SEC chromatogram (Figure 10).
3. In addition to the effects noted in hypothesis '2.' above, there is the possibility that the non-acetylated hexose polymers are a completely different type of hemicellulose with different types of hexose units and/or linkages than those of the partially acetylated hexose polymers. Results from the monomer and linkage analysis tend to support this hypothesis as Fraction N3 was enriched in a D-galactosyl, especially 1-4 linked D-galactopyranosyl. The non-acetylated hexose polymers that were enriched in the MALDI-ToF mass spectra of Fraction N3 could be due the non-acetylated  $\beta$ -(1,4)-galactan known to be present in *P. radiata* compression wood [18, 19]

### 3.2.3 Alkaline De-acetylation of Neutral Polysaccharides

The de-acetylation method gave effective de-acetylation and produced results similar to those reported in the literature for the de-acetylation of *O*-acetylated-glucogalactomannans (AcGGM) [36]. The acetylated hexose series were removed and the non-acetylated hexose series became clearer and in some cases more abundant when compared to control spectra (Figure 18 and Figure 19). The de-acetylation also allowed higher DP hexose polymers to be distinguished from the baseline noise.

De-acetylated hexose polymers with a large range of DP could be observed in the mass spectra of Fraction N2 (Figure 20). When the region above an  $m/z$  of 6000 in the mass spectra of Fraction N2 was observed closely the hexose repeating pattern became indistinguishable from baseline noise at a point corresponding to a DP of approximately 47.

Before and after de-acetylation, the mass spectrum of N3 had a very low abundance population of peaks consistent with neutral pentose polymers. These pentose polymers had DPs as high as 11 and became more obvious after de-acetylation (Figure 19).

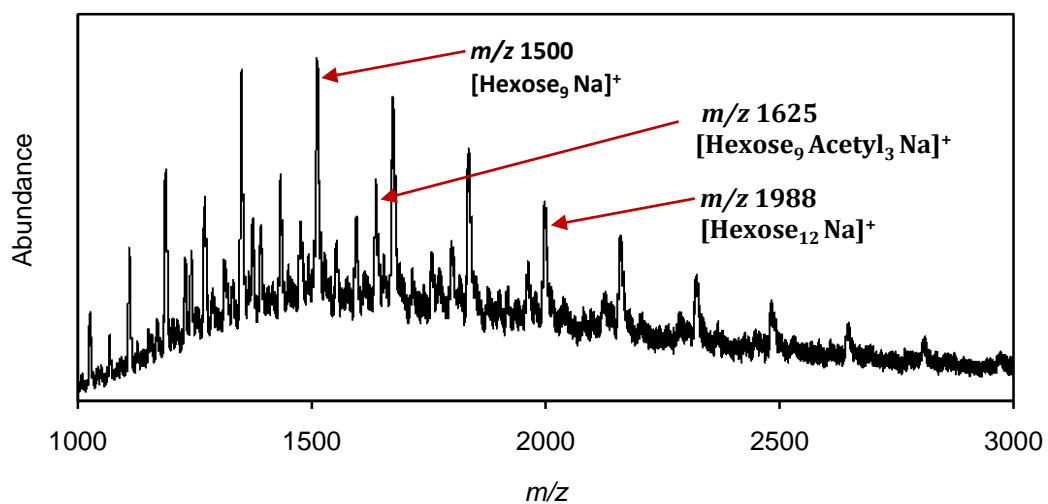


Figure 18: MALDI-ToF mass spectrum of Fraction N3 control before de-acetylation (THAP matrix, positive ion mode).

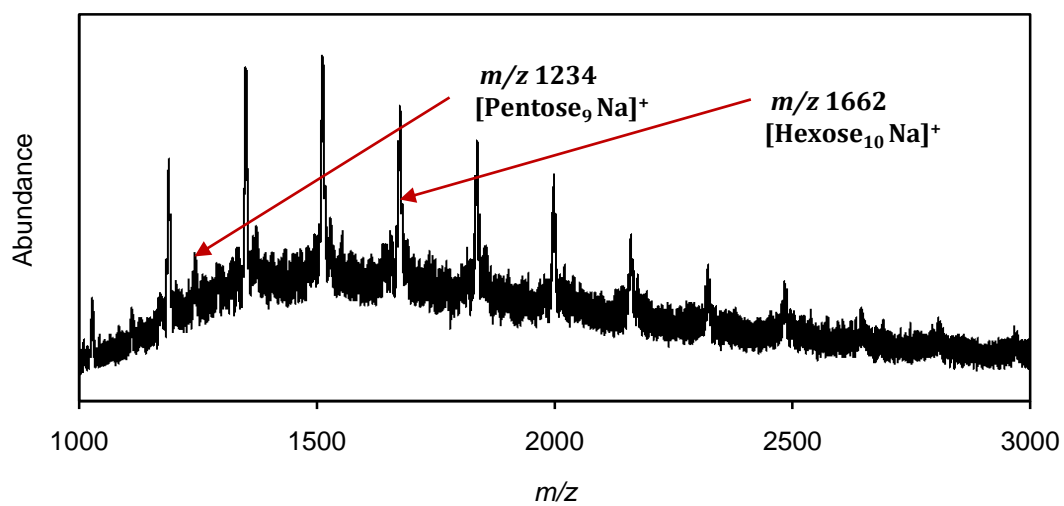


Figure 19: MALDI-ToF-MS Fraction N3 after de-acetylation with NH<sub>4</sub>OH (THAP matrix, positive ion mode).

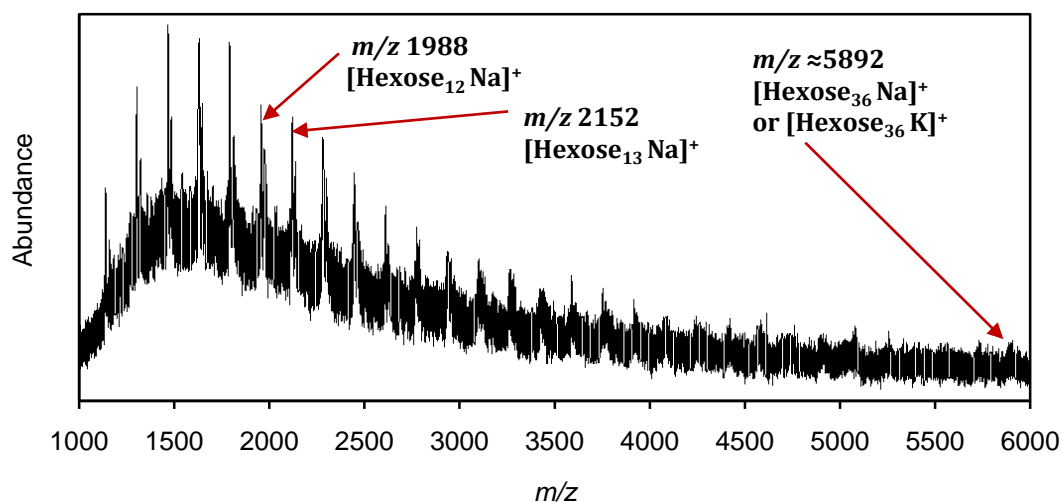


Figure 20: MALDI-ToF-MS of Fraction N2 after de-acetylation with  $NH_4OH$  (THAP matrix, positive ion mode).

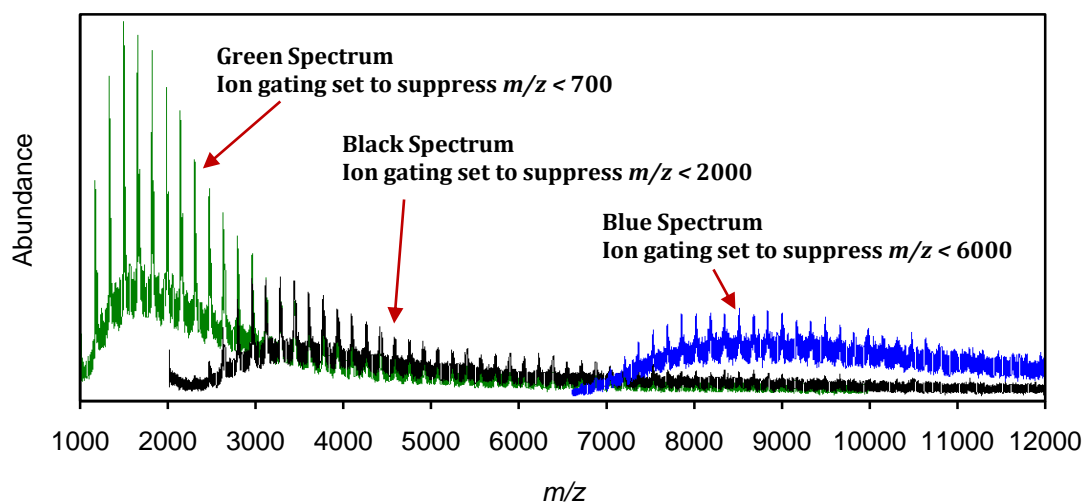


Figure 21: Ion gating changes on N1 after de-acetylation with  $NH_4OH$  (THAP matrix, positive ion mode).

Green spectrum used standard ion gating to suppress (mainly matrix) ions below  $m/z$  700. Black spectrum had ion gating set to suppress ions with  $m/z$  less than 2000. Blue spectrum had ion gating set to suppress ions with  $m/z$  less than 6000 and the detector set to monitor a higher mass range at increased electronic gain.

The spectra of fraction N1 was clear enough to observe hexose polymer patterns after de-acetylation. Hexose polymers with a DP range of approximately 6 to 55 were initially detected with the most abundant ions below  $m/z$  3000 (green spectrum, Figure 21).

The gating settings on the MALDI-ToF were modified to suppress ions with  $m/z$  smaller than 2000 and another 300 laser shots were acquired (black spectrum, Figure 21). This ion gating change appeared to increase the sensitivity and improve the detection of higher DP ions, to a point where polymer ions as high as DP 79 ( $m/z \approx 12850$ ) could just be observed above the baseline noise. A further increase in the gating settings to suppress ions with  $m/z$  smaller than 6000, together with an increase in the electronic gain on the detector that was the focused on a higher mass range with another 300 laser shots acquired, improved the detection of the higher molecular weight hexose polymers in the 7000 to 14000 Da range (blue spectrum, Figure 21). Increasing the ion gating settings further did not appear to provide significant improvement in the detection of polysaccharides above 10,000 Da.

The detection of abundant hexose polymer ions below  $m/z$  3000 in fraction N1 was not expected from the SEC apparent molecular weight results and indicates a number of potential problems could be occurring in the MALDI-ToF method used. These potential problems might include:

1. The separation on the SEC is poor with large overlaps causing some smaller polymers ( $\approx 1500$ Da) that should elute in Fraction N3 to mix and elute in Fraction N1 where only polymers in an 80,000Da to 8,000 Da range are expected. Column overload could be the cause of this huge loss of resolution. However, evidence against this explanation was obtained from re-injections of the nine smaller fractions of neutral polysaccharides (Figure 11, page 49) which each gave relatively sharp chromatogram peaks. This suggests that a large contamination of Fraction N1 with smaller polymers ( $\approx 1500$  Da) does not appear to have occurred.
2. The tendency of MALDI to preferentially ionise smaller carbohydrates in polydisperse samples at the expense of larger ones is greatly amplifying a trace contamination of smaller polymers while the larger polymers that make up the bulk of Fraction N1 by weight are suppressed in the mass spectrum.

3. Larger polymers might make up most of the sample if measuring weight, non-end-group NMR integrals or RI response. However, each molecule of a smaller polymer weighs less and therefore smaller molecules could still constitute most of the sample if measuring the number of molecules present. The mass spectrometer detector counts the abundance of each ion, which should be somewhat proportional to the number of molecules in the original sample. This concept is demonstrated in a hypothetical sample containing only 4 different sizes of hexose polymers (Table 2).

**Table 2: Simplified hypothetical hexose polymer sample <sup>a</sup>**

<b>DP</b>	<b>MW of hexose polymer (g/mol or Da)</b>	<b>Amount (µg)</b>	<b>Composition by mass</b>	<b>Amount (mol)</b>	<b>Composition by number of molecules <sup>b</sup></b>
6	991	0.05	6%	$5.0 \times 10^{-5}$	30%
7	1153	0.05	6%	$4.3 \times 10^{-5}$	26%
53	8774	0.4	50%	$4.6 \times 10^{-5}$	27%
62	10071	0.3	38%	$3.0 \times 10^{-5}$	18%
<sup>a.</sup> Hypothetical sample contains higher molecular weight hemicelluloses with a small amount of contamination by lower molecular weight hemicelluloses.					
<sup>b.</sup> Because MALDI-TOF-MS will count ions it is likely spectra peak areas and heights will reflect composition of sample by number of molecules.					

4. The MALDI method (especially at 95% laser power) is fragmenting larger polymers from the sample and causing them to appear in the mass spectra as much smaller fragmentation ions. Fragmentation is known to occur with polysaccharides as they move between the MALDI plate and the detector [109] but it is claimed that this fragmentation will not be a significant problem when using a ‘cooler’ matrix like THAP or 2,5-DHB [109]. However, literature reporting of MALDI mass spectra of polysaccharides (free carbohydrates, not glycoconjugates) larger than about 10,000Da is rare [106, 109] and a ‘cooler’ matrix like DHB is known to cause significant fragmentation of some synthetic polymers such as poly(tetrahydrofuran) [121]. So this explanation cannot be discounted.

**Table 3: Average MW values for de-acetylated neutral hexose polymers (calculated using Polytools).**

<b>Fraction</b>	<b>Ion gating (<i>m/z</i>)</b>	<b>M<sub>n</sub> (Da)<sup>a</sup></b>	<b>M<sub>w</sub> (Da)<sup>b</sup></b>	<b>Pd<sup>c</sup></b>	<b>DP<sup>d</sup></b>	<b>DP range<sup>e</sup></b>
N3	700	1755.08	1898.58	1.08176	10.77	17
N2	700	2577.4	3469.5	1.34613	15.91	45
N1	700	2304.51	2763.69	1.19925	14.20	56
	2000	4012.08	4734.18	1.17998	24.71	53
	6000	9157.88	9361.26	1.02221	56.53	39
<p><sup>a.</sup> <b>M<sub>n</sub> = number-averaged molecular weight.</b></p> <p><sup>b.</sup> <b>M<sub>w</sub> = weight-averaged molecular weight.</b></p> <p><sup>c.</sup> <b>pd = polydispersity.</b></p> <p><sup>d.</sup> <b>DP = mean degree of polymerization.</b></p> <p><sup>e.</sup> <b>DP range = range in the numbers of hexose units contained in polymers.</b></p>						

Analysis of MALDI-ToF spectra mass lists with Polytools was also carried out on the major neutral hexose series that were detected in de-acetylated samples of fractions N1, N2, and N3 in positive ion mode. Polytools calculated average values for the hexose polymer distribution found in each fraction (Table 3). The mass lists of N1 spectra where ion gating suppression settings had been increased were also analysed with Polytools, although the calculated values (Table 3) should not be compared directly with the values for the other fractions as the method had been radically changed to ignore lower mass ions.

These averages generated by Polytool software do depend on choices made by the programs user. These choices include the accuracy of the peak picking and whether peak heights or peak areas were used for the calculation. The rise in the baseline under the hexose series appeared to distort both peak height and peak area values. Calculations using peak heights generally gave higher average values than calculations using peak areas. For consistency peak area (integral) was used to calculate all values listed in Table 1 and Table 3.

The mass list peaks were all picked manually from the spectra to reduce the chances of the Polytool software getting confused by the excess of data in the computer picked mass lists. The mass accuracy limit was set to 30 mass units. This mass accuracy limit was very high but allowed the software to count Na<sup>+</sup> and K<sup>+</sup> adducts in the same series for the neutral polysaccharides.

The Na<sup>+</sup> adducts were generally the dominant peaks in hexose polymers below  $m/z$  5000. At around  $m/z$  5000 Na<sup>+</sup> and K<sup>+</sup> adduct peaks were at about equal intensity, and above  $m/z$  5000 the K<sup>+</sup> adducts appeared to dominate. Na<sup>+</sup> and K<sup>+</sup> adduct peaks for each hexose polymer size appeared to start blending together at higher  $m/z$  values, likely to be due to loss of resolution and isotope variations at higher masses.

### 3.3 Nuclear Magnetic Resonance Spectroscopy (NMR) Analysis

#### 3.3.1 Anionic (Acidic) Fractions

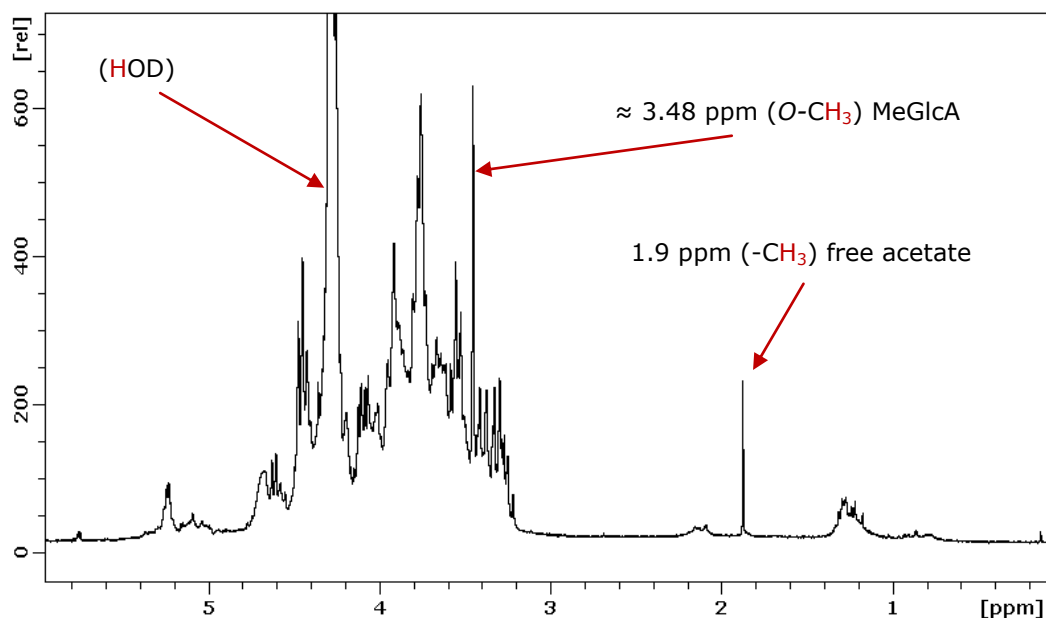
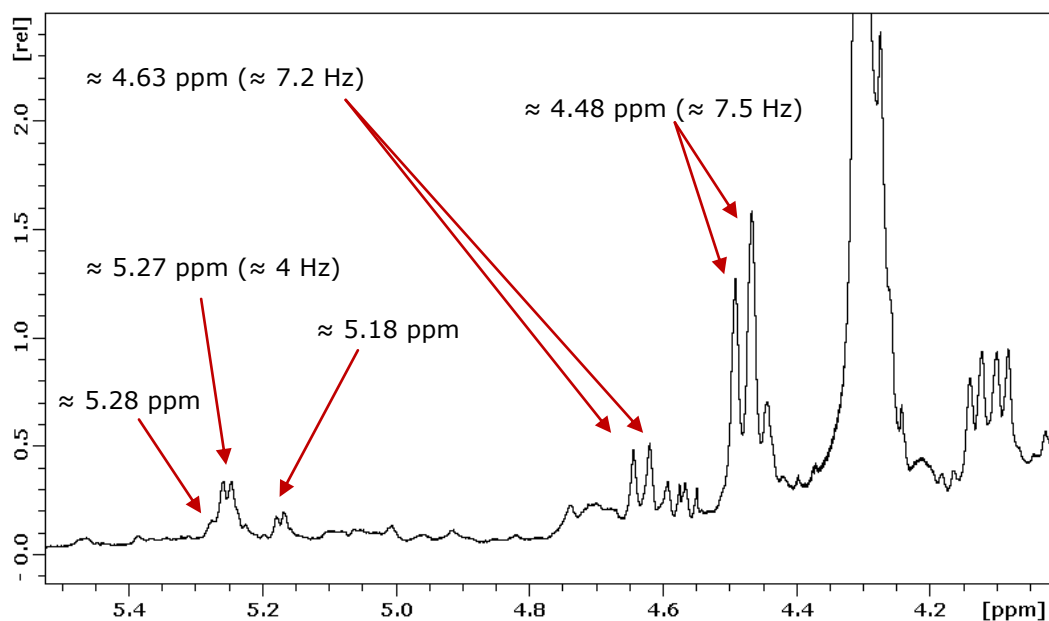


Figure 22: <sup>1</sup>H NMR of Fraction A2 in D<sub>2</sub>O (70°C probe temperature).

<sup>1</sup>H NMR analysis of Fractions A2 and A3 provided additional evidence for the presence of 4-*O*-methyl- $\alpha$ -D-glucuronic acid groups attached to the pentose polymers. Sharp singlets at approximately 3.48 ppm were observed rising above the carbohydrate envelope region (Figure 22) in the spectra of both fractions and are at a similar shift to literature values for the -OCH<sub>3</sub> groups of 4-*O*-methylglucuronic acid attached to xylans [90]. A weak 4-*O*-methyl signal was also observed in Fraction N1 (Figure 24), but any 3.48 ppm signal present in the N2 and N3 spectra were not discernable above the carbohydrate signals in Fractions N2 and N3. This is consistent with MALDI-ToF evidence (Table 1, page 55) that shows most of the acidic polysaccharides are eluted during the SEC before Fraction N1 was collected but that there is a small amount of acidic polymers contaminating N1.



**Figure 23: Anomeric region of  $^1\text{H}$  NMR of Fraction A2 in  $\text{D}_2\text{O}$  (70°C probe temperature)**

Some signals in the anomeric region of the proton NMR of Fraction A2 (Figure 23) were very similar to those published for a softwood and hardwood 4-*O*-methylglucuronoxylans [21, 83]. The doublet at  $\approx 4.63$  ppm ( $^3J_{\text{H,H}} \approx 7.2$  Hz) was a very close match to the signal assigned to the H-1 proton on 1,2,4-linked  $\beta$ -D-xylopyranosyl units where 4-*O*-methyl- $\alpha$ -D-glucopyranosyluronic acids are attached [83, 105].

The signals around 4.48 ppm (Figure 23) might be a doublet with an  $^3J_{\text{H,H}}$  of approximately 7.5 Hz, and is a very close match to the signal assigned to H-1 protons of 1,4-linked  $\beta$ -D-xylopyranosyl backbone units [21, 83, 105]. If this is a doublet then it has been distorted by overlapping signals. The overlapping signals would likely be due to the H-1 signal of 1,6 linked  $\beta$ -D-galactopyranosyl at 4.47 ppm, [21]. The acidic fractions were found to be enriched in 1,6-linked D-galactopyranosyl units (Figure 30) and Fraction A2 was found to contain very high levels of D-galactosyl (Table 7, page 83).

There is more uncertainty about assigning the signals (Figure 23) at shifts around 5.28 ppm, 5.26 ppm, and 5.18 ppm based on literature examples. Some literature assigns signals around 5.27 ppm as being from the H-1 signal of 1-linked  $\alpha$ -L-arabinofuranosyl branches [21]. Others assign a broad singlet somewhere between 5.2 ppm and 5.3 ppm as the H-1 signal of 4-*O*-methyl- $\alpha$ -D-glucopyranosyluronic acids linked to a xylan backbone [21, 35, 90]. Based on the literature assignments and information about the composition of Fraction A2 (Table 7, page 83 and Table 9, page 91) a tentative assignment of these signals would be that the doublet around 5.26 ppm is from H-1 signal of terminal  $\alpha$ -L-arabinofuranosyl units, that is superimposed over a less intense broader signal that extends out towards 5.28 ppm from the H-1 of 4-*O*-methyl- $\alpha$ -D-glucopyranosyluronic acids linked to the C-2 position of the xylan backbone.

This NMR evidence from the acidic fractions is consistent with these fractions containing a 1,4-linked  $\beta$ -D-xylopyranosyl backbone with 1,2,4 linked  $\beta$ -D-xylopyranosyl branch points and 4-*O*-methyl- $\alpha$ -D-glucopyranosyluronic acids attached to these branch points. 1-linked  $\alpha$ -L-arabinofuranosyl units are likely to be present, but it is uncertain if they are attached to the D-xylopyranosyl backbone or separate arabinogalactan polymers. Some correlations found in monomer composition across the fractions (page 85), suggested that most of the L-arabinosyl units are not associated with D-xylosyl units, but could be associated with D-galactosyl units.

### 3.3.2 Neutral Fractions

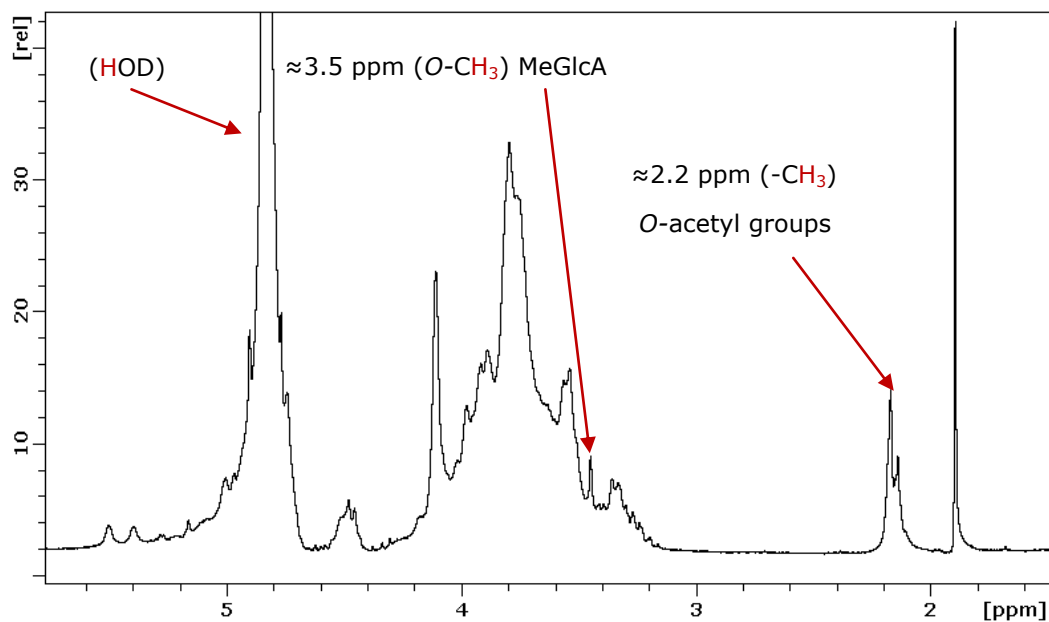


Figure 24:  $^1\text{H}$  NMR of Fraction N1 in  $\text{D}_2\text{O}$ . (27°C probe temperature)

Most signals consistent with partially-acetylated hexose polymers [89]. Some evidence of trace 4-O-methylglucuronic acid (MeGlcA) contamination [90].

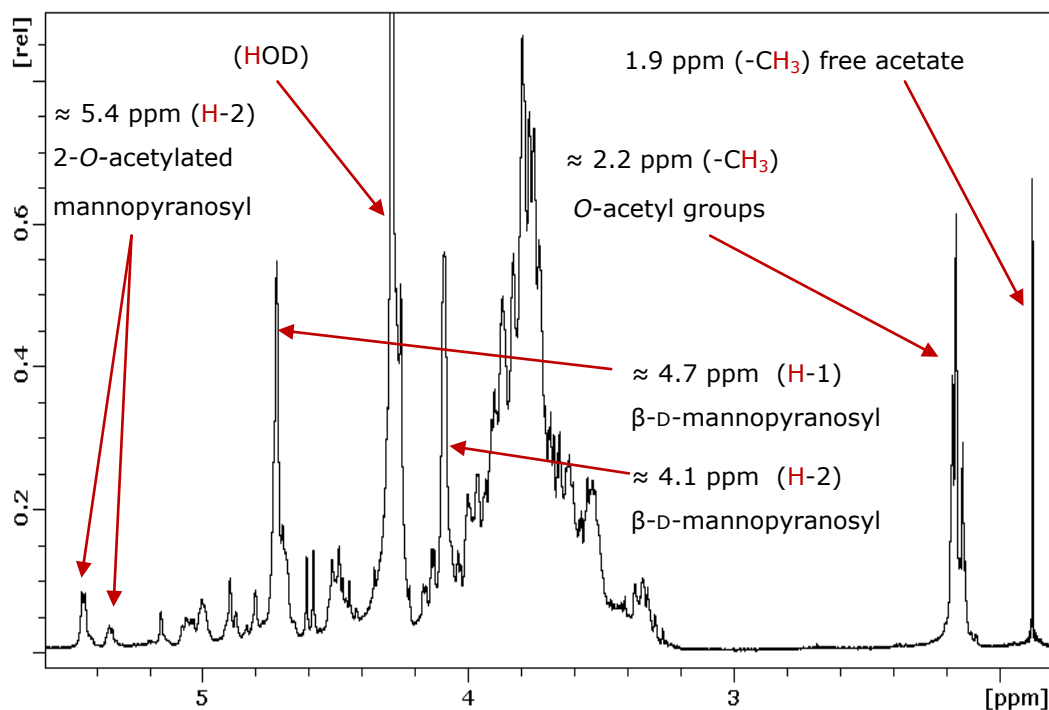
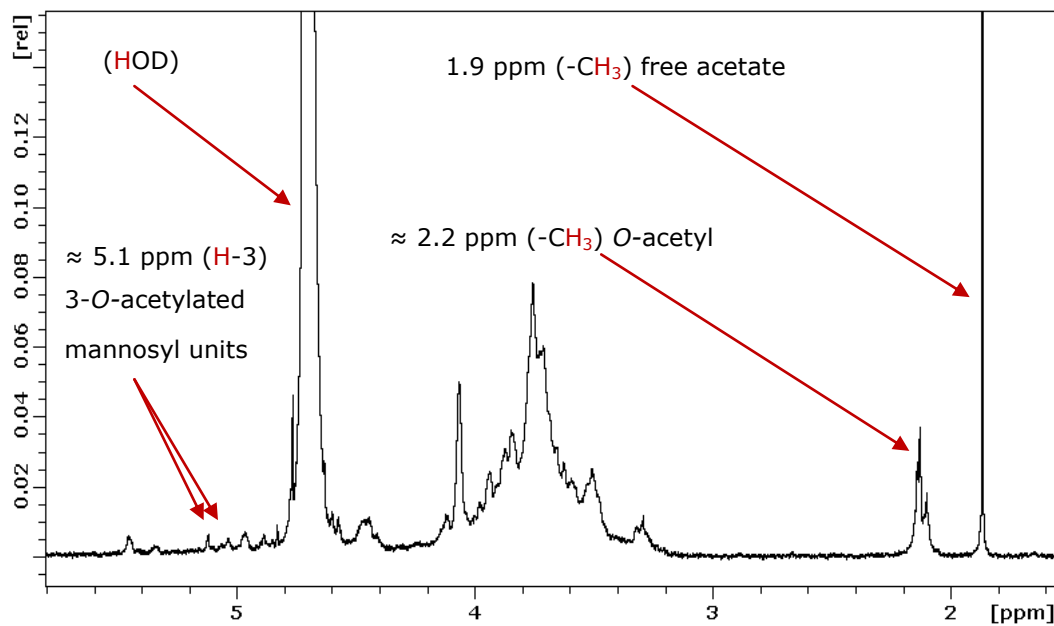


Figure 25:  $^1\text{H}$  NMR of Fraction N2 in  $\text{D}_2\text{O}$ . (70°C probe temperature)

Assignments based on literature [21, 36, 90].

A large broad group of overlapping signals around 2.2 ppm were observed in the  $^1\text{H}$  spectra of Fractions N1, N2, and N3 (Figure 24 and Figure 25) that is consistent with literature shift values for *O*-acetyl groups attached to xylans [35] or galactoglucomannans [89]. Only very low intensity signals were observed between 2.1 and 2.3 ppm in fractions A1, A2 and A3. This is consistent with earlier MALDI-ToF results (pages 54 and 53) where no acetyl groups were detected attached to the acidic polysaccharides, and the literature reports of softwood xylans that are generally free of acetyl groups [26].



**Figure 26:**  $^1\text{H}$  NMR of Fraction N2 in  $\text{D}_2\text{O}$  acquired two weeks after Figure 25. (70°C probe temperature) Assignments based on literature [21, 89].

A sharp singlet signal at 1.9 ppm was a major presence in most proton NMR spectra (Figure 22 to Figure 26). This shift has been attributed to acetate in the literature [36, 90]. When present in the neutral fractions its present is likely due to de-acetylation after the SEC step. This is because free acetate ions would carry a charge, so should elute with the acidic polysaccharide fractions during SEC if it is formed during prehydrolysis or isolation steps. In Fraction N2, the 1.9 ppm signal appeared to increase in relative intensity when further NMR experiments were carried out on the same sample after two weeks of storage in D<sub>2</sub>O at room temperature. In addition the relative intensity of *O*-acetyl signals around 2.2 ppm was reduced after storage (Figure 26). These changes during the storage, processing, or analysis of the polysaccharides will increase the uncertainty when estimating the degree of acetylation of the polymers.

Initial attempts to estimate the average degree of acetylation from NMR spectra involved integration of carbohydrate signals between 4.2 ppm and 3.0 ppm, *O*-acetyl signals around 2.2 ppm, and the free acetate signals around 1.9 ppm. The integral values for *O*-acetyl and acetate were each divided by 3 (number of protons in each acetyl group) to give N values (number of acetyl groups). The integral values for carbohydrate signals between 4.2 ppm and 3.0 ppm were divided by 6 (this assumed that neutral fractions were mostly hexoses and that each hexose unit contributes 6 protons to this region: H-2, H-3, H-4, H-5, H-6a and H-6b, [36]) to give N values (number of hexose groups). The *O*-acetyl and acetate N values were then each divided by the N values for the hexose to produce NMR average DS<sub>Ac</sub> values (Equation 2, Equation 3, Table 4).

**Equation 2: Estimating Observed DS<sub>Ac</sub>**

$$DS_{Ac} (\text{observed}) \approx \frac{\left( \frac{\text{integral of } O\text{-acetyl signals around 2.2 ppm}}{3 \text{ (protons)}} \right)}{\left( \frac{\text{integral of signals between 4.2 ppm and 3.0 ppm}}{6 \text{ (protons)}} \right)}$$

**Equation 3: Estimating 'Original' DS<sub>Ac</sub>**

$$DS_{Ac} (\text{'original'}) \approx DS_{Ac} (\text{observed}) + \left[ \frac{\left( \frac{\text{integral of free acetate signals around 1.9 ppm}}{3 \text{ (protons)}} \right)}{\left( \frac{\text{integral of signals between 4.2 ppm and 3.0 ppm}}{6 \text{ (protons)}} \right)} \right]$$

The separate  $DS_{Ac}$  values for *O*-acetyl and acetate were then added together to give an ‘Original  $DS_{Ac}$ ’ value (Table 4). ‘Original  $DS_{Ac}$ ’ is based on the assumption that all free acetate detected in the neutral fractions was originally attached to hemicelluloses as *O*-acetyl groups when the neutral polymers eluted from the SEC system, and that further handling, storage in aqueous solution at room temperature, and during acquisition of the NMR spectra at 70°C has caused de-acetylation of the hemicelluloses. In Table 4 ‘Observed  $DS_{Ac}$ ’ refers to the *O*-acetyl groups still attached to the polysaccharide when the NMR spectrum was recorded; it is therefore based on fewer assumptions than the ‘Original  $DS_{Ac}$ ’ values.

**Table 4: Estimated degrees of acetylation for neutral fractions and comparison to literature values.**

<b>Fraction</b>	<b>NMR spectrum</b>	<b>Observed DS<sub>Ac</sub><sup>a</sup></b>	<b>‘Original’ DS<sub>Ac</sub><sup>b</sup></b>
N1	Figure 24	0.19	0.28
N2	Figure 25	0.16	0.20
N2 after 2 weeks of storage	Figure 26	0.13	0.22
N3		0.04	0.07
N2 (anomeric method) <sup>c</sup>	Figure 25	0.15	0.18
<b>Literature values of DS<sub>Ac</sub> for <i>O</i>-acetylated hexose polymers from water extracts of wood</b>			
<b>Hemicellulose source</b>	<b>Analysis method</b>	<b>DS<sub>Ac</sub></b>	
Spruce AcGGMs from microwave heat fractionation (water, 190°C, 5 min) [106]	Obtained by de-acetylation and acetic acid analysis by HPLC	0.31	
Birch <i>O</i> -acetyl glucomannans from process water (mechanical pulping) [36]	NMR	0.2	
Aspen <i>O</i> -acetyl glucomannans from two water extractions (80°C, 30 min ) after DMSO extraction [36]	NMR	0.3	
Spruce AcGGMs from microwave heat fractionation (water, 200°C, 2 min) [89]	NMR	0.28 (higher MW fraction) 0.25 (lower MW fraction)	
<p><sup>a.</sup> Observed DS<sub>Ac</sub> refers to the acetyl groups attached when the NMR was acquired.</p> <p><sup>b.</sup> ‘Original’ DS<sub>Ac</sub> was calculated based on the assumption that all the free acetate detected was attached to the carbohydrates when eluted from the SEC system then de-acetylated before the NMR was acquired.</p> <p><sup>c.</sup> Used integrals of hexose H-1 signals instead of H-(2 to 6) carbohydrate signals for calculating DS<sub>Ac</sub> values.</p>			

A second set of  $DS_{Ac}$  values was calculated for N2 by integrating and using the anomeric H-1 signals around the HOD peak (Figure 25) to estimate the relative number of hexose units. This second set of values was compared to the values from the other method. The two sets were close, but differed by  $\approx 0.02$  (12%). This provides an indication of the error in these methods. The main source of error in the H-1 method is likely to be due to the HOD peak overlap interfering with some of the H-1 signals.

In the first integration method the six non-H-1 protons for each hexose present in an *O*-acetylated (galacto)glucomannan were all assumed to be integrated between 4.2 ppm and 3.0 ppm. A significant source of error in this use of integrals is caused by each 3-*O* or 2-*O* acetyl group attached to a hexose shifting a single hexose proton out of the area that was integrated (between 4.2 ppm and 3.0 ppm) [36, 89]. This means that each hexose with a single attached acetyl group will only contribute 5 protons instead of 6 protons to this area (between 4.2 ppm and 3.0 ppm) and any hexose that is acetylated at both 3-*O* and 2-*O* positions should only contribute 4 protons to the area integrated between 4.2 ppm and 3.0 ppm. Potential improvements to the accuracy of the  $DS_{Ac}$  estimates could be obtained by adding in the integrals of the H-2 and H-3 signals that are outside the area between 4.2 ppm and 3.0 ppm, if they are free of interference and can be correctly assigned. Another approach to mitigate this error could be a mathematical adjustment of Equations 2 and 3 using the  $DS_{Ac}$  estimates in Table 4 to account for 'hexose protons with signals between 4.2 ppm and 3.0 ppm' =  $(6 - DS_{Ac})$  instead of 6. This would generate a new adjusted set of  $DS_{Ac}$  estimates which could have greater accuracy.

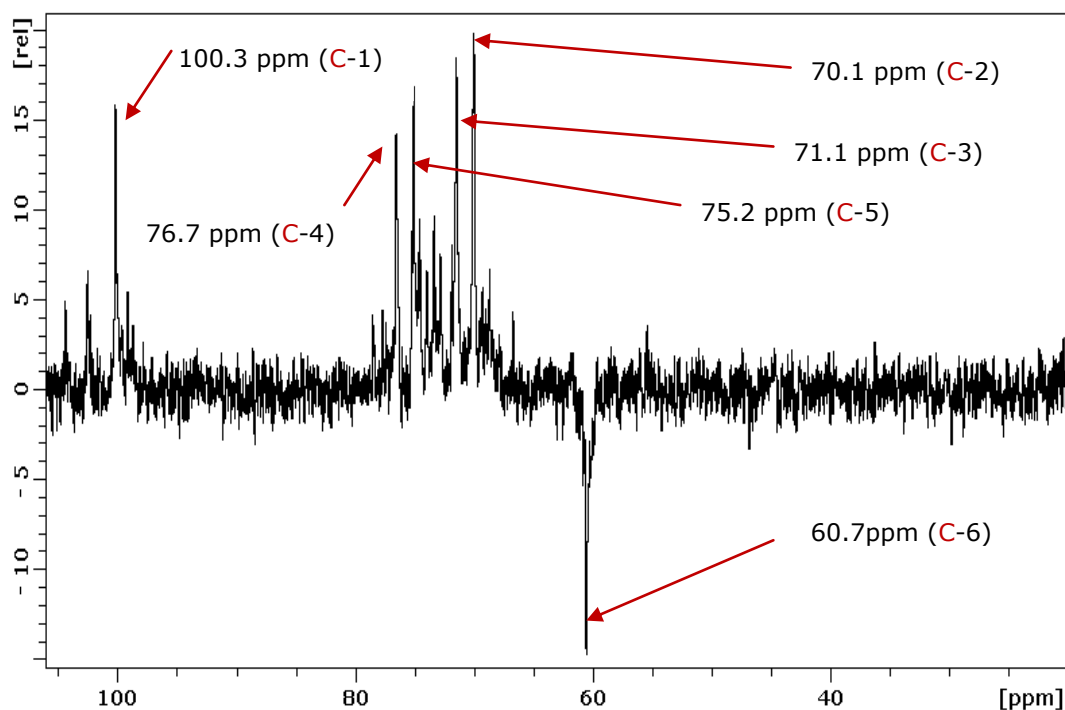


**Figure 27:**  $^{13}\text{C}$  DEPT135 of Fraction N2 in  $\text{D}_2\text{O}$ . ( $37^\circ\text{C}$  probe temperature)

The signals of the most abundant hexopyranosyl repeating unit are assigned and are likely to be from the  $\beta$ -(1  $\rightarrow$  4)-linked D-mannopyranosyl backbone of the AcGGM polymers [21, 122].

Trials of one dimensional  $^{13}\text{C}$  NMR on various fractions generally produced poor signal/noise ratios and were time consuming to collect making them of little value for assigning signals. However, the DEPT135 of Fraction N1 recorded on the 300 MHz machine showed six dominant signals of similar intensity (Figure 27). These signals were consistent with a single major hexose repeating unit as assigned. These six hexose carbon shifts were very similar to those reported in the literature for  $\beta$ -(1 $\rightarrow$ 4)-linked D-mannopyranosyl dominated oligosaccharide fragments of acetylated-GGM from aloe gel [122]. They also followed a similar pattern to those assigned to the  $\beta$ -(1  $\rightarrow$ 4)-linked D-mannopyranosyl backbone of spruce AcGGM [21], although the shifts were each approximately 1 ppm less in Figure 27 which could be due to differences in referencing. *O*-acetyl groups gave weak signals around 20 ppm, but these were not easy to discern above baseline noise. A number of less intense carbohydrate signals were also observed.

### 3.4 Acid Hydrolysis and Monomer Composition Analysis

#### 3.4.1 Analysis of Neutral Components by Conversion to Alditol Acetates

**Table 5: Monosaccharide components by mol ratio relative to D-mannose**

	D-galactose	D-glucose	D-xylose	D-mannose	L-arabinose
<b>Crude</b>	0.31	0.27	0.48	1.00	0.15
<b>A1</b>	n.d.	n.d.	n.d.	n.d.	n.d.
<b>A2</b>	2.91	0.87	1.08	1.00	0.88
<b>A3</b>	1.96	0.77	5.26	1.00	0.74
<b>N1</b>	0.06	0.25	0.05	1.00	0.00
<b>N2</b>	0.24	0.27	0.08	1.00	0.09
<b>N3</b>	0.80	0.35	1.11	1.00	0.42

**Table 6: Monosaccharide composition of samples in mol%**

	D-galactose	D-glucose	D-xylose	D-mannose	D-arabinose
<b>Crude</b>	14%	12%	22%	45%	7%
<b>A1</b>	n.d.	n.d.	n.d.	n.d.	n.d.
<b>A2</b>	43%	13%	16%	15%	13%
<b>A3</b>	20%	8%	54%	10%	8%
<b>N1</b>	5%	18%	4%	73%	0%
<b>N2</b>	14%	16%	5%	59%	6%
<b>N3</b>	22%	9%	30%	27%	11%

Monosaccharide composition after acid hydrolysis was obtained for the crude samples and for five of the fractions from SEC (Table 5 and Table 6). The GC-MS analysis of Fraction A1 showed no clear results for alditol acetates, which could have been due in part to it being the least concentrated fraction and more susceptible to losses during handling.

The relative proportions of D-galactosyl, D-xylosyl, and L-arabinosyl residues increased in the neutral polysaccharides as their apparent molecular weight decreased. This meant that larger polysaccharides in Fraction N1 contained the highest proportion of D-mannosyl residues while, the smaller polysaccharides in Fraction N3 contained higher proportions of D-galactosyl, D-xylosyl, and L-arabinosyl residues, and Fraction N2 was part way between.

Unexpectedly high amounts of D-galactosyl units were found in Fraction A2 and to a lesser extent Fraction A3. This indicates that there is a significant amount of hexose-based polymers in the acidic fractions that was not evident in the MALDI-ToF-MS spectra (Figure 13 and Figure 14). This could be due to poor ionisation of the D-galactosyl-based polymers or that there is such a large diversity in size and structure of these polymers that very few molecules ever have the same molecular weight. Another possibility is that these D-galactosyl-based polymers could be extremely large and gave only a few low intensity peaks in the high mass range and thus were missed during the observations of the MALDI-ToF mass spectra.

The possibility of the D-galactosyl-based polymers containing varying sized lignin and/or protein fragments covalently bound cannot be ruled out, given evidence of lignin-hemicellulose-complexes in softwoods [9, 17, 123] and arabinogalactan-proteins compounds reported to be present in *P. radiata* [31]. The fact that the mass spectra (Figure 12, Figure 13, and Figure 14) appeared completely free of any hexose-based polymers shows that although MALDI-ToF-MS can provide detailed qualitative information, any attempt at quantifying different polymers present should be treated with caution.

### 3.4.2 Analysis of Acidic Components by Ion Chromatography and NMR

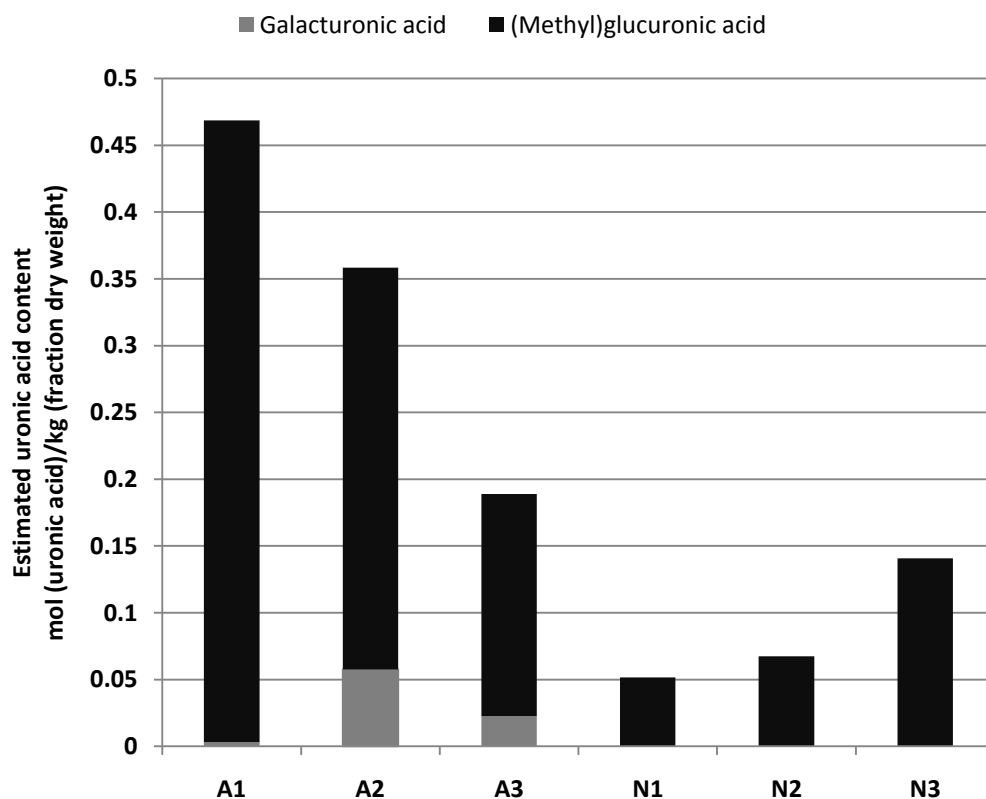


Figure 28: Estimated uronic acid content of the fractions as a proportion of fraction dryweight.

A single peak eluting at approximately 3.9 min was detected in all acidic fractions and was assumed to be D-galacturonic acid based on the retention time being similar to that of D-galacturonic acid standards. This peak assigned to D-galacturonic acid was not present in the neutral fractions, except for an insignificant trace amount detected in Fraction N2. The integration of this peak eluting at 3.9 min along with the calibration formula (Figure 7) were used to calculate the D-galacturonic acid content of the six SEC fractions (Figure 28).

Estimating the D-glucuronic acid content was made more complicated by the presence of two peaks eluting with retention times close to that of the D-glucuronic acid standard (4.7 min). These two peaks with poor resolution were observed in the chromatograms of the crude polysaccharides and the Fractions A1, A2, and A3. In contrast, only a single peak (with a retention time that appeared closer to the latter of the two peaks) was observed in the chromatograms from the neutral Fractions N1, N2, and N3. This indicates the presence of two types of molecules with retention times close to D-glucuronic acid in the acidic-polymer-derived fractions, but only a single type of molecule in the neutral-polymer-derived fractions.

The sample of acidic components from fraction N2 was analysed using proton NMR. No clear *O*-methyl signal around 3.48 ppm could be observed rising above the other carbohydrate signals in the spectrum. This result suggested that the uronic acid produced from acid hydrolysis of the Fraction N2 is the un-methylated glucuronic acid.

In order to narrow down the possibilities of where the *O*-methylated hexuronic acid (tentatively assumed to be 4-*O*-methylglucuronic acid) is eluting on the ion chromatography system, the four narrower Bio-Gel fractions of acidic components (from the complete hydrolysis of the crude sample) were each analysed by proton NMR and the ion chromatography method. Each of these four fractions was found to be a complex mixture of different components. However, relative enrichment or depletion of various components was observed across the four fractions, in both the NMR spectrum and ion chromatogram. In these four fractions, enrichment in *O*-methyl NMR signals (integral relative to the integrals of other carbohydrate signals) was observed to occur when the first of the two peaks that eluted around 4.7 minutes in the ion chromatogram was enriched (relative to the other peaks in the ion chromatogram). This evidence suggests that 4-*O*-methyl D-glucuronic acid and un-methylated D-glucuronic acid nearly co-eluted from the column. However, it does not rule out the possibility that the MeGlcA is eluting somewhere else and enrichment is being hidden by unknown factors such as other components in the samples. In the present situation the lack of a verified 4-*O*-methylglucuronic acid standard means that conclusively proving exactly how 4-*O*-methylglucuronic acid behaves on this ion chromatography system is still unresolved.

When estimating the uronic acid content, the D-glucuronic acid peak and the slightly earlier peak suspected to be 4-*O*-methylglucuronic acid were integrated together due to their poor resolution and referred to as (methyl)glucuronic acid.

The possibility of some uronic acids still having neutral sugars attached as aldobiouronic acids [24] adds further uncertainty to this method. It was tentatively assumed in the absence of standards that any aldobiouronic acids would have a similar retention time and molar detector response, and simply cause broadening of the corresponding uronic acid peak.

When estimating the uronic acid content, a further assumption was made. 4-*O*-methylglucuronic acid was assumed to have the same peak area to mol responses (molar detector response) as D-glucuronic acid and D-galacturonic acid.

This method for estimating uronic acid content was developed rapidly from some previous work [124] and is unlikely to be optimised. The method also was not validated against other existing methods for estimating uronic acid content [27, 35, 42, 125]. Identification and quantification of uronic acids from lignocellulosic sources is often very difficult and unreliable across many different methods as indicated by an inter-laboratory comparison study [27].

The determined uronic acid contents in the SEC fractions showed some distinct trends (Figure 28). Total uronic acids present in acidic fractions decreased with elution time with fractions A1, A2 and A3 containing 0.47, 0.36 and 0.19 mol/kg uronic acids, respectively. This pattern supports the theory that polysaccharides with more anionic groups are ion excluded to a greater extent under the of SEC conditions used in the separation [26]. In contrast, total uronic acid content in the neutral fractions increased with elution time and, as expected, the levels were lower than in the acidic fractions. This suggests that the neutral fraction polysaccharides containing these (methyl)glucuronic acid residues are likely to be smaller in molecular weight and relatively independent of the dominant *O*-acetylated galactoglucomannans.

Only glucuronic acid was detected in the neutral fractions and results so far indicate a lack of *O*-methyl groups. The fact that polysaccharides containing glucuronic acid are not 'ion excluded' [26, 103] and appear in the neutral fractions, can be explained if the glucuronic acid is ester linked, therefore losing its anionic behaviour. In other lignocellulosic materials, evidence of 4-*O*-methylglucuronic acids on hemicelluloses being ester-linked to lignin has been documented [51]. These results suggested that the un-methylated glucuronic acid is ester linked and present in these neutral fractions.

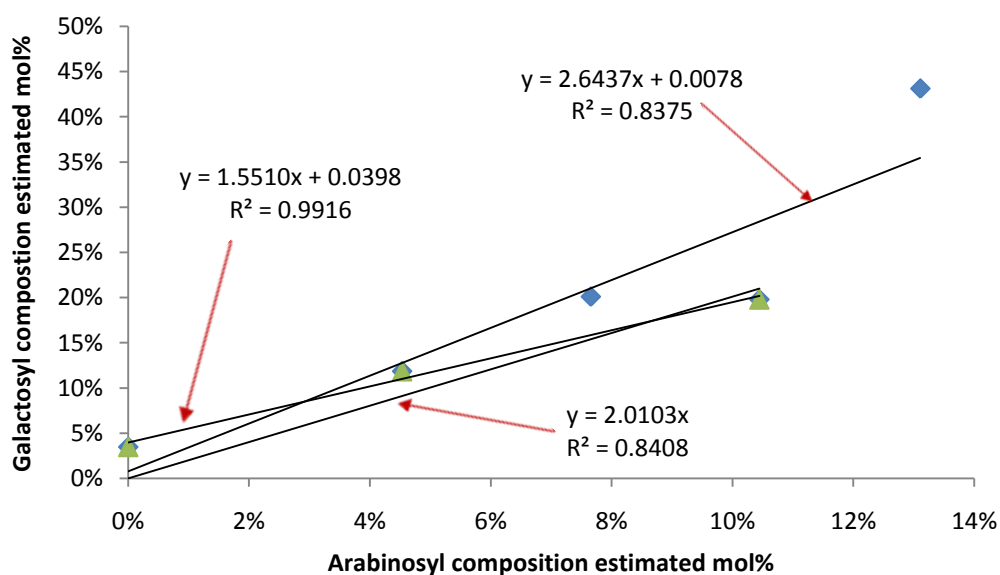
### 3.4.3 Interpretation of Monomer Composition Information

Table 7: Estimated mol% of monomer components

Component	N1	N2	N3	A2	A3
D-galactosyl <sup>a</sup>	3.5%	11.9%	19.8%	43.1%	20.1%
D-glucosyl <sup>a</sup>	14.3%	13.0%	8.6%	12.9%	7.9%
D-xylosyl <sup>a</sup>	3.1%	4.1%	27.5%	16.1%	54.1%
D-mannosyl <sup>a</sup>	56.6%	48.8%	24.8%	14.8%	10.3%
L-arabinosyl <sup>a</sup>	0.0%	4.5%	10.4%	13.1%	7.7%
acetyl <sup>b</sup>	21.8%	16.8%	6.9%	0.0%	0.0%
D-galacturonic acid <sup>c</sup>	0.0%	0.0%	0.0%	0.9%	0.3%
(Methyl) D-glucuronic acid <sup>c</sup>	0.7%	0.9%	2.0%	4.9%	2.5%
<p><sup>a.</sup> Neutral monosaccharide mol% were taken from the alditol acetate GC-MS results with the assumption that these monosaccharides made up most of the fraction dryweight not attributed to acetyl or uronic acid content. Fraction dryweights used were based on measurements of the first fourteen SEC runs.</p> <p><sup>b.</sup> Acetyl group mol% was estimated from NMR integrals with adjustments made using the hexose/pentose ratio in each neutral fraction produced from alditol acetate results.</p> <p><sup>c.</sup> Uronic acid contents were calculated as un-methylated units based on ion chromatography results.</p>					

Table 7 is the results from Table 6 adjusted to include estimated contents of uronic acids and acetyl groups. As these values come from different experiments each with their own set of uncertainties, errors, and assumptions it is unlikely that the mol% composition values in Table 7 are an accurate representation of the absolute composition of each fraction. However, these values provide a tool for comparing different fractions and for understanding how different components are related in terms of behaviour on the SEC column and/or being linked to each other.

In an attempt to understand the relationships between different components, when all the fractions likely contain some level of mixing of polysaccharide types, a number of correlation plots were generated. These involved plotting the mol% data for one component against another component and generating a linear “least squares” line of best fit and an  $R^2$  correlation coefficient. This was repeated across many combinations of the different components. The entire dataset (A2, A3, N1, N2, and N3) and the neutral fraction dataset (N1, N2, and N3) were both used to generate lines in order to assess how relationships between different components could change due to the different SEC behaviour in the acidic fractions. An example of the plots generated is shown in Figure 29. The linear regression equations linking the components, together with their respective  $R^2$  values are shown in Table 8 (full table in Appendix page 111). The  $R^2$  values can then be used to compare the strength of different linear correlations to test which components are likely to be linked together in which polymer types. The slopes of these lines of best fit could give insight into the average ratio of different components especially when forced through the origin (zero point).



**Figure 29: Plot of correlations between estimated content of D-galactosyl and L-arabinosyl**  
**Three linear correlations shown: dataset of only neutral fractions (N1, N2 and N3) with an  $R^2 = 0.9916$ , dataset of only neutral fractions (N1, N2 and N3) zero forced with an  $R^2 = 0.8408$ , and the total dataset (A2, A3, N1, N2 and N3) with an  $R^2 = 0.8375$**

**Table 8: Useful linear correlations between mol % estimates of different components**

Y axis, Mol%	X axis, Mol%	Linear Formula, Full Dataset	Linear Formula, Neutral Dataset	Linear Formula, Zero forced <sup>a</sup>
<b>D-Mannosyl</b>	<b>D-Glucosyl</b>	$y = 5.0797x - 0.2647$ $R^2 = 0.5028$	$y = 5.601x - 0.2358$ $R^2 = 0.9999$	$y = 3.7069x$ $R^2 = 0.8809$
<b>D-Mannosyl</b>	<b>Acetyl</b>	$y = 2.076x + 0.122$ $R^2 = 0.9896$	$y = 2.1696x + 0.105$ $R^2 = 0.9893$	$y = 2.765x$ $R^2 = 0.9023$
<b>D-Galactosyl</b>	<b>L-Arabinosyl</b>	$y = 2.6437x + 0.0078$ $R^2 = 0.8375$	$y = 1.551x + 0.0398$ $R^2 = 0.9916$	$y = 2.0103x$ $R^2 = 0.8408$
<b>D-Xylosyl</b>	<b>(Methyl) glucuronic acid</b>	$y = 3.7397x + 0.1272$ $R^2 = 0.0898$	$y = 19.711x - 0.124$ $R^2 = 0.9819$	$y = 11.352x$ $R^2 = 0.7667$
<b>D-Galactosyl</b>	<b>Galacturonic acid</b>	$y = 33.08x + 0.1123$ $R^2 = 0.8407$	$y = 98.019x + 0.116$ $R^2 = 0.0002^b$	$y = 47.466x$ $R^2 = 0.355$
<b>D-Glucosyl</b>	<b>Acetyl</b>	$y = 0.1884x + 0.0961$ $R^2 = 0.4183$	$y = 0.387x + 0.061$ $R^2 = 0.9877$	$y = 0.7315x$ $R^2 = 0.0736$
<b>D-Xylosyl</b>	<b>L-Arabinosyl</b>	$y = 1.7332x + 0.0858$ $R^2 = 0.1775$	$y = 2.4225x - 0.005$ $R^2 = 0.8417$	$y = 2.3612x$ $R^2 = 0.8408$
<b>L-Arabinosyl</b>	<b>(Methyl)gluc uronic acid<sup>c</sup></b>	$y = 2.6172x + 0.0137$ $R^2 = 0.7445$	$y = 7.252x - 0.0381$ $R^2 = 0.9267$	$y = 4.6754x$ $R^2 = 0.7841$
<p><sup>a.</sup> Zero forced linear formula used the neutral fraction datasets.</p> <p><sup>b.</sup> Very little or no galacturonic acid was detected in neutral fractions.</p> <p><sup>c.</sup> (Methyl)glucuronic acid represents the content of glucuronic acid in addition to estimated content of what was tentatively assigned as methylglucuronic acid. In the neutral fractions only the un-methylated glucuronic acid appeared to be present.</p>				

Discerning the strongest associations between components involved first rejecting all linear formula with negative slopes (Table 12, page 111). Comparing the  $R^2$  values from both the neutral and full datasets allowed the strongest associations to be found. The zero (origin) forced linear formula slopes (most from the neutral fraction dataset) were used to estimate average ratios of different components. The findings from this analytical process follow below:

- D-mannosyl content, acetyl content, and D-glucosyl content all have very strong associations to each other ( $R^2 = 0.9893, 0.9999$ ) over the neutral fractions indicating that a single polymer type accounts for close to all the D-mannosyl, acetyl, and D-glucosyl residues found in the neutral fractions. The average mol ratio of components in this polymer is estimated to be 3.7 : 1.3 : 1 (D-mannosyl : acetyl : D-glucosyl) based on the relative gradients of the zero forced linear formulas and appears reasonably consistent across Fractions N1, N2, and N3. This ratio is close to ratios reported for a type of water-soluble *O*-acetylated galactoglucomannan isolated from Norway spruce and radiata pine [4, 17, 21, 30, 106].
- The strong association between D-mannosyl content and D-glucosyl content becomes inconsistent and weaker ( $R^2 = 0.5028$ ) when the acidic fractions are included in the dataset. This indicates that a large proportion of the D-glucosyl in the acidic fractions is not associated with the same glucomannan polymer that dominates the neutral fractions. Another type of high-glucosyl glucomannan, glucan or cellulose could be soluble only when attached in some way to an anionic group. The presence of (cellulose or glucomannan)-lignin-(anionic galactan or xylan) type complexes [9, 11, 126], could be potential explanations for this D-glucosyl enrichment in the acidic fractions.

- D-galactosyl content and L-arabinosyl content have a very strong association to each other ( $R^2 = 0.9916$ ) in the neutral fractions which weakens slightly ( $R^2 = 0.8375$ ) when the acidic fractions are added. These associations are much stronger than the ones between L-arabinosyl and D-xylosyl contents ( $R^2 = 0.8417, 0.1775$ ) and indicates that the majority of D-galactosyl and L-arabinosyl residues found across all fractions are likely to be attached together in similar polymer types. This does not discount the hypothesis that some L-arabinosyl units are attached to xylans or that some D-galactosyl units are attached to the glucomannan polymers, it only indicates that the majority of D-galactosyl and L-arabinosyl residues are not attached to xylans and glucomannans. The average mol ratio of these components is estimated to be 2 : 1 (D-galactosyl : L-arabinosyl), which represents a significantly higher proportion of L-arabinosyl residues than normally reported for softwood arabinogalactans [4, 29].
- D-xylosyl content and glucuronic acid content have a stronger association ( $R^2 = 0.9819$ ) in the neutral fractions than D-galactosyl content and glucuronic acid ( $R^2 = 0.8713$ ). This indicates that the glucuronic acid detected in the neutral fractions could be linked to xylan-based polymers.

The strong associations detailed above provide evidence that the majority of the two specified components are travelling together in consistent proportions when fractionated on the SEC system. The causes of these associations could have a number of different potential explanations. The most likely explanation for a strong association is that most of the two components are covalently linked in the same type of polymer and also that the polymer type keeps similar proportions of different components regardless of the polymer's size. However, alternative explanations such as the two components each being part of two or more independent polymer types which all happen to have very similar SEC behaviour cannot be discounted based on this evidence.

### 3.5 Linkage Analysis

The method used is unlikely to be effective for detecting the points where the uronic acids are attached to the polysaccharides due to the difficulty experienced with reducing the carboxylic acid groups and the resistance of the uronic acid linkages to acid hydrolysis [115]. Alternative reduction methods involving esterification and/or activation of the acid, often in conjunction with the use of stronger reducing agents are reported in the literature [41, 44, 115]. However, due to time and material constraints these methods were not successfully applied to these samples. These methods are recommended if a more complete picture of uronic acid attachment is a focus of any future research.

The two most abundant PMAAs detected in the crude polysaccharide samples were consistent with 1,4-linked D-xylopyranosyl and 1,4-linked D-mannopyranosyl units. The 1,4-linked D-xylopyranosyl PMAA was dominant in the acidic fractions and the 1,4-linked D-mannopyranosyl PMAA was dominant in the neutral fractions, especially the sample from Fraction N1.

The PMAAs which were detected and identified, their retention times, and the deduced linkages from which they were likely produced are displayed in Table 10. Approximate proportions of total-ion peak areas are displayed in Table 9 along with deduced linkages. Caution is recommended in interpretation of these proportions as large variations were observed between the duplicates of the crude samples. The ratios between 1,4-linked D-mannopyranosyl PMAA and 1,4-linked D-glucopyranosyl PMAA peak areas were also very different from that which would be expected, given the D-mannosyl and D-glucosyl ratios from the monomer composition analysis (Table 7, page 83).

The linkages deduced from the PMAA indicate that Fraction N1 was the closest to containing a single type of polysaccharide and that the polysaccharide is structurally consistent with a typical softwood (galacto)glucomannan [17, 21, 30]. It likely contains a 1,4-linked backbone of D-mannopyranosyl and D-glucopyranosyl with a small amount of 1-linked terminal D-galactopyranosyl branches linked to the C-6 oxygen of some backbone D-mannopyranosyl units. (Table 9). Smaller amounts of other linkages were detected which often increase in relative abundance in the composite neutral fraction sample. This is evidence for an increase in structural diversity in the smaller molecular weight neutral polysaccharides.

The smaller molecular weight neutral polymers (Fractions N2 and N3) appear to be shorter (galacto)glucomannan fragments and a mixture of other types of polysaccharide. These other types of polysaccharide could include pentose based arabinan, xylan, and/or arabinoxylan. Some of the D-galactosyl enrichment in Fraction N3 (page 77) is likely due to 1,4-linked D-galactopyranosyl based polymers which is consistent with them being fragments of a compression wood galactan from *P. radiata* [19].

Evidence for some branching of the 1,4-linked D-xylopyranosyl backbone at the C-3 oxygen was found in the acidic fractions (and to a lesser extent in the neutral fractions). The literature [25] suggests that these branches should be terminal L-arabinofuranosyl units. However, only very small amounts of terminal L-arabinofuranosyl PMAAs were detected. Possible reasons for this include (i) that the L-arabinofuranosyl units are more vulnerable to decomposition in the severe acid hydrolysis step [92], (ii) that some of the uronic acid branch points are unexpectedly being detected by this method, or (iii) that another group is attached to this branch point.

A number of other PMAA were detected in very small abundance and had shorter retention times than anything listed in the primary literature source [115]. Some of the mass spectra of these PMAA were consistent with what was expected to be produced from the reducing end monomer, especially 4-linked hexoses. However, the absence of standards of these PMAAs or relative retention times from literature limits the confirmation of their identities. One of the more prominent PMAA peaks of this type had a mass spectrum that was very similar to the 4-*O*-acetyl-1,2,3,5,6-penta-*O*-methyl-D-glucitol PMAA produced from the lactose standard, yet had a slightly shorter retention time suggesting that it could be from another reducing-end 4-linked hexose. One possibility could be 4-*O*-acetyl-1,2,3,5,6-penta-*O*-methyl-D-mannitol.

Major contaminant peaks were present in the gas chromatograms of all PMAA samples and they did not have mass spectra consistent with PMAAs. The  $m/z$  149 ion found in the mass spectrum of these peaks indicates phthalate ester type contaminants [127], perhaps due to the use of plastic vial lids during steps such as acid hydrolysis.

**Table 9: Linkages deduced from detected partially methylated alditol acetates, approximate proportions represented as percentage of total indentified PMAA peak area within each sample.**

<b>Deduced Linkage</b>	<b>Crude</b>	<b>Acidic Fractions (A1, A2 and A3 combined)</b>	<b>Neutral Fractions(N1, N2 and N3 combined)</b>	<b>Fraction N1</b>
1,4 linked D-mannopyranosyl	32%	12%	36%	41%
1,4 linked D-xylopyranosyl	17%	24%	8%	2%
1,4 linked D-glucopyranosyl	17%	15%	23%	32%
Terminal D-galactopyranosyl	6%	15%	7%	7%
Terminal D-mannopyranosyl and/or Terminal D-glucopyranosyl	7%	<1%	7%	3%
1,5 linked L-arabinofuranosyl and/or 1,4 linked L-arabinopyranosyl	4%	15%	4%	<1%
Terminal L-arabinofuranosyl	4%	<1%	1%	<1%
1,4,6 linked D-mannopyranosyl	3%	0%	4%	7%
Terminal D-xylopyranosyl	1%	1%	0%	2%
1,4 linked D-galactopyranosyl	2%	<1%	5%	<1%
1,3 linked D-galactopyranosyl	4%	3%	1%	2%
1,4,6 linked D-galactopyranosyl	3%	3%	3%	4%
1,3,4 linked D-xylopyranosyl	<1%	8%	1%	<1%
1,6 linked D-galactopyranosyl	1%	4%	0%	0%

**Table 10: Partial methylated alditol acetates detected and identified.**

<b>Partially Methylated Alditol Acetate (Identified by comparison of mass spectrum and retention times)</b>	<b>Deduced Linkage(s)</b>	<b>Retention time (min)</b>
1,4,5-tri- <i>O</i> -acetyl-1-deuterio-2,3,6-tri- <i>O</i> -methyl-D-mannitol	1,4-linked D-mannopyranosyl	17.82
1,4,5-tri- <i>O</i> -acetyl-1-deuterio-2,3-di- <i>O</i> -methyl-D-xylitol	1,4-linked D-xylopyranosyl	16.54
1,4,5-tri- <i>O</i> -acetyl-1-deuterio-2,3,6-tri- <i>O</i> -methyl-D-glucitol	1,4-linked D-glucopyranosyl	18.46
1,5-di- <i>O</i> -acetyl-1-deuterio-2,3,4,6-tetra- <i>O</i> -methyl-D-galactitol	Terminal-D-galactopyranosyl	15.82
1,5-di- <i>O</i> -acetyl-1-deuterio-2,3,4,6-tetra- <i>O</i> -methyl-D-(mannitol/glucitol)	Terminal-D-(manno and/or gluco)pyranosyl	15.02
1,4,5-tri- <i>O</i> -acetyl-1-deuterio-2,3-di- <i>O</i> -methyl-L-arabinitol	1,5-linked L-arabinofuranosyl and/or 1,4-linked L-arabinopyranosyl	15.95
1,4-di- <i>O</i> -acetyl-1-deuterio-2,3,5-tri- <i>O</i> -methyl-L-arabinitol	Terminal-L-arabinofuranosyl	12.32
1,4,5,6-tetra- <i>O</i> -acetyl-1-deuterio-2,3-di- <i>O</i> -methyl-D-mannitol	1,4,6-linked D-mannopyranosyl	20.20
1,5-di- <i>O</i> -acetyl-1-deuterio-2,3,4-tri- <i>O</i> -methyl-D-xylitol	Terminal-D-xylopyranosyl	13.42
1,4,5-tri- <i>O</i> -acetyl-1-deuterio-2,3,6-tri- <i>O</i> -methyl-D-galactitol	1,4-linked D-galactopyranosyl	18.26
1,3,5-tri- <i>O</i> -acetyl-1-deuterio-2,4,6-tri- <i>O</i> -methyl-D-galactitol	1,3-linked D-galactopyranosyl	17.38
1,4,5,6-tetra- <i>O</i> -acetyl-1-deuterio-2,3-di- <i>O</i> -methyl-D-galactitol	1,4,6-linked D-galactopyranosyl	20.82
1,4,3,5-tetra- <i>O</i> -acetyl-1-deuterio-2- <i>O</i> -methyl-D-xylitol	1,3,4-linked D-xylopyranosyl	19.21
1,5,6-tri- <i>O</i> -acetyl-1-deuterio-2,3,4-tri- <i>O</i> -methyl-D-galactitol	1,6-linked D-galactopyranosyl	19.38
4- <i>O</i> -acetyl-1,2,3,5,6-penta- <i>O</i> -methyl-D-(mannitol/glucitol)	4-linked reducing end D-(mannosyl/glucosyl)	11.43

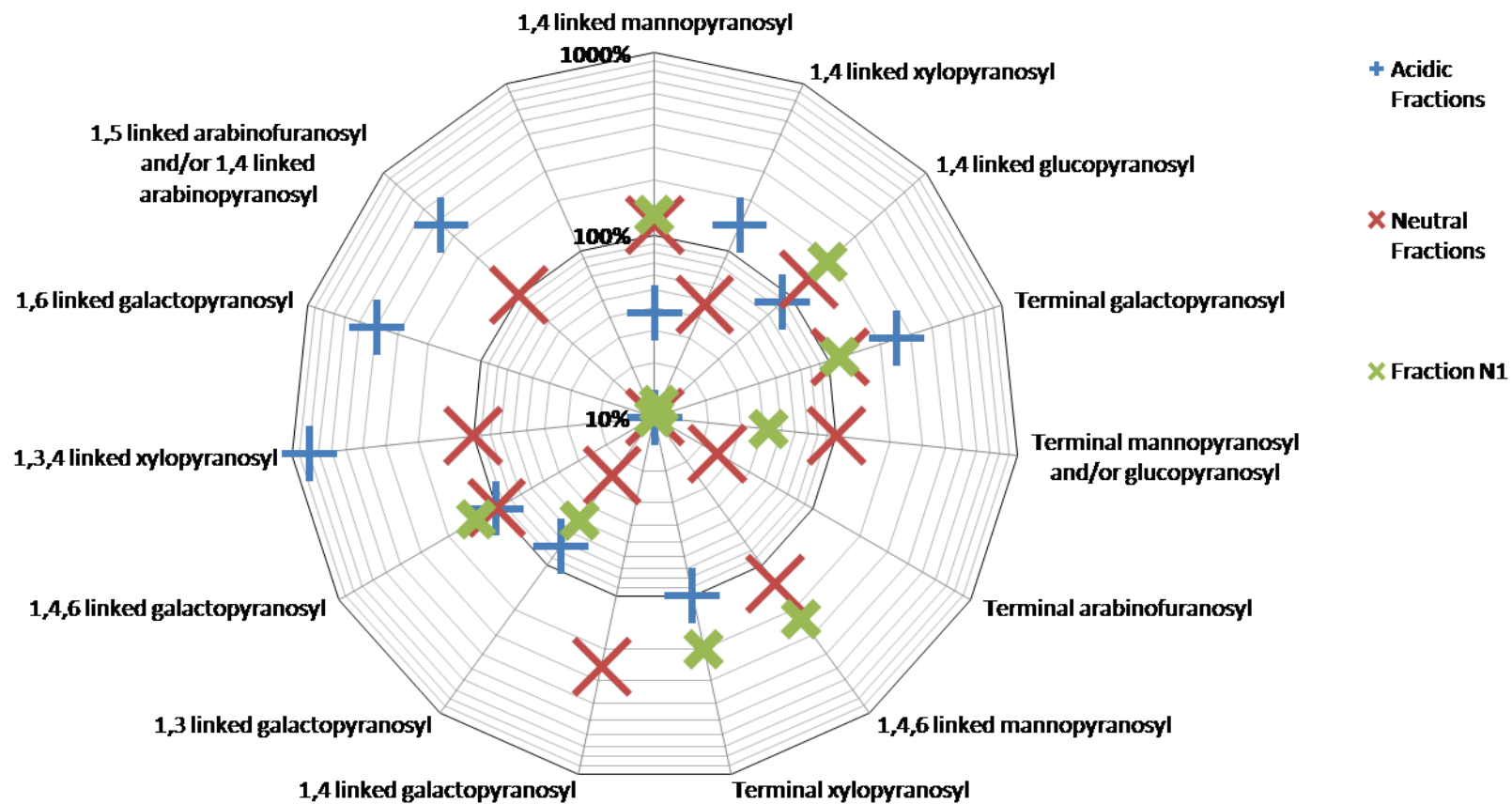


Figure 30:Relative enrichment and depletion of detected linkages

All points calculated by dividing the linkage composition proportion in the fraction by the linkage composition proportion in the crude(unfractionated) sample.

Enrichment in a linkage is indicated by the fraction's point falling between the 100% and 1000% lines. Relative depletion in a linkage is indicated by the fraction's point falling between the 100% line and the centre. The 100% line represents the relative composition of the crude (unfractionated) sample. Scale is logarithmic.

The composite sample of all the neutral fractions had a far greater diversity of linkages than those detected in Fraction N1 (Figure 30). This along with the monomer composition results (Table 7, page 83) indicates that the lower molecular weight polymers in Fraction N3 (and to a lesser extent Fraction N2) are a mixture of many different polymer types. From the linkage analysis results it can be deduced that these non-mannan polymers are composed of mainly of: 1,4-linked D-xylopyranosyl, 1,4-linked D-galactopyranosyl, and 1,5-linked L-arabinofuranosyl units with indication of some branching at 1,3,4-linked D-xylopyranosyl and 1,4,6-linked D-galactopyranosyl units.

The composite sample of the acidic fractions also indicates a high diversity of linkages and polymer types (Figure 30). These minor polymers are likely to be composed of: terminal-D-galactopyranosyl, 1,4-linked D-glucopyranosyl, 1,4-linked D-mannopyranosyl, 1,6-linked D-galactopyranosyl, 1,4,6-linked D-galactopyranosyl, and 1,3-linked D-galactopyranosyl linkages. A PMAA consistent with 1,5-linked L-arabinofuranosyl was detected, however the same PMAA (1,4,5-tri-*O*-acetyl-1-deuterio-2,3-di-*O*-methyl-L-arabinitol) would be produced from 1,4-linked L-arabinopyranosyl. Literature often assigns this PMAA as 1,5-linked L-arabinofuranosyl [31, 32]. Further NMR work, possibly after partial hydrolysis and fractionation is recommended to deduce if these L-arabinosyl units are in the furanose or pyranose ring forms.

## Chapter 4 Summary and Conclusions

### 4.1 Types of Polysaccharides in the Prehydrolysate

**Table 11: Estimated yields of different polymer types identified**

	% by mass of crude polymeric carbohydrates isolated <sup>a</sup>	g/kg dry woodchips <sup>a</sup>
Neutral O-acetylated (galacto)glucomannans <sup>b</sup>	54%	10.9
Neutral (arabinoglucurono)xylans <sup>c</sup>	6%	1.1
Neutral galactans, arabinogalactans & arabinans <sup>d</sup>	8%	1.6
Anionic glucans and/or glucomannans <sup>e</sup>	7%	1.4
Anionic (arabino)glucuronoxylans <sup>f</sup>	12%	2.3
Anionic galactans, arabinogalactans & arabinans <sup>g</sup>	11%	2.1
<p><sup>a.</sup> These values were estimated based on evidence from throughout the results section and are based on a number of assumptions. They are presented to give rough proportions of the different types of polysaccharides found in this prehydrolysate.</p> <p><sup>b.</sup> All glucosyl, mannosyl and acetyl units in the neutral fractions were assumed to be part of these polymers along with 1 galactosyl unit per 5 glucosyl units (based on N1 ratios).</p> <p><sup>c.</sup> All (methyl)glucuronic acid groups and xylosyl units in the neutral fractions are assumed to be part of this polymer. The carboxylic acid group is assumed to be ester linked making it neutral.</p> <p><sup>d.</sup> All arbinosyl and galactosyl units in the neutral fractions are assumed to be part of these polymers with the exception of the small amount of galactosyl attached to AcGGMs<sup>b</sup>.</p> <p><sup>e.</sup> This is the glucosyl and mannosyl units present in the acidic fractions. It is unknown what else these components are attached to.</p> <p><sup>f.</sup> All xylosyl units were assumed to be part of these polymers along with 1 MeGlcA residue per 10 xylosyl units.</p> <p><sup>g.</sup> All galactosyl and arabinosyl units in acidic fractions assumed to be part of these polymers along with all uronic acids not assumed to be attached to the xylans<sup>f</sup>.</p>		

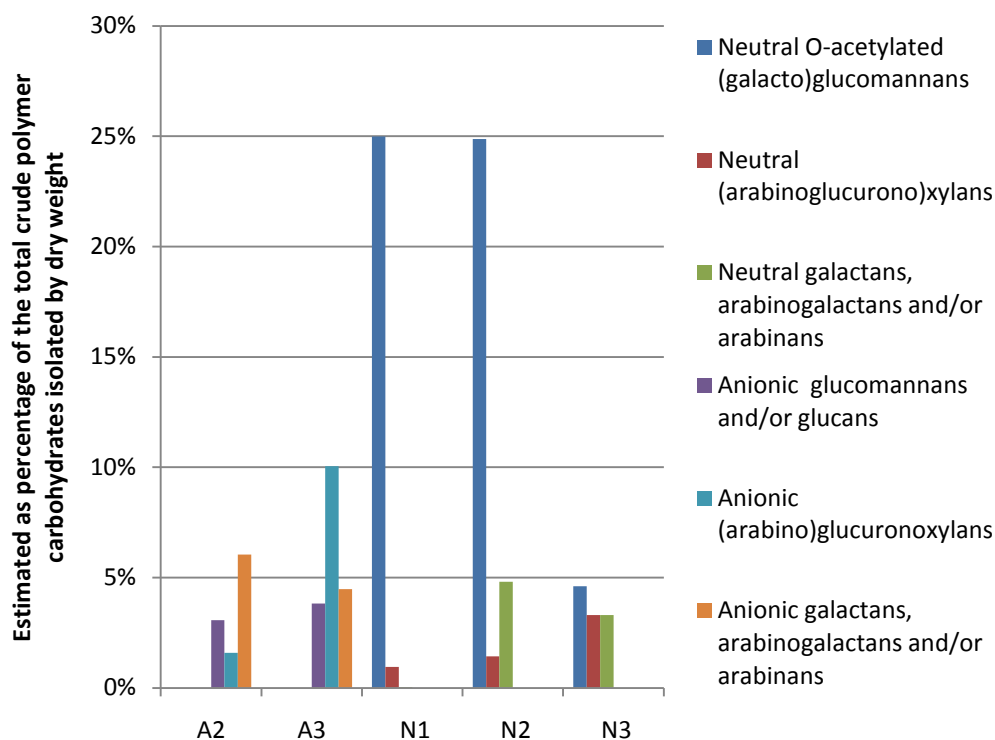


**Figure 31: Estimated distribution of different types of polymer across the major fractions. Used similar assumptions to those listed in Table 11.**

#### 4.1.1 *O*-acetylated (galacto)glucmannans (AcGGMs)

The ratios of components attributed to this polymer type in the neutral fractions N1, N2 and N3 were approximately 3.7 : 1.3 : 1 : 0.2 (D-mannosyl : acetyl : D-glucosyl : D-galactosyl) and this appears to account for close to all the D-mannosyl, acetyl, and D-glucosyl units in these fractions. However the majority of D-galactosyl units present in this prehydrolysate are not attached to this polymer type.

A backbone of  $\beta$ -1,4-linked D-mannopyranosyl and  $\beta$ -1,4-linked D-glucopyranosyl units were found along with terminal  $\alpha$ -D-galactopyranosyl units likely to be attached at 1,4,6-linked D-mannopyranosyl branch points.

Evidence of variation in *O*-acetyl group attachment was found with NMR signals consistent with literature examples [21] of acetyl groups at C-2 and C-3 positions of some mannosyl units.

These neutral *O*-acetylated (galacto)glucomannan hemicellulose fragments were the only polysaccharides that could be recovered from the prehydrolysate at a yield representing greater than 1% of original wood dry weight. In total they comprise approximately 54% of the dry weight of the crude polysaccharide isolated from the prehydrolysate (calculated based on D-mannosyl content). These AcGGMs dominate the neutral fractions and can be recovered in greater purity in the higher molecular weight fractions such as Fraction N1.

A great variation in apparent molecular weight, from disaccharides through to polymers as high as 62,000 Da were observed for this polymer-type. MALDI-ToF-MS average molecular weights of the de-acetylated polymers were  $M_n \approx 2600$ ,  $M_w \approx 3500$ . This corresponds to an average DP of  $\approx 16$  hexose units. The average molecular weight could actually be much higher as the MALDI-ToF-MS method appears biased towards lower molecular weight polysaccharides and the method had difficulty detecting neutral carbohydrates larger than about 10,000 Da.

The average degree of acetylation  $DS_{Ac}$  was around 0.3 across all size ranges of these AcGGMs. However, there was a slight trend towards a higher  $DS_{Ac}$  for higher molecular weight (N1) polymers, and a lower  $DS_{Ac}$  for smaller molecular weight (N3) polymers (Table 14, page 114).

A postulated structure for a typical *O*-acetylated (galacto)glucomannan in this prehydrolysate with a molecular weight of  $\approx 2780$  Da is presented in Figure 32. The proposed structure is based on the results of this thesis study and the comparison of NMR signals obtained with those reported in the literature [21]. Given that the ratio of D-galactosyl units to D-mannosyl units in these polymers was calculated to be very low, a majority of polymer molecules of this molecular weight may contain no D-galactosyl units. Uncertainty also exists over the distribution (random, evenly spaced, or clustered) of the acetyl and D-glucosyl groups along the polymer backbone.

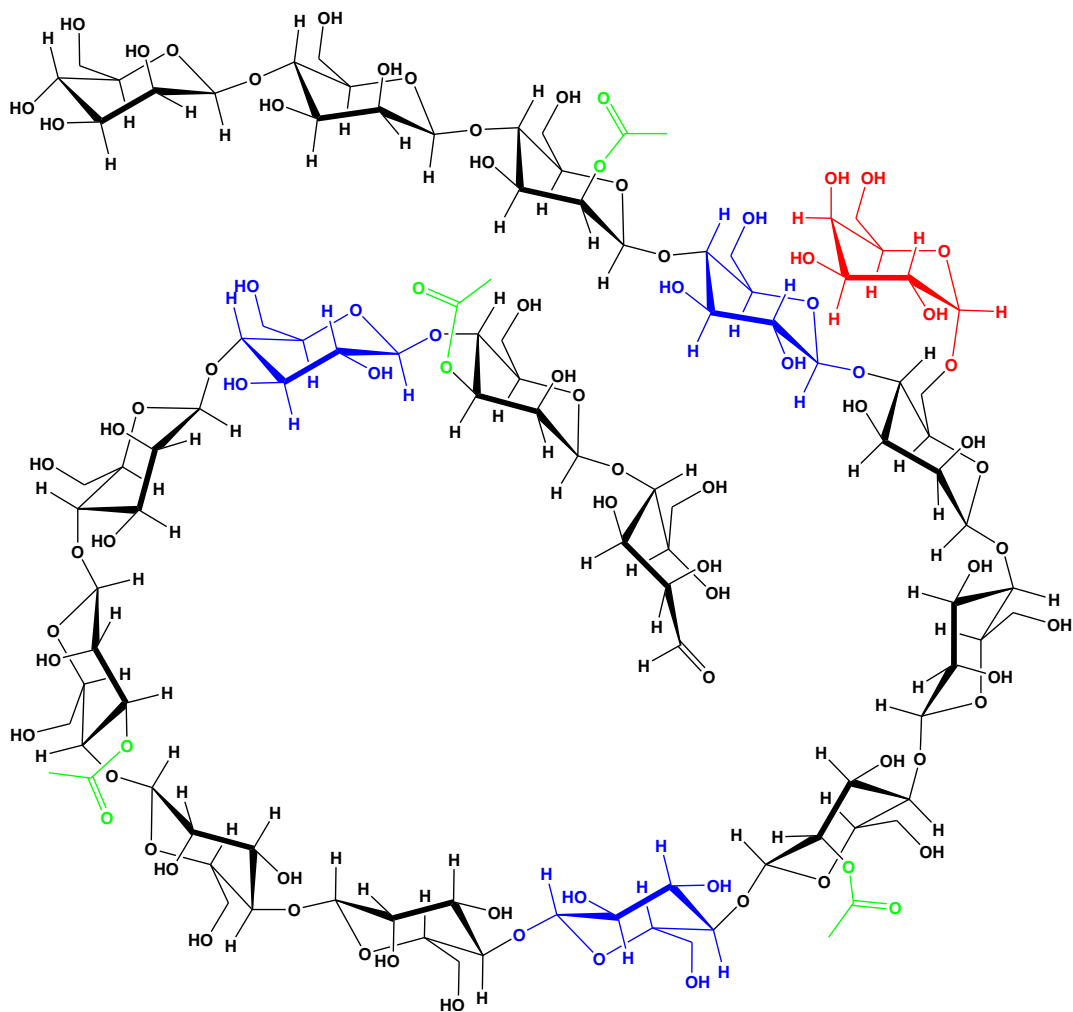


Figure 32: Postulated structure of a typical *O*-acetylated (galacto)glucomannan molecule  $\approx$  2780 Da that could be found in the prehydrolysate.

#### 4.1.2 (Arabino)4-*O*-methylglucuronoxylans

Estimated to account for  $\approx 12\%$  (by dry weight) of the of the polysaccharides isolated from the prehydrolysate (Table 11), these polymers identified as (arabino)4-*O*-methylglucuronoxylans exhibit anionic behaviour. They have a backbone of  $\beta$ -1,4-linked D-xylopyranosyl units and some evidence was obtained from this study for terminal  $\alpha$ -L-arabinofuranosyl being attached at  $\beta$ -1,3,4-linked D-xylopyranosyl branch points. There is evidence from NMR spectra of 1,2,4-linked D- xylopyranosyl branch points consistent with 4-*O*-methyl- $\alpha$ -D-glucopyranosyluronic acids that are attached at the *O*-2 position. A large proportion of the polymeric D-xylosyl content present in this prehydrolysate appears to be contained within this type of polysaccharide. However, the results indicate that the majority of L-arabinosyl content present in the prehydrolysate is not attached to this type of polysaccharide.

Evidence presented in this thesis is consistent with the attachment of 4-*O*-methylglucuronic acid groups but there is not enough evidence in this thesis alone to completely eliminate the prospect of another hexuronic acid containing a single *O*-methyl group being present instead. However, information in the literature on softwood composition and identified hemicellulose structures [24-30] indicates that significant quantities of another *O*-methylated hexuronic acid is unlikely to occur.

These anionic xylan-based polymers, detected in Fractions A1, A2, A3, and as a contaminant in Fraction N1, usually consisted of between 5 and 40 pentose units, and gave very clear MALDI-ToF mass spectra. Each polysaccharide molecule usually contained between 1 and 4 attached groups that are consistent with 4-*O*-methylglucuronic acid. The average mol ratio of (pentose : 4-*O*-methylglucuronic acid) trends from  $\approx 13 : 1$  in small polymers with a single uronic acid group towards  $\approx 7 : 1$  for the larger polymers with four attached uronic acid groups. This 7 : 1 ratio is getting closer to those reported the literature for samples considered to be 'native' softwood (arabino)4-*O*-methylglucuronoxylan [25, 30].

A postulated structure for a typical kind of (arabino)4-*O*-methylglucuronoxylan found in this prehydrolysate with a molecular weight of  $\approx 2511$  Da is presented in Figure 33. Uncertainty exists over the distribution (random, evenly spaced, or clustered) of the 4-*O*-methylglucuronic acid groups along the polymer backbone and how common the small L-arabinofuranosyl branches are. A potential site for an ester linkage to lignin complexes is also indicated in Figure 34 (page 105).

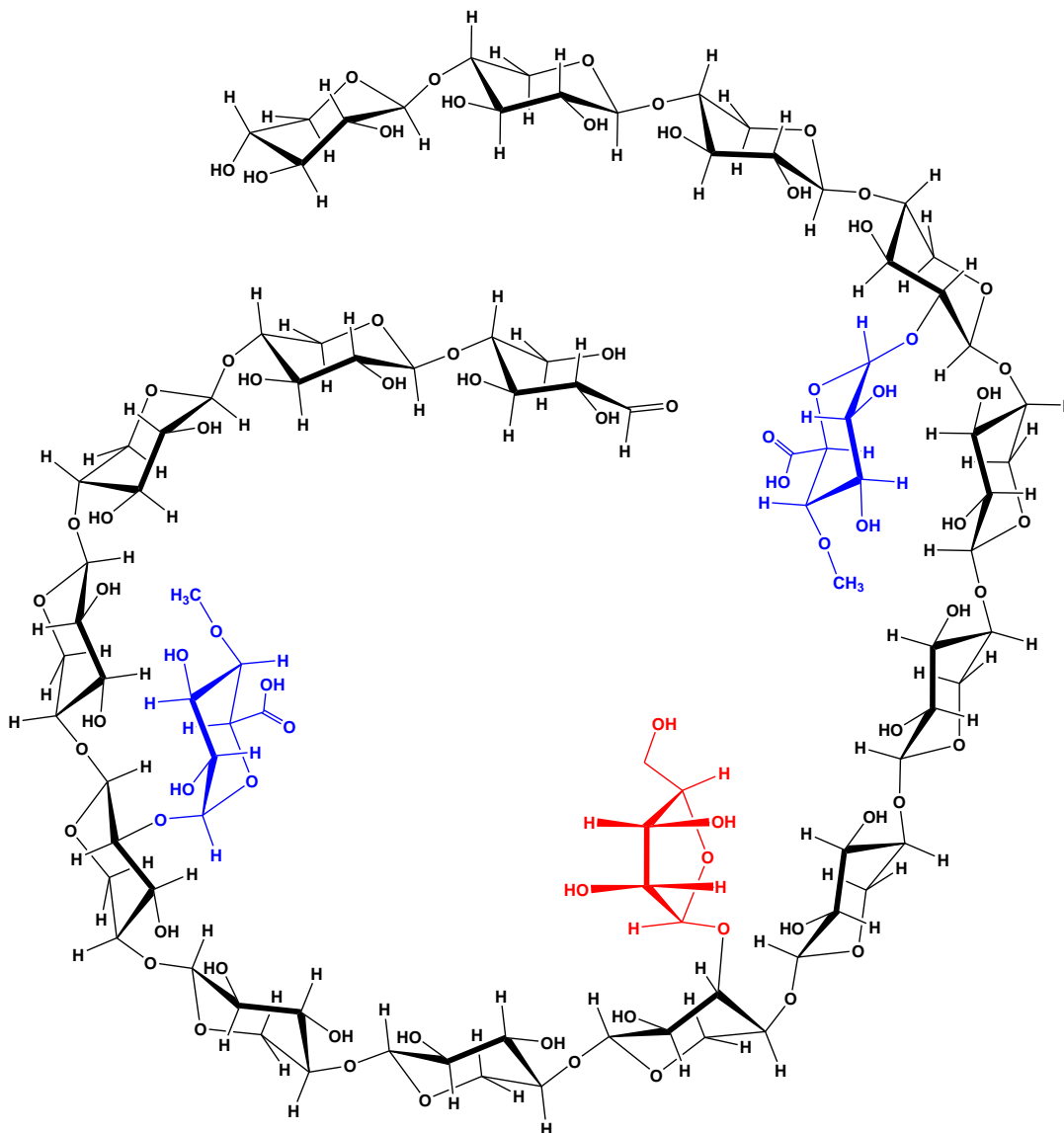


Figure 33: Postulated structure of a typical (arabino)4-*O*-methylglucuronoxylan molecule  $\approx 2511$  Da that could be found in the prehydrolysate.

### **4.1.3 (Arabino)xylans**

Evidence for a small amount of purely pentose oligomers with sizes less than 10 pentose units was found in the MALDI-ToF mass spectra of some neutral fractions. These could be parts of (arabino)4-*O*-methylglucuronoxylans that have been hydrolysed between two uronic acid groups during the prehydrolysis process and thus contain no acidic groups and are size-limited based on the uronic acid spacing on xylan backbones in the native polysaccharide. The evidence of 1,4-linked D-xylopyranosyl units detected in the neutral fractions supports their presence.

### **4.1.4 Galactans**

A backbone of 1,4-linked D-galactopyranosyl was detected in the neutral fractions. Such structures have been reported to be enriched in the compression wood of radiata pine trees [18, 19]. Their presence could explain the D-galactosyl enrichment in Fraction N3 (and to a lesser extent Fraction N2) and the corresponding neutral non-acetylated hexose polymers that show up clearly in the MALDI-ToF-MS of those fractions. These polymers appear to mostly contain between 5 and 30 hexose units. Other D-galactosyl-based polymers could also be present and might have some of the linkages noted below in the arabinogalactans section.

### **4.1.5 Arabinogalactans**

The acidic fractions and the lower-molecular-weight neutral fractions were enriched in both L-arabinosyl and D-galactosyl residues. Evidence of 1,5 linked L-arabinofuranosyl (and/or 1,4 linked L-arabinopyranosyl), 1,3 linked D-galactopyranosyl, 1,6 linked D-galactopyranosyl, 1,4,6 linked D-galactopyranosyl, and terminal D-galactopyranosyl was found in the linkage analysis and this is consistent with polysaccharides described in the literature as arabinogalactans [15, 29, 31, 128].

There appears to be a strong association between L-arabinosyl and D-galactosyl content across all the fractions analysed. This could mean that most L-arabinosyl and D-galactosyl units are linked together in the same polymer type, or that separate galactan and arabinan polymers behave in a very similar way during SEC fractionation. If arabinogalactans account for the bulk of L-arabinosyl and D-galactosyl content detected then the D-galactosyl : L-arabinosyl unit ratio is calculated to be approximately 2:1. Both D-galacturonic and (methyl) D-glucuronic acid also showed the strongest correlations in the acidic fractions to D-galactosyl content, suggesting that the majority of uronic acids present in the acidic fractions are attached to types of D-galactosyl-based polymers. With the evidence indicating that the methylated glucuronic acids are attached to xylan-based backbones, it is likely that the non-methylated glucuronic acids are the ones causing the apparent association to the D-galactosyl-based polymers

Despite the presence anionic groups (that should be attached to these polymers) and the high D-galactosyl content of the acidic fractions (especially A2), no clear MALDI-ToF mass spectra of hexose-based anionic polymers were obtained from the acidic fractions. This could be due to extremely high structural diversity in these arabinogalactans that causes very few polymer molecules to ever have exactly the same molecular weight. This structural diversity might be partially caused by covalent bonds to lignin [126] or protein derived structures [31].

#### **4.1.6 Glucans**

Evidence for D-glucosyl enrichment in the acidic fractions compared to the (galacto)glucomannans in the neutral fractions was discovered. Relative enrichment in 1,4-linked D-glucopyranosyl PMAA compared to 1,4-linked D-mannopyranosyl PMAA was also found in the acidic fractions. Glucans, high-glucosyl-content-glucomannans, or cellulose fragments bound [10] to anionic complexes could explain this enrichment.

#### 4.1.7 Arabinans

It is uncertain how much of the L-arabinosyl residues detected could exist as independent polymers free of attachment to D-galactosyl or D-xylosyl backbones. If they do exist they will contain some of the linkages noted under the arabinogalactan heading (page 101).

#### 4.1.8 Other Polysaccharides

The content of D-galacturonic and D-glucuronic acid appeared to be associated to some extent with D-galactosyl content. This could be in the form of galactans or arabinogalactans with attached uronic acid groups. Some pectin-derived polysaccharides with a very high uronic acid content could also be present in the acidic fractions.

The neutral fractions contained quantities of glucuronic acid which appeared to be associated with the smaller molecular weight polysaccharides. The hypothesis that these glucuronic acids are ester-linked would explain how they avoided “ion exclusion” during SEC fractionation. It is unknown exactly what type of polysaccharide these glucuronic acid/ester groups are attached to but results suggest xylan or galactan type polymers. The lack of *O*-methyl groups in some neutral fractions indicates that these ester-linked glucuronic acids are unmethylated. If these neutral glucuronic acid containing polysaccharides are produced from the partial hydrolysis of native arabino-4-*O*-methylglucuronoxylan (Figure 34), then all the glucuronic acids would need to be methylated except those involved in ester-linkages in order for it to be consistent with these results. A less convoluted explanation would be that these neutral polysaccharides containing glucuronic acid are produced from some polymer-type other than arabino-4-*O*-methylglucuronoxylans, such as arabinogalactans.

## 4.2 Causes of the Diversity and Complexity of Polysaccharides in this Prehydrolysate

There are two main reasons for the great diversity of polymer types in this prehydrolysate. The first reason is the variations from the biological construction of the hemicelluloses within the original wood material. The second cause of diversity is the way hemicelluloses partially de-polymerised during the prehydrolysis process. Both of these causes interact to influence the size, structure, charge, and composition of the water-soluble polymeric carbohydrates that exists in this prehydrolysate. When the native *O*-acetylated (galacto)glucomannan in the original wood partially depolymerises during the prehydrolysis process, the resulting polysaccharide fragments appear as neutral partially-acetylated hexoses of various sizes.

The presence of carboxylic groups adds additional complexity to the different types of polysaccharides formed when native hemicelluloses such as xylans are partially de-polymerised during prehydrolysis. For these hemicelluloses, the distribution of the uronic acid groups along the backbone influences the types of polysaccharide fragments formed during the prehydrolysis. A model native arabino-4-*O*-methylglucuronoxylan is used to demonstrate how this diversity could be generated (Figure 34). Similar processes could be occurring to galactans.

When the native xylan is hydrolysed twice between two uronic acid groups a neutral (arabino)xylan oligomers can form that contains only pentose units. Due to the resistance of the xylosyl-glucuronic acid linkage to acid hydrolysis [92], the size of the pentose-only oligomers is likely to be limited by the maximum spacing between two glucuronic acid groups on the xylosyl backbone. Only small neutral pentose-only oligomers were observed in the MALDI-ToF mass spectrum of the neutral fractions (Figure 19, page 61).

When the polysaccharide fragments formed during the prehydrolysis of the native xylans include one or more glucuronic acid groups, then the polymeric fragment can have anionic charges and will behave very differently on the SEC columns or the MALDI-ToF-MS.

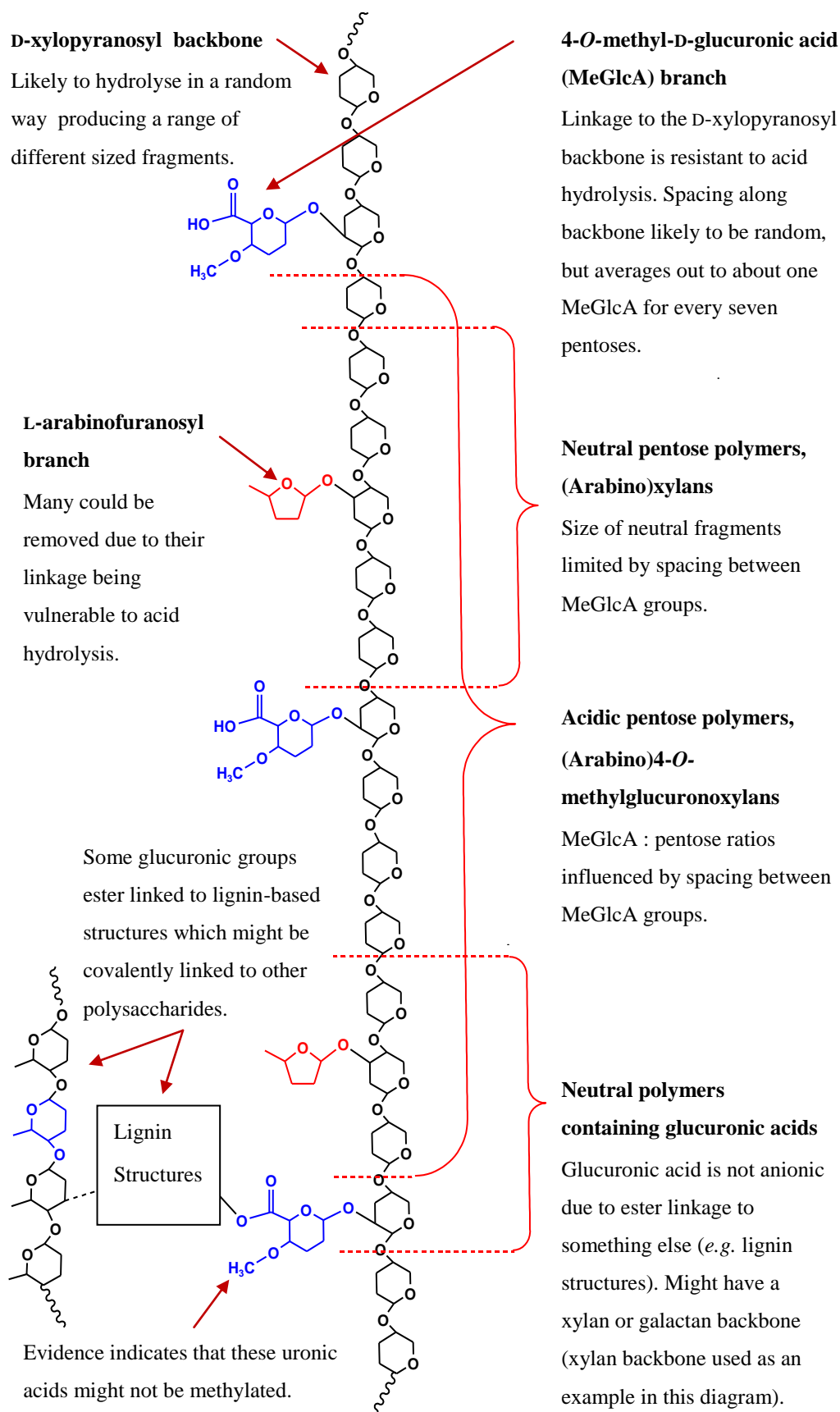


**Figure 34: Ways that the native softwood xylan could fragment during prehydrolysis.**  
(-OH groups not shown) Native softwood xylan structures postulated based a number of literature sources [3, 6, 10, 25, 30] and evidence obtained in this study.

## **4.3 Future Research Suggestions**

### **4.3.1 NMR**

Mainly one-dimensional  $^1\text{H}$  NMR was used to identify methylation, quantify acetylation and to provide limited supporting information to complement the results from other methods such as linkage analysis by GC-MS. This NMR work was often reliant on comparison with literature assignments for similar polysaccharides. There is scope to use additional NMR analysis to obtain much more information about the polysaccharides in the prehydrolysate.

#### **4.3.1.1 Whole Polymer NMR Assignment**

A combination of one-dimensional  $^1\text{H}$  and  $^{13}\text{C}$  NMR along with a series of two-dimensional experiments could be carried out in an attempt to assign all signals from the polymers in order to gain more information and greater certainty about fine structural details. Such determinations have been carried out on spruce AcGGMs [21]. Polysaccharides might need to be partially hydrolysed prior to analysis to reduce problems with signal broadening and low signal intensity common with analysing large polymers [21]. Standards of well characterized and/or synthetic oligomers could reduce the reliance on literature assignments to confirm signal identities.

#### **4.3.1.2 Quantification of Linkages and Components by NMR**

The integration of NMR signals could provide an alternative to derivatisation techniques for analysing the proportions of different monosaccharides and linkages present in samples of these polysaccharides. The advantages of using NMR would be in observing the polymer in its intact form and eliminating the problems of losses and/or changes in components during derivatisation and hydrolysis methods [115]. However, NMR integration also has disadvantages such as a need to select key diagnostic signals free from interference.

#### 4.3.1.3 *O*-Acetyl Group Stability, Migration, and Kinetics.

During the  $^1\text{H}$  NMR analysis of Fraction N2 in multiple experiments over a number of weeks the proportion of *O*-acetyl groups attached to the polysaccharides decreased along with a similar magnitude increase in free acetate signal. This change suggests that the *O*-acetylated (galacto)glucomannans were gradually de-acetylating when dissolved in  $\text{D}_2\text{O}$  and stored for weeks at room temperature or while they were heated up to  $70^\circ\text{C}$  for NMR analysis. Due to the clear separation of the *O*-acetyl signals from the free acetate signals and the fact are both signals are well separated from the carbohydrate or HOD signals,  $^1\text{H}$  NMR could provide a convenient way of studying this de-acetylation process.

The extent of *O*-acetylation can influence properties of (galacto)glucomannans such as their solubility, emulsifying abilities and sorption to cellulose [17, 50, 74, 76, 129]. Studying the stability of these acetyl groups and the mechanisms that will remove them could be relevant to any potential applications where the degree of acetylation is considered important.

An investigation to aid understanding of the mechanisms involved and the kinetics of the de-acetylation, would likely involve isolated acetylated (galacto)glucomannans dissolved in either polar protic or polar aprotic solvents at a range of acidity/basicity conditions at different time/temperature conditions and monitoring de-acetylation by observing the change in NMR signal intensities. The H-2 and H-3 signals on the D-mannopyranosyl backbone could also be monitored in order to find out if 3-*O*-acetylation is more stable than 2-*O*-acetylation, or the extent of *O*-acetyl migration that has been reported to occur [17].

### **4.3.2 Enzyme Hydrolysis**

A variety of different enzymes could be used to selectively hydrolyse some of the linkages in these polysaccharides. The released oligomers could be separated by chromatography and further analysed by methods such as NMR. Selective enzyme hydrolysis may well be a useful tool for assisting the isolation of desirable hemicellulose fragments from a complex mixture of hemicelluloses present in prehydrolysates like the one studied in this thesis. Enzymes could be used to break down the less desirable/useful polysaccharides in the sample to low molecular weight oligomers thus allowing the desired polysaccharides to be more easily isolated based on them retaining higher molecular weights.

An example of an analytical use of enzymatic hydrolysis, would in testing the hypothesis that the non-acetylated hexoses that appear in the MALDI-ToF mass spectrum of Fraction N3 are mostly galactan-based. Enzymes that specifically hydrolyse common galactosyl linkages [130] could be used prior to MALDI-ToF-MS to drastically reduce the molecular weights of any galactans, thus confirming their prevalence.

### **4.3.3 Ion Chromatography**

The use of a heated conductivity cell detector after ion chromatography to identify and quantify uronic acid content is not an established method for analysing polysaccharides from lignocellulosics. This study found that when the detector was calibrated using D-glucuronic acid and D-galacturonic acid standards it appeared to provide adequate quantification of these uronic acids over a wide concentration range. Given the problems reported for the established techniques for identifying and quantifying different uronic acids from plant biomass [27], the method that was partially developed for this thesis might be worthy of further development and optimisation. This would likely involve testing the repeatability of the method, testing a number of different types of plant samples, and comparing the results to those obtained by a number of different established techniques. The behaviour of uronic acids derivatives (MeGlcA and aldobiouronic acids) on the IC column and their detector response would also need to be studied further. However, authenticated standards of these uronic acid derivatives (or close analogues) would likely be required for such a study.

#### **4.3.4 MALDI-ToF-MS**

One of the disadvantages of using the MALDI-ToF techniques when analysing polysaccharides is the difficulty experienced in detecting neutral polymers of higher molecular mass. Detection of these neutral polysaccharides may be improved if the polysaccharides are derivatised prior to analysis by MALDI-ToF-MS. One approach might be to covalently bond a molecule containing a carboxylic acid group, or multiple carboxylic acid groups, to the reducing end of neutral polysaccharides so that they may ionise in a similar way to acidic polysaccharides in the MALDI-ToF. Alternatively, introducing an oxidising step that changes the reducing end aldehydes into carboxylic acids may also achieve the same result.

#### **4.3.5 Linkage Analysis**

Complete characterisation of the uronic acids and identification of their points of linkage was not possible in this thesis using the methods available. Alternative methods involving complete reduction of the uronic acid have been suggested (page 88). The use of such methods on the polysaccharides from this prehydrolysate could allow the uronic acid attachments to be deduced and the NMR assignments to be confirmed.

### 4.3.6 Larger Scale Processing of Prehydrolysates

Extraction of potentially useful hemicelluloses from prehydrolysates such as the type studied in this thesis will need to be done on a larger scale and be economically viable. The most relevant findings from this thesis for guiding any design of larger scale processing likely would involve the *O*-acetylated (galacto)glucomannans (AcGGMs) because they are the most abundant type of polysaccharide found in the prehydrolysate.

The large quantities of AcGGMs could be possibly separated from most of the other carbohydrates by taking advantage of the two key differences that distinguishes the AcGGMs from most of the other types of polysaccharide found in the prehydrolysate. These are (i) the observation that the vast majority of *O*-acetylated (galacto)glucomannans in the prehydrolysate are non-anionic, and (ii) the higher the molecular weight a non-anionic polymer was, the more likely that polymer was an *O*-acetylated (galacto)glucomannan. Therefore targeting a non-anionic high molecular weight fraction for separation should isolate a fraction containing a high proportion of AcGGMs. This separation, which would likely involve a combination of ion exchange and ultrafiltration steps [17]. Attempting to improve the isolation of AcGGMs by using galactan and/or xylan cleaving enzyme [130, 131] treatments prior to ultrafiltration (or other separation steps based on molecular weight), could be worth investigating.

# Appendix 1

**Table 12: Extended table of linear correlations between mol % estimates of different components of correlation graphs between monomer components**

Y axis, Mol%	X axis, Mol%	Linear Formula, Full Dataset	Linear Formula, Neutral Dataset	Linear Formula( Zero Forced).
D-Mannosyl	D-Glucosyl	$y = 5.0797x - 0.2647$ $R^2 = 0.5028$	$y = 5.601x - 0.2358$ $R^2 = 0.9999$	$y = 3.7069x$ $R^2 = 0.8809$
D-Mannosyl	Acetyl	$y = 2.076x + 0.122$ $R^2 = 0.9896$	$y = 2.1696x + 0.1054$ $R^2 = 0.9893$	$y = 2.765x$ $R^2 = 0.9023$
D-Mannosyl	(Methyl) glucuronic acid	$y = -9.6238x + 0.523$ $R^2 = 0.6175$	$y = -23.853x + 0.724$ $R^2 = 0.996$	$y = 25.06x$ $R^2 = -4.108$
D-Mannosyl	D-Xylosyl	$y = -0.7956x + 0.478$ $R^2 = 0.657$	$y = -1.178x + 0.5703$ $R^2 = 0.9612$	$y = 1.3465x$ $R^2 = -7.663$
D-Mannosyl	D-Galactosyl	$y = -1.0803x + 0.523$ $R^2 = 0.5975$	$y = -1.9443x + 0.662$ $R^2 = 0.9111$	$y = 2.3249x$ $R^2 = -4.901$
D-Mannosyl	L-Arabinosyl	$y = -3.4163x + 0.555$ $R^2 = 0.716$	$y = -3.1023x + 0.589$ $R^2 = 0.9561$	$y = 3.702x$ $R^2 = -7.018$
D-Mannosyl	Galacturonic acid	$y = -33.082x + 0.395$ $R^2 = 0.4304$	$y = 3617x + 0.4069$ $R^2 = 0.0802$	$y = 21671x$ $R^2 = -5.916$
D-Galactosyl	L-Arabinosyl	$y = 2.6437x + 0.0078$ $R^2 = 0.8375$	$y = 1.551x + 0.0398$ $R^2 = 0.9916$	$y = 2.0103x$ $R^2 = 0.8408$
D-Galactosyl	D-Xylosyl	$y = 0.1818x + 0.1586$ $R^2 = 0.067$	$y = 0.5174x + 0.0574$ $R^2 = 0.7693$	$y = 0.6009x$ $R^2 = -0.576$
D-Galactosyl	(Methyl) glucuronic acid	$y = 8.6268x + 0.0064$ $R^2 = 0.9693$	$y = 10.957x - 0.0158$ $R^2 = 0.8719$	$y = 9.8865x$ $R^2 = 0.8618$
D-Galactosyl	Galacturonic acid	$y = 33.08x + 0.1123$ $R^2 = 0.8407$	$y = 98.019x + 0.1164$ $R^2 = 0.0002$	$y = 47.466x$ $R^2 = 0.355$
D-Galactosyl	Acetyl	$y = -1.2351x + 0.309$ $R^2 = 0.6842$	$y = -1.0497x + 0.276$ $R^2 = 0.9608$	$y = 0.5106x$ $R^2 = -1.52$
D-xylosyl	L-Arabinosyl	$y = 1.7332x + 0.0858$ $R^2 = 0.1775$	$y = 2.4225x - 0.0053$ $R^2 = 0.8417$	$y = 2.3612x$ $R^2 = 0.8408$
D-Xylosyl	D-Glucosyl	$y = -6.6469x + 0.963$ $R^2 = 0.8293$	$y = -4.5774x + 0.663$ $R^2 = 0.9642$	$y = 0.7484x$ $R^2 = -0.395$
D-Xylosyl	(Methyl) glucuronic acid	$y = 3.7397x + 0.1272$ $R^2 = 0.0898$	$y = 19.711x - 0.1237$ $R^2 = 0.9819$	$y = 11.352x$ $R^2 = 0.7667$

<b>D-Xylosyl</b>	<b>Galacturonic acid</b>	$y = 9.5729x + 0.1852$ $R^2 = 0.0347$	$y = -4958.1x + 0.153$ $R^2 = 0.2176$	$y = 1825.2x$ $R^2 = -1.004$
<b>D-Xylosyl</b>	<b>Acetyl</b>	$y = -1.6061x + 0.356$ $R^2 = 0.5706$	$y = -1.7335x + 0.378$ $R^2 = 0.9117$	$y = 0.4031x$ $R^2 = -0.707$
<b>L-Arabinosyl</b>	<b>Galacturonic acid</b>	$y = 8.6071x + 0.0495$ $R^2 = 0.4749$	$y = -306.18x + 0.052$ $R^2 = 0.0058$	
<b>L-Arabinosyl</b>	<b>(Methyl)glucuronic acid</b>	$y = 2.6172x + 0.0137$ $R^2 = 0.7445$	$y = 7.252x - 0.0381$ $R^2 = 0.9267$	$y = 4.6754x$ $R^2 = 0.7841$
<b>L-Arabinosyl</b>	<b>D-Glucosyl</b>	$y = -0.8099x + 0.163$ $R^2 = 0.2083$	$y = -1.7234x + 0.256$ $R^2 = 0.9529$	$y = 0.3331x$ $R^2 = -0.46$
<b>D-Glucosyl</b>	<b>Acetyl</b>	$y = 0.1884x + 0.0961$ $R^2 = 0.4183$	$y = 0.387x + 0.061$ $R^2 = 0.9877$	$y = 0.7315x$ $R^2 = 0.0736$
<b>D-Glucosyl</b>	<b>D-Galactosyl</b>	$y = -0.03x + 0.1192$ $R^2 = 0.0237$	$y = -0.3463x + 0.160$ $R^2 = 0.9066$	
<b>D-Glucosyl</b>	<b>Galacturonic acid</b>	$y = 0.4661x + 0.1121$ $R^2 = 0.0044$	$y = 662.63x + 0.1146$ $R^2 = 0.0845$	$y = 5748.7x$ $R^2 = -14.84$
<b>D-Glucosyl</b>	<b>(Methyl)glucuronic acid</b>	$y = -0.2369x + 0.119$ $R^2 = 0.0192$	$y = -4.2606x + 0.171$ $R^2 = 0.9969$	

## Appendix 2

**Table 13: Summary Table.**

<b>Physical Measurements</b>	<b>A1</b>	<b>A2</b>	<b>A3</b>	<b>N1</b>	<b>N2</b>	<b>N3</b>
Retention time at collection start (min)	14.5	17.5	20.5	23.5	26.5	29.5
Dry weight of fraction, 1 <sup>st</sup> 14 runs (mg)	0.5	1.7	3.1	5.1	5.8	2
Dry weight of fraction (% by mass)	3%	9%	17%	28%	32%	11%
<b>Acidic Polysaccharides</b>	<b>A1</b>	<b>A2</b>	<b>A3</b>	<b>N1</b>	<b>N2</b>	<b>N3</b>
<b>MALDI-ToF-MS results</b>						
Primary repeating unit, <b>pentose</b> (Da)	132	132	132	132	-	-
Attached group unit, MeGlcA (Da)	191	191	191	191	-	-
Numbers of MeGlcA found per polymer	2,3,4	1,2,3, 4	1,2,3	1	-	-
≈DP range of polymers with 1 MeGlcA	-	5-19	5-19	5-19	-	-
≈DP range of polymers with 2 MeGlcA	9-22	6-28	5-25	-	-	-
≈DP range of polymers with 3 MeGlcA	13-33	10-28	10-28	-	-	-
≈DP range of polymers with 4 MeGlcA	21-39	21-31	-	-	-	-
Polytool calculated mean values						
M <sub>n</sub> of polymers with 1 MeGlcA (Da)	-	1698	1748	1696	-	-
M <sub>n</sub> of polymers with 2 MeGlcA (Da)	2458	2336	2178	-	-	-
M <sub>n</sub> of polymers with 3 MeGlcA (Da)	3087	3066	-	-	-	-
M <sub>w</sub> of polymers with 4 MeGlcA (Da)	3853	3939	-	-	-	-
M <sub>w</sub> of polymers with 1 MeGlcA (Da)	-	1753	1832	1775	-	-
M <sub>w</sub> of polymers with 2 MeGlcA (Da)	2523	2440	2271	-	-	-
M <sub>w</sub> of polymers with 3 MeGlcA (Da)	3144	3122	-	-	-	-
M <sub>w</sub> of polymers with 4 MeGlcA (Da)	3898	3999	-	-	-	-
DP of polymers with 1 MeGlcA	-	12.86	13.24	12.85	-	-
DP of polymers with 2 MeGlcA	18.67	17.70	16.50	-	-	-
DP of polymers with 3 MeGlcA	23.40	23.22	-	-	-	-
DP of polymers with 4 MeGlcA	29.00	29.69	-	-	-	-

**Table 14: Summary Table (continued).**

<b>Neutral polysaccharides</b>	<b>A1</b>	<b>A2</b>	<b>A3</b>	<b>N1</b>	<b>N2</b>	<b>N3</b>
<b>MALDI-ToF-MS results</b>						
Primary repeating unit, <b>pentose</b> (Da)	-	-	-	-	-	132
≈DP range of polymers	-	-	-	-	-	5-11
Primary repeating unit, <b>hexose</b> (Da)	-	-	-	162	162	162
Attached group unit, 0-acetyl (Da)	-	-	-	42	42	42
≈DP range of de-acetylated polymers	-	-	-	5-79	5-47	5-36
Polytool calculated mean values						
M <sub>n</sub> of de-acetylated polymers (Da)	-	-	-	2304 <sup>a</sup>	2577	1899
M <sub>w</sub> of de-acetylated polymers (Da)	-	-	-	2764 <sup>a</sup>	3470	1755
DP of de-acetylated polymers	-	-	-	14.2 <sup>a</sup>	15.9	10.8
<b>SEC results</b>						
SEC estimated M <sub>w</sub> upper value(Da)	-	-	-	80000	12000	1500
SEC estimated M <sub>w</sub> lower value(Da)	-	-	-	10000	1300	180
Mean Apparent M <sub>w</sub> sub-fraction 1 (Da)	-	-	-	62000	8900	1200
Mean Apparent M <sub>w</sub> sub-fraction 2 (Da)	-	-	-	31000	4600	500
Mean Apparent M <sub>w</sub> sub-fraction 3 (Da)	-	-	-	22000	2300	340
<b>Estimated DS<sub>Ac</sub> (Proton NMR Results)</b>	<b>A1</b>	<b>A2</b>	<b>A3</b>	<b>N1</b>	<b>N2</b>	<b>N3</b>
Observed degree of acetylation DS <sub>Ac</sub>	Trace	Trace	Trace	0.19	0.16	0.04
'Original' degree of acetylation DS <sub>Ac</sub>	N/A	N/A	N/A	0.28	0.20	0.07
Calculated mean DS <sub>Ac</sub> of AcGGMs <sup>b</sup>	N/A	N/A	N/A	0.31	0.27	0.21
<sup>a.</sup> Much higher values were obtained when method was drastically altered. <sup>b.</sup> Assumes that only AcGGMs are acetylated.						

## References

1. MAF. *National Exotic Forest Description*. 2009 [cited 02/02/2010]; Available from: <http://www.maf.govt.nz/mafnet/publications/nefd/>.
2. Kelley, S.S., *Lignocellulosic biorefineries: Reality, hype, or something in between?*, in *Materials, Chemicals, and Energy from Forest Biomass*, D.S. Argyropoulos, Editor. 2006, American Chemical Society Washington, DC.
3. Sjöström, E., *Wood Chemistry: Fundamentals and Applications*. 1981, New York, NY: Academic Press Inc.
4. Kininmonth, J.A. and Whitehouse, L.J., *Properties and uses of New Zealand Radiata pine*. Vol. 1. 1991: NZ Ministry of Forestry, Forest Research Institute
5. Wiedenhoef, A.C. and Miller, R.B., *Structure and function of wood*, in *Handbook of Wood Chemistry and Wood Composites*, R.M. Rowell, Editor. 2005, CRC Press: Boca Raton.
6. Rowell, R.M., Rowell, J.S., Pattersen, R., Han, J.S., and Tshabalala, M.A., *Cell wall chemistry*, in *Handbook of Wood Chemistry and Wood Composites*, R.M. Rowell, Editor. 2005, CRC Press: Boca Raton.
7. Sun, R., Sun, X., F, and Tomkinson, J., *Hemicelluloses and their derivatives*, in *Hemicelluloses: Science and Technology*, P. Gatenholm and M. Tenkanen, Editors. 2002, American Chemical Society: Washington, DC.
8. Aimi, H., Matsumoto, Y., and Meshitsuka, G., *Lignin fragments rich in detached side-chain structures found in water-soluble LCC*. *Journal of Wood Science*, 2005. **51**(3): p. 252-255.
9. Lawoko, M., Henriksson, G., and Gellerstedt, G., *Characterisation of lignin-carbohydrate complexes (LCCs) of spruce wood (Picea abies L.) isolated with two methods*. *Holzforschung*, 2006. **60**(2): p. 156-161.
10. Lawoko, M., Henriksson, G., and Gellerstedt, G., *Structural differences between the lignin-carbohydrate complexes present in wood and in chemical pulps*. *Biomacromolecules*, 2005. **6**(6): p. 3467-3473.
11. Jin, Z.F., Katsumata, K.S., Lam, T.B.T., and Iiyama, K., *Covalent linkages between cellulose and lignin in cell walls of coniferous and nonconiferous woods*. *Biopolymers*, 2006. **83**(2): p. 103-110.
12. Altaner, C.M. and Jarvis, M.C., *Modelling polymer interactions of the 'molecular Velcro' type in wood under mechanical stress*. *Journal of Theoretical Biology*, 2008. **253**(3): p. 434-445.
13. Caffall, K.H. and Mohnen, D., *The structure, function, and biosynthesis of plant cell wall pectic polysaccharides*. *Carbohydrate Research*, 2009. **344**(14): p. 1879-1900.
14. Hafren, J. and Westermark, U., *Distribution of acidic and esterified polygalacturonans in sapwood of spruce, birch and aspen*. *Nordic Pulp & Paper Research Journal*, 2001. **16**(4): p. 284-290.
15. Willfor, S., Sundberg, A., Hemming, J., and Holmbom, B., *Polysaccharides in some industrially important softwood species*. *Wood Science and Technology*, 2005. **39**(4): p. 245-258.

16. Saarimaa, V., Vahasalo, L., Sundberg, A., Pranovich, A., Holmbom, B., Svedman, M., and Orsa, F., *Influence of pectic acids on aggregation and deposition of colloidal pitch*. Nordic Pulp & Paper Research Journal, 2006. **21**(5): p. 613-619.
17. Willfor, S., Sundberg, K., Tenkanen, M., and Holmbom, B., *Spruce-derived mannans - A potential raw material for hydrocolloids and novel advanced natural materials*. Carbohydrate Polymers, 2008. **72**(2): p. 197-210.
18. Mast, S.W., Donaldson, L., Torr, K., Phillips, L., Flint, H., West, M., Strabala, T.J., and Wagner, A., *Exploring the ultrastructural localization and biosynthesis of beta(1,4)-galactan in Pinus radiata compression wood*. Plant Physiology, 2009. **150**(2): p. 573-583.
19. Nanayakkara, B., *Chemical Characterisation of Compression Wood in Plantation Grown Pinus Radiata*. 2007, The University of Waikato: Hamilton.
20. Wagner, A., Donaldson, L., Kim, H., Phillips, L., Flint, H., Steward, D., Torr, K., Koch, G., Schmitt, U., and Ralph, J., *Suppression of 4-coumarate-CoA ligase in the coniferous gymnosperm Pinus radiata*. Plant Physiology, 2009. **149**(1): p. 370-383.
21. Hannuksela, T. and Hervé du Penhoat, C., *NMR structural determination of dissolved O-acetylated galactoglucomannan isolated from spruce thermomechanical pulp*. Carbohydrate Research, 2004. **339**(2): p. 301-312.
22. Capek, P., Alföldi, J., and Lisková, D., *An acetylated galactoglucomannan from Picea abies L. Karst.* Carbohydrate Research, 2002. **337**(11): p. 1033-1037.
23. Capek, P., Kubacková, M., Alföldi, J., Bilisics, L., Lisková, D., and Kákoniová, D., *Galactoglucomannan from the secondary cell wall of Picea abies L. Karst.* Carbohydrate Research, 2000. **329**(3): p. 635-645.
24. Adams, G.A., *Uronic acids from white spruce* Canadian Journal of Chemistry, 1959. **37**: p. 29-34.
25. Jacobs, A., Larsson, P.T., and Dahlman, O., *Distribution of uronic acids in xylans from various species of soft- and hardwood as determined by MALDI mass spectrometry*. Biomacromolecules, 2001. **2**(3): p. 979-990.
26. Jacobs, A., Lundqvist, J., Stålbrand, H., Tjerneld, F., and Dahlman, O., *Characterization of water-soluble hemicelluloses from spruce and aspen employing SEC/MALDI mass spectroscopy*. Carbohydrate Research, 2002. **337**(8): p. 711-717.
27. Willfor, S., Pranovich, A., Tamminen, T., Puls, J., Laine, C., Suurnakki, A., Saake, B., Uotila, K., Simolin, H., Hemming, J., and Holmbom, B., *Carbohydrate analysis of plant materials with uronic acid-containing polysaccharides-A comparison between different hydrolysis and subsequent chromatographic analytical techniques*. Industrial Crops and Products, 2009. **29**(2-3): p. 571-580.
28. McDonald, A.G. and Clark, T.A., *Characterization of oligosaccharides released by steam explosion of sulfur-dioxide impregnated Pinus radiata*. Journal of Wood Chemistry and Technology, 1992. **12**(1): p. 53-78.

29. Willfor, S. and Holmbom, B., *Isolation and characterisation of water soluble polysaccharides from Norway spruce and Scots pine*. Wood Science and Technology, 2004. **38**(3): p. 173-179.
30. Haslemore, R.M., *The structure of polysaccharides extracted from Pinus Radiata*. 1973, The University of Otago: Dunedin.
31. Putoczki, T.L., Pettolino, F., Griffin, M.D.W., Moller, R., Gerrard, J.A., Bacic, A., and Jackson, S.L., *Characterization of the structure, expression and function of Pinus radiata D. Don arabinogalactan-proteins*. Planta, 2007. **226**(5): p. 1131-1142.
32. McDonald, A.G., Clare, A.B., Meder, A.R., and Appita, A. *Chemical characterisation of the neutral water soluble components from radiata pine high temperature TMP fibre*. in *53rd Appita Annual Conference*. 1999. Rotorua, New Zealand: Appita Inc.
33. Andrew, I.G. and Little, J.W.L., *A xyloglucan in etiolated seedlings of Pinus radiata*. Phytochemistry, 1997. **46**(2): p. 203-207.
34. Jacobs, A., Lundqvist, J., Stalbrand, H., Tjerneld, F., and Dahlman, O., *Characterization of water-soluble hemicelluloses from spruce and aspen employing SEC/MALDI mass spectroscopy*. Carbohydrate Research, 2002. **337**(8): p. 711-717.
35. Teleman, A., Tenkanen, M., Jacobs, A., and Dahlman, O., *Characterization of O-acetyl-(4-O-methylglucurono)xylan isolated from birch and beech*. Carbohydrate Research, 2002. **337**(4): p. 373-377.
36. Teleman, A., Nordström, M., Tenkanen, M., Jacobs, A., and Dahlman, O., *Isolation and characterization of O-acetylated glucomannans from aspen and birch wood*. Carbohydrate Research, 2003. **338**(6): p. 525-534.
37. Guilloux, K., Gaillard, I., Courtois, J., Courtois, B., and Petit, E., *Production of arabinoxylan-oligosaccharides from flaxseed (Linum usitatissimum)*. Journal of Agricultural and Food Chemistry, 2009. **57**(23): p. 11308-11313.
38. Yadav, M.P., Moreau, R.A., and Hicks, K.B., *Phenolic acids, lipids, and proteins associated with purified corn fiber arabinoxylans*. Journal of Agricultural and Food Chemistry, 2007. **55**(3): p. 943-947.
39. Geng, Z.C., Sun, J.X., Liang, S.F., Zhang, F.Y., Zhang, Y.Y., Xu, F., and Sun, R.C., *Characterization of water- and alkali-soluble hemicellulosic polymers from sugarcane bagasse*. International Journal of Polymer Analysis and Characterization, 2006. **11**(3): p. 209-226.
40. Dinand, E. and Vignon, M.R., *Isolation and NMR characterisation of a (4-O-methyl--glucurono)--xylan from sugar beet pulp*. Carbohydrate Research, 2001. **330**(2): p. 285-288.
41. Fares, K., Renard, C., Crepeau, M.J., and Thibault, J.F., *Characterization of hemicelluloses of sugar beet roots grown in Morocco*. International Journal of Food Science and Technology, 2004. **39**(3): p. 303-309.
42. Fares, K., Renard, C., R'Zina, Q., and Thibault, J.F., *Extraction and composition of pectins and hemicelluloses of cell walls of sugar beet roots grown in Morocco*. International Journal of Food Science and Technology, 2001. **36**(1): p. 35-46.

43. Jacobs, A., Palm, M., Zacchi, G., and Dahlman, O., *Isolation and characterization of water-soluble hemicelluloses from flax shive*. Carbohydrate Research, 2003. **338**(18): p. 1869-1876.
44. Komiyama, H., Kato, A., Aimi, H., Ogihara, J., and Shimizu, K., *Chemical structure of kenaf xylan*. Carbohydrate Polymers, 2008. **72**(4): p. 638-645.
45. Komiyama, H., Enomoto, A., Sueyoshi, Y., Nishio, T., Kato, A., Ishii, T., and Shimizu, K., *Structures of aldouronic acids liberated from kenaf xylan by endoxylanases from Streptomyces sp.* Carbohydrate Polymers, 2009. **75**(3): p. 521-527.
46. da Silva, B.P., de Medeiros Silva, G., and Parente, J.P., *Chemical properties and adjuvant activity of a galactoglucomannan from Acrocomia aculeata*. Carbohydrate Polymers, 2009. **75**(3): p. 380-384.
47. Schröder, R., Nicolas, P., Vincent, S.J.F., Fischer, M., Reymond, S., and Redgwell, R.J., *Purification and characterisation of a galactoglucomannan from kiwifruit (Actinidia deliciosa)*. Carbohydrate Research, 2001. **331**(3): p. 291-306.
48. Hoch, G., *Cell wall hemicelluloses as mobile carbon stores in non-reproductive plant tissues*. Functional Ecology, 2007. **21**(5): p. 823-834.
49. Sarkar, P., Bosneaga, E., and Auer, M., *Plant cell walls throughout evolution: towards a molecular understanding of their design principles*. Journal of Experimental Botany, 2009. **60**(13): p. 3615-3635.
50. Hannuksela, T. and Holmbom, B., *Sorption of mannans to different fiber surfaces: An evolution of understanding*, in *Hemicelluloses: Science and Technology*, P. Gatenholm and M. Tenkanen, Editors. 2002, American Chemical Society: Washington, DC.
51. Gatenholm, P. and Tenkanen, M., eds. *Hemicelluloses: Science and Technology*. ACS Symposium Series. 2002, American Chemical Society: Washington, DC.
52. Zhang, Y., Brown, G., Whetten, R., Loopstra, C.A., Neale, D., Kieliszewski, M.J., and Sederoff, R.R., *An arabinogalactan protein associated with secondary cell wall formation in differentiating xylem of loblolly pine*. Plant Molecular Biology, 2003. **52**(1): p. 91-102.
53. Kaparaju, P., Serrano, M., Thomsen, A.B., Kongjan, P., and Angelidaki, I., *Bioethanol, biohydrogen and biogas production from wheat straw in a biorefinery concept*. Bioresource Technology, 2009. **100**(9): p. 2562-2568.
54. Mao, C.B. and Ni, Y.H., *Integrated Forest Biorefinery: Concept and processes*. Second International Papermaking and Environment Conference, Proceeding, Books a and B, ed. L. Wang, Y. Ni, Q. Hou, and Z. Liu. 2008, Beijing: China Light Industry Press. 3-7.
55. Chirat, C., Picon, G., Viardin, M.T., Lachenal, D., Lloyd, J.A., and Suckling, I. *Hemicelluloses extraction from eucalyptus and softwood wood chips : Pulp properties and ethanol production*. in *Proceedings of 15th ISWFPC Conference*. 2009. Oslo, Norway.
56. Liu, X., Zhang, Z., Chi, C.C., and Ge, W.W., *Influence of water pre-hydrolyzing eucalyptus chips on the following alkaline pulping*. Proceedings of International Conference on Pulping, Papermaking and Biotechnology 2008: ICPPB '08, Vol 2, ed. Y. Jin, H. Zhai, and Z. Li. 2008, Nanjing: Nanjing Forestry Univ. 120-123.

57. Martin, R.S., Perez, C., and Briones, R., *Simultaneous production of ethanol and kraft pulp from pine (Pinus radiata) using steam explosion*. *Bioresource Technology*, 1995. **53**(3): p. 217-223.
58. Hannuksela, T., Holmbom, B., Mortha, G., and Lachenal, D. *Effect of sorbed galactoglucomannans and galactomannans on pulp and paper handsheet properties, especially strength properties*. in *5th International Paper and Coating Chemistry Symposium*. 2003. Montreal, Canada: Ab Svensk Papperstidning.
59. Lloyd, J.A., Suckling I. D., Allison, R. W., Manley-Harris, M., McDonald-Wharry, J. S., Lachenal, D., and Chirat, C. . *Hot-water prehydrolysis of radiata pine - hemicellulose extraction*. in *Proceedings of 15th ISWFPC Conference*. 2009. Oslo, Norway.
60. Parajo, J.C., Dominquez, H., and Dominguez, J.M., *Study of charcoal adsorption for improving the production of xylitol from wood hydrolysates*. *Bioprocess Engineering*, 1996. **16**(1): p. 39-43.
61. Araque, E., Parra, C., Freer, J., Contreras, D., Rodríguez, J., Mendonça, R., and Baeza, J., *Evaluation of organosolv pretreatment for the conversion of Pinus radiata D. Don to ethanol*. *Enzyme and Microbial Technology*, 2008. **43**(2): p. 214-219.
62. Ballesteros, I., Oliva, J.M., Navarro, A.A., Gonzalez, A., Carrasco, J., and Ballesteros, M. *Effect of chip size on steam explosion pretreatment of softwood*. in *21st Symposium on Biotechnology for Fuels and Chemicals*. 1999. Ft Collins, Colorado: Humana Press Inc.
63. Ewanick, S.M., Bura, R., and Saddler, J.N., *Acid-catalyzed steam pretreatment of lodgepole pine and subsequent enzymatic hydrolysis and fermentation to ethanol*. *Biotechnology and Bioengineering*, 2007. **98**(4): p. 737-746.
64. Ferrari, M.D., Neirotti, E., Alborno, C., and Saucedo, E., *Ethanol production from eucalyptus wood hemicellulose hydrolysate by Pichia stipitis*. *Biotechnology and Bioengineering*, 1992. **40**(7): p. 753-759.
65. Monavari, S., Galbe, M., and Zacchi, G., *The influence of solid/liquid separation techniques on the sugar yield in two-step dilute acid hydrolysis of softwood followed by enzymatic hydrolysis*. *Biotechnology for Biofuels*, 2009. **2**: p. 9.
66. Pienkos, P.T. and Zhang, M., *Role of pretreatment and conditioning processes on toxicity of lignocellulosic biomass hydrolysates*. *Cellulose*, 2009. **16**(4): p. 743-762.
67. Soderstrom, J., Galbe, M., and Zacchi, G., *Separate versus simultaneous saccharification and fermentation of two-step steam pretreated softwood for ethanol production*. *Journal of Wood Chemistry and Technology*, 2005. **25**(3): p. 187-202.
68. Saka, S. and Miyafuji, H., *Bioethanol production from lignocellulosics using supercritical water*, in *Materials, Chemicals, and Energy from Forest Biomass*, D.S. Argyropoulos, Editor. 2006, American Chemical Society Washington, DC.
69. Jin, B., Yin, P.H., Ma, Y.H., and Zhao, L., *Production of lactic acid and fungal biomass by Rhizopus fungi from food processing waste streams*. *Journal of Industrial Microbiology & Biotechnology*, 2005. **32**(11-12): p. 678-686.

70. Tay, A. and Yang, S.T., *Production of L(+)-lactic acid from glucose and starch by immobilized cells of Rhizopus oryzae in a rotating fibrous bed bioreactor*. Biotechnology and Bioengineering, 2002. **80**(1): p. 1-12.
71. Moldes, A.B., Torrado, A., Converti, A., and Dominguez, J.M., *Complete bioconversion of hemicellulosic sugars from agricultural residues into lactic acid by Lactobacillus pentosus*. Applied Biochemistry and Biotechnology, 2006. **135**(3): p. 219-227.
72. Lucian, L.A., Argyropoulos, D.S., Adamopoulos, L., and Gaspar, A., R., *Materials, chemicals, and energy from forest biomass: A review*, in *Materials, Chemicals, and Energy from Forest Biomass*, D.S. Argyropoulos, Editor. 2006, American Chemical Society Washington, DC.
73. Hannuksela, T., Tenkanen, M., and Holmbom, B., *Sorption of dissolved galactoglucomannans and galactomannans to bleached kraft pulp*. Cellulose, 2002. **9**(3-4): p. 251-261.
74. Mikkonen, K.S., Tenkanen, M., Cooke, P., Xu, C., Rita, H., Willför, S., Holmbom, B., Hicks, K.B., and Yadav, M.P., *Mannans as stabilizers of oil-in-water beverage emulsions*. LWT - Food Science and Technology, 2009. **42**(4): p. 849-855.
75. Xu, C.L., Pranovich, A., Hemming, J., Holmbom, B., Albrecht, S., Schols, H.A., and Willfor, S. *Hydrolytic stability of water-soluble spruce O-acetyl galactoglucomannans*. in *2nd International Cellulose Conference (ICC 2007)*. 2007. Tokyo, Japan: Walter De Gruyter & Co.
76. Mikkonen, K.S., Yadav, M.P., Cooke, P., Willfor, S., Hicks, K.B., and Tenkanen, M., *Films from spruce galactoglucomannan blended With poly(vinyl alcohol), corn arabinoxylan, and konjac glucomannan*. Bioresources, 2008. **3**(1): p. 178-191.
77. Soderqvist Lindblad, M., Albertsson, A.-C., Ranucci, E., Laus, M., and Giani, E., *Biodegradable polymers from renewable sources: Rheological characterization of hemicellulose-based hydrogels*. Biomacromolecules, 2005. **6**(2): p. 684-690.
78. Hansen, N.M.L. and Plackett, D., *Sustainable films and coatings from hemicelluloses: A review*. Biomacromolecules, 2008. **9**(6): p. 1493-1505.
79. Soderqvist Lindblad, M., Sjoberg, J., Albertsson, A.C., and Hartman, J., *Hydrogels from polysaccharides for biomedical applications*, in *Materials, Chemicals, and Energy from Forest Biomass*, D.S. Argyropoulos, Editor. 2006, American Chemical Society Washington, DC.
80. Voepel, J., Sjoberg, J., Reif, M., Albertsson, A.C., Hultin, U.K., and Gasslander, U., *Drug diffusion in neutral and ionic hydrogels assembled from acetylated galactoglucomannan*. Journal of Applied Polymer Science, 2009. **112**(4): p. 2401-2412.
81. Phan The, D., Debeaufort, F., Voilley, A., and Luu, D., *Biopolymer interactions affect the functional properties of edible films based on agar, cassava starch and arabinoxylan blends*. Journal of Food Engineering, 2009. **90**(4): p. 548-558.
82. Hartman, J., Albertsson, A.C., Lindblad, M.S., and Sjoberg, J., *Oxygen barrier materials from renewable sources: Material properties of softwood hemicellulose-based films*. Journal of Applied Polymer Science, 2006. **100**(4): p. 2985-2991.

83. Moine, C., Krausz, P., Chaleix, V., Sainte-Catherine, O., Kraemer, M., and Gloaguen, V., *Structural characterization and cytotoxic properties of a 4-O-methylglucuronoxylan from Castanea sativa*. Journal of Natural Products, 2007. **70**(1): p. 60-66.
84. Sukhov, B.G., Aleksandrova, G.P., Grishchenko, L.A., Feoktistova, L.P., Sapozhnikov, A.N., Proidakova, O.A., T'Kov, A.V., Medvedeva, S.A., and Trofimov, B.A., *Nanobiocomposites of noble metals based on arabinogalactan: Preparation and properties*. Journal of Structural Chemistry, 2007. **48**(5): p. 922-927.
85. Esker, A., Becker, U., Jamin, S., Beppu, S., Rennecker, S., and Glasser, W., *Self-assembly behavior of co- and heteropolysaccharides related to hemicelluloses*, in *Hemicelluloses: Science and Technology*, P. Gatenholm and M. Tenkanen, Editors. 2002, American Chemical Society: Washington, DC.
86. Kenealy, W.R., Houtman, C.J., Laplaza, J., Jeffries, T.W., and Horn, E.G., *Pretreatments for converting wood into paper and chemicals*, in *materials, chemicals, and energy from forest biomass*, D.S. Argyropoulos, Editor. 2006, American Chemical Society Washington, DC.
87. Sears, K.D., Beelik, A., Casebier, R.L., Engen, R.J., Hamilton, J.K., and Hergert, H.L., *Southern pine prehydrolysates: Characterization of polysaccharides and lignin fragments*. Journal of Polymer Science: Part C, 1971(36): p. 425-443.
88. Song, T., Pranovich, A., Sumerskiy, I., and Holmbom, B., *Extraction of galactoglucomannan from spruce wood with pressurised hot water*. Holzforschung, 2008. **62**(6): p. 659-666.
89. Lundqvist, J., Teleman, A., Junel, L., Zacchi, G., Dahlman, O., Tjerneld, F., and Stålbrand, H., *Isolation and characterization of galactoglucomannan from spruce (Picea abies)*. Carbohydrate Polymers, 2002. **48**(1): p. 29-39.
90. Teleman, A., Lundqvist, J., Tjerneld, F., Stalbrand, H., and Dahlman, O., *Characterization of acetylated 4-O-methylglucuronoxylan isolated from aspen employing H-1 and C-13 NMR spectroscopy*. Carbohydrate Research, 2000. **329**(4): p. 807-815.
91. Berlin, A., Maximenko, V., Gilkes, N., and Saddler, J., *Optimization of enzyme complexes for lignocellulose hydrolysis*. Biotechnology and Bioengineering, 2007. **97**(2): p. 287-296.
92. Biermann, C.J., *Hydrolysis and other cleavages of glycosidic linkages in polysaccharides*, in *Advances in Carbohydrate Chemistry and Biochemistry*. 1988, Academic Press, Inc.
93. Gilbert, H.J., Stålbrand, H., and Brumer, H., *How the walls come crumbling down: recent structural biochemistry of plant polysaccharide degradation*. Current Opinion in Plant Biology, 2008. **11**(3): p. 338-348.
94. Moreira, L.R.S. and Filho, E.X.F., *An overview of mannan structure and mannan-degrading enzyme systems*. Applied Microbiology and Biotechnology, 2008. **79**(2): p. 165-178.
95. Andersson, S.-I., Samuelson, O., Ishihara, M., and Shimizu, K., *Structure of the reducing end-groups in spruce xylan*. Carbohydrate Research, 1983. **111**(2): p. 283-288.

96. Villaverde, J.J., Li, J.B., Ek, M., Ligeró, P., and de Vega, A., *Native lignin structure of miscanthus x giganteus and its changes during acetic and formic acid fractionation*. Journal of Agricultural and Food Chemistry, 2009. **57**(14): p. 6262-6270.
97. Xu, F., Liu, C.F., Geng, Z.C., Sun, J.X., Sun, R.C., Hei, B.H., Lin, L., Wu, S.B., and Je, J., *Characterisation of degraded organosolv hemicelluloses from wheat straw*. Polymer Degradation and Stability, 2006. **91**(8): p. 1880-1886.
98. Parajo, J.C., Dominguez, H., and Dominguez, J.M., *Study of the adsorption steps to improve the production of xylitol from wood hydrolysates*. Afinidad, 1997. **54**(467): p. 51-54.
99. Sanz, M.L. and Martínez-Castro, I., *Recent developments in sample preparation for chromatographic analysis of carbohydrates*. Journal of Chromatography A, 2007. **1153**(1-2): p. 74-89.
100. Curling, S.F., Fowler, P.A., and Hill, C.A.S., *Development of a method for the production of hemicellulosic gels from Sitka spruce*. Carbohydrate Polymers, 2007. **69**(4): p. 673-677.
101. Westbye, P., Kohnke, T., Glasser, W., and Gatenholm, P., *The influence of lignin on the self-assembly behaviour of xylan rich fractions from birch (Betula pendula)*. Cellulose, 2007. **14**(6): p. 603-613.
102. Cruz, J.M., Dominguez, J.M., Dominguez, H., and Parajo, J.C., *Solvent extraction of hemicellulosic wood hydrolysates: a procedure useful for obtaining both detoxified fermentation media and polyphenols with antioxidant activity*. Food Chemistry, 1999. **67**(2): p. 147-153.
103. Ponder, G.R. and Richards, G.N., *Arabinogalactan from Western larch .I. Effect of uronic acid groups on size exclusion chromatography*. Journal of Carbohydrate Chemistry, 1997. **16**(2): p. 181-193.
104. Cardoso, S.M., Silva, A.M.S., and Coimbra, M.A., *Structural characterisation of the olive pomace pectic polysaccharide arabinan side chains*. Carbohydrate Research, 2002. **337**(10): p. 917-924.
105. Barbat, A., Gloaguen, V., Moine, C., Sainte-Catherine, O., Kraemer, M., Rogniaux, H., Ropartz, D., and Krausz, P., *Structural characterization and cytotoxic properties of a 4-O-methylglucuronoxylan from Castanea sativa. 2. Evidence of a structure-activity relationship*. Journal of Natural Products, 2008. **71**(8): p. 1404-1409.
106. Lundqvist, J., Jacobs, A., Palm, M., Zacchi, G., Dahlman, O., and Stalbrand, H., *Characterization of galactoglucomannan extracted from spruce (Picea abies) by heat-fractionation at different conditions*. Carbohydrate Polymers, 2003. **51**(2): p. 203-211.
107. Stahl, B., Linos, A., Karas, M., Hillenkamp, F., and Steup, M., *Analysis of fructans from higher plants by matrix-assisted laser desorption/ionization mass spectrometry*. Analytical Biochemistry, 1997. **246**(2): p. 195-204.
108. Lastovickova, M. and Chmelik, J., *Simple and fast method for recognition of reducing and nonreducing neutral carbohydrates by matrix-assisted laser desorption/ionization time-of-flight mass spectrometry*. Journal of Agricultural and Food Chemistry, 2006. **54**(14): p. 5092-5097.
109. Harvey, D.J., *Matrix-assisted laser desorption/ionization mass spectrometry of carbohydrates and glycoconjugates*. International Journal of Mass Spectrometry, 2003. **226**(1): p. 1-35.

110. Chan, P.K. and Chan, T.W.D., *Effect of sample preparation methods on the analysis of dispersed polysaccharides by matrix-assisted laser desorption/ionization time-of-flight mass spectrometry*. Rapid Communications in Mass Spectrometry, 2000. **14**(19): p. 1841-1847.
111. Williams, D. and Young, M.K., *Analysis of neutral isomeric low molecular weight carbohydrates using ferrocenyl boronate derivatization and tandem electrospray mass spectrometry*. Rapid Communications in Mass Spectrometry, 2000. **14**(22): p. 2083-2091.
112. Manley-Harris, M., *Structural studies by NMR spectroscopy of the major oligomers from alkali-degraded arabinogalactan from Larix occidentalis*. Carbohydrate Polymers, 1997. **34**: p. 243-249.
113. Ray, B., Loutelier-Bourhis, C., Lange, C., Condamine, E., Driouch, A., and Lerouge, P., *Structural investigation of hemicellulosic polysaccharides from Argania spinosa: characterisation of a novel xyloglucan motif*. Carbohydrate Research, 2004. **339**(2): p. 201-208.
114. Maslen, S.L., Goubet, F., Adam, A., Dupree, P., and Stephens, E., *Structure elucidation of arabinoxylan isomers by normal phase HPLC-MALDI-TOF/TOF-MS/MS*. Carbohydrate Research, 2007. **342**(5): p. 724-735.
115. Carpita, N.C. and Shea, E.M., *Linkage structure of carbohydrates by gas chromatography-mass spectrometry (GC-MS) of partially methylated alditol acetates*, in *Analysis of Carbohydrates by GLC and MS*, C.J. Biermann and G.D. McGinnis, Editors. 1988, CRC Press, Inc.
116. Xu, C.L., Pranovich, A., Vahasalo, L., Hemming, J., Holmbom, B., Schols, H.A., and Willfor, S., *Kinetics of acid hydrolysis of water-soluble spruce o-acetyl galactoglucomannans*. Journal of Agricultural and Food Chemistry, 2008. **56**(7): p. 2429-2435.
117. Sims, I.M. and Newman, R.H., *Structural studies of acidic xylans exuded from leaves of the monocotyledonous plants Phormium tenax and Phormium cookianum*. Carbohydrate Polymers, 2006. **63**(3): p. 379-384.
118. Chattopadhyay, K., Adhikari, U., Lerouge, P., and Ray, B., *Polysaccharides from Caulerpa racemosa: Purification and structural features*. Carbohydrate Polymers, 2007. **68**(3): p. 407-415.
119. Cai, Y., Jiang, Y.J., and Cole, R.B., *Anionic adducts of oligosaccharides by matrix-assisted laser desorption/ionization time-of-flight mass spectrometry*. Analytical Chemistry, 2003. **75**(7): p. 1638-1644.
120. *CCRC Spectral Database PMAA*. 2009 [cited 21/09/2009]; Available from: <http://www.crc.uga.edu/specdb/ms/pmaa/pframe.html>.
121. Wetzel, S.J., Guttman, C.M., and Girard, J.E., *The influence of matrix and laser energy on the molecular mass distribution of synthetic polymers obtained by MALDI-TOF-MS*. International Journal of Mass Spectrometry, 2004. **238**(3): p. 215-225.
122. Chun-hui, L., Chang-hai, W., Zhi-liang, X., and Yi, W., *Isolation, chemical characterization and antioxidant activities of two polysaccharides from the gel and the skin of Aloe barbadensis Miller irrigated with sea water*. Process Biochemistry, 2007. **42**(6): p. 961-970.
123. Balakshin, M.Y., Capanema, E.A., and Chang, H.M., *MWL fraction with a high concentration of lignin-carbohydrate linkages: Isolation and 2D NMR spectroscopic analysis*. Holzforschung, 2007. **61**(1): p. 1-7.

124. Davey, C., *Development of an Ion Chromatography Method for the Analysis of Nitric Acid Oxidation Reactions of Common Sugars*. 2008, The University of Waikato: Hamilton.
125. Tamaki, Y., Konishi, T., Fukuta, M., and Tako, M., *Isolation and structural characterisation of pectin from endocarp of Citrus depressa*. Food Chemistry, 2008. **107**(1): p. 352-361.
126. Choi, J.W., Choi, D.H., and Faix, O., *Characterization of lignin-carbohydrate linkages in the residual lignins isolated from chemical pulps of spruce (Picea abies) and beech wood (Fagus sylvatica)*. Journal of Wood Science, 2007. **53**(4): p. 309-313.
127. Gibeaut, D.M. and Carpita, N.C., *Clean-up procedure for partially methylated alditol acetate derivatives of polysaccharides*. Journal of Chromatography 1991. **587**: p. 284-287.
128. Laine, C., Tamminen, T., and Hortling, B., *Carbohydrate structures in residual lignin-carbohydrate complexes of spruce and pine pulp*. Holzforschung, 2004. **58**(6): p. 611-621.
129. Ebringerová, A., Hromádková, Z., Hříbalová, V., Xu, C., Holmbom, B., Sundberg, A., and Willför, S., *Norway spruce galactoglucomannans exhibiting immunomodulating and radical-scavenging activities*. International Journal of Biological Macromolecules, 2008. **42**(1): p. 1-5.
130. Luonteri, E., Laine, C., Uusitalo, S., Telemann, A., Siika-aho, M., and Tenkanen, M., *Purification and characterization of Aspergillus beta-D-galactanases acting on beta-1,4- and beta-1,3/6-linked arabinogalactans*. Carbohydrate Polymers, 2003. **53**(2): p. 155-168.
131. Verbruggen, M.A., Spronk, B.A., Schols, H.A., Beldman, G., Voragen, A.G.J., Thomas, J.R., Kamerling, J.P., and Vliegthart, J.F.G., *Structures of enzymically derived oligosaccharides from sorghum glucuronoarabinoxylan*. Carbohydrate Research, 1998. **306**(1-2): p. 265-274.